Theoretical Modeling of Terahertz (THZ) Radiation Emissions from Free Electron Laser (FEL)

THESIS

SUBMITTED TO DELHI TECHNOLOGICAL UNIVERSITY
FOR THE AWARD OF THE DEGREE OF

DOCTOR OF PHILOSOPHY

BY

JYOTSNA PANWAR
(2K14/Ph.D/AP/02)

DEPARTMENT OF APPLIED PHYSICS
DELHI TECHNOLOGICAL UNIVERSITY
SHAHBAD DAULATPUR, MAIN BAWANA ROAD,
DELHI-110042, INDIA

NOVEMBER, 2018

CERTIFICATE

This is to certify that the thesis entitled **"Theoretical Modeling of Terahertz (THz) Radiation Emissions from Free Electron Laser (FEL)"** submitted by **Ms. Jyotsna Panwar** to Delhi Technological University in partial fulfilment for the award of Ph.D. degree in Physics is a bonafide record of the research work carried out by her under our supervision and guidance.

The results of the thesis have not been submitted to any other Institution or University for the award of any other degree or diploma.

Prof. Suresh C. Sharma
Supervisor
Former HOD, Dept. of Applied Physics
Delhi Technological University
Delhi

Prof. Rinku Sharma
Co-Supervisor
HOD, Dept. of Applied Physics
Delhi Technological University
Delhi

CANDIDATE'S DECLARATION

I, herby certify that the thesis titled **"Theoretical Modeling of Terahertz (THz) Radiation Emissions from Free Electron Laser (FEL)"** submitted in the fulfilment of the requirements for the award of the degree of Doctor of Philosophy is an authentic record of my research work carried out under the guidance of Prof. Suresh C. Sharma and Prof. Rinku Sharma. Any material borrowed or referred to is duly acknowledged.

Jyotsna Panwar
(2K14/PhD/AP/02)
Dept. of Applied Physics
Delhi Technological University
Delhi, India

Dedicated

to

My Family

ACKNOWLEDGEMENTS

I would like to convey my indebted thanks and gratitude to everyone who supported, encouraged and cooperated me in successful completion of my research work.

Prior and foremost, I am grateful to the almighty for entrusting potential, morale, strength and a right direction to me to accomplish my work.

I express profound gratitude to my research supervisor and former HOD, Applied Physics, Prof. Suresh C. Sharma for his faith, fruitful discussions and worthy guidance to me. He supported me all through my research work with his expertise and endurance. He provided motivation, sound ideas and great advice to me throughout my thesis writing.

I am also thankful to my Co-Supervisor and HOD, Applied Physics, Prof. Rinku Sharma for helping me out in my work through her great support.

A very special gratitude goes out to Delhi Technological University for providing me the necessary research facilities and fellowship for carrying out thesis work.

I would like to thank the administration and Library for their willing cooperation and assistance.

I owe regards to the faculty and staff members of the Department of Applied Physics. I also thank my labmates Ms. Pratibha Malik, Ms. Neha Gupta, Mr. Ravi Gupta, Ms. Kavita Rani, Ms. Ruchi Sharma, Ms. Umang Sharma, Ms. Monika Yadav, Ms. Anshu, Ms. Renu, and Ms. Suman Dahiya for their discussions and suggestions.

Moreover, I am grateful to Ms. Umang Sharma and Ms. Sumandeep for providing a friendly environment and helping me out in completion of my work.

I am highly thankful to my father (Mr. Devender Singh Panwar) and mother (Ms. Sunita Panwar) for providing me the moral and material support. Their love and belief have been a great hand in making me to complete my thesis and reach this point in the field of academics. I am grateful to my brother (Mr. Tarun Panwar), my sister-in-law (Ms. Namita) for their affection and inspiration and especially to my twin nieces (Ms. Hunar and Ms. Harnoor), who have been there for creating a happy, joyful and stress free environment. I would also thank my fiancé (Lieut Sudhir Tomar) for being so understanding and motivating.

Finally, I apologize all others unnamed who assisted me in various ways in the completion of my research work.

Jyotsna Panwar

ABSTRACT

The research in the subject of terahertz (THz) radiation has gained a great awareness since nineties to fill the THz gap in the electromagnetic spectra due to the existing significant properties and resulting applications in diverse areas such as medical, spectroscopy, communications and others. The non-ionizing and high penetration potential of the THz radiation has enabled numerous techniques involving both optics and electronics to be proposed to study the emission and detection of THz radiation.

The thesis focuses on designing of analytical models to study the emission of high power THz radiation by employing premodulated electron beams using free electron laser (FEL) as a classical device. The role of premodulation of the beam in generation of the THz radiation is discussed. To study the efficient emission of the radiation, plasma based medium such as surface plasma wave, Langmuir wave are used as wigglers in FEL. Slow wave structure involving a waveguide with dielectric lining is also used as a Cerenkov FEL for THz emission. The power, amplitude and efficiency of the radiation wave are evaluated to have an analysis of the output radiation. We have studied the effect of parameters of the electron beam, wiggler, plasma and other factors affecting the tunability of the THz radiation. The route followed in the analytical treatment of the analysis involves fluid theory which deals with the interaction of premodulated electron beam, electromagnetic wave and a pump signal. The softwares used for obtaining the results are MATLAB and MATHEMATICA.

CONTENTS

LIST OF FIGURES

LIST OF PUBLICATIONS

International Refereed Journals

1. **Jyotsna Panwar** and Suresh C. Sharma, *Terahertz radiation emission using plasma-filled dielectric liner with the effects of pre-modulated relativistic electron beam*, Contribution to Plasma Physics **58**, 917-924 (2018).
2. **Jyotsna Panwar**, and Suresh C. Sharma, *Modeling the emission of high power terahertz radiation using Langmuir wave as a wiggler*, Phys. Plasmas **24**, 083101 (2017).
3. Suresh C. Sharma, **Jyotsna Panwar** and Rinku Sharma, *Modeling of terahertz radiation emission from a free-electron laser*, Contribution to Plasma Physics **57**, 167-175 (2017).
4. **Jyotsna Panwar**, Suresh C. Sharma and Rinku Sharma, *Terahertz Radiation Emission from A Surface Wave Pumped Free Electron Laser*, Journal of Atomic, Molecular, Condensate & Nano Physics **6**, 169-178 (2015).
5. **Jyotsna Panwar** and Suresh C. Sharma, *Relativistic electron beam driven THz radiation using plasma slab* IEEE Trans. On Plasma Sci. (Communicated).

International Conference Proceedings

6. **J Panwar**, S C Sharma, P Malik, M Yadav and R Sharma, *Generation of high power sub millimeter radiation using free electron laser*, IOP Conf. Series: Materials Science and Engineering **331**, 012014 (2018).
7. Pratibha Malik, Suresh C. Sharma, **Jyotsna Panwar** and Rinku Sharma, *Numerical analysis of THz radiation wave using upper hybrid wave wiggler*, , IOP Conf. Series: Materials Science and Engineering **331**, 012021 (2018).
8. **Jyotsna Panwar**, Suresh C. Sharma and Rinku Sharma, *Terahertz radiation generation by using modulated electron beam with plasma wave wiggler*, Journal of Physics: Conference series **836**, 1-4 (2017).

9. **Jyotsna Panwar**, Suresh C. Sharma, Pratibha Malik, and Rinku Sharma, *Terahertz output radiation tunability with free electron laser*, in International Conference on Advances in Applied Sciences, Engineering and Technology at K. R. Mangalam University, Gurgaon, August 17-18, 2017. (Accepted for Publication).

10. **Jyotsna Panwar**, Suresh C. Sharma and Rinku Sharma, *Emission of high power radiation using free electron lasers*, abstract in International Symposium on Nonlinear Waves in Fluids and Plasmas, from 1-2 March 2017, IIT Delhi.

11. **Jyotsna Panwar**, Suresh C. Sharma and Rinku Sharma, *Tunability of high power radiation generated using strong field free electron laser*, abstract in 18th International Conference on Physics of Highly Charged Ions, HCI, 11-16 Sep. 2016, at Kielce, Poland.

Chapter 1

INTRODUCTION

The electromagnetic (EM) spectra covers a wide frequency ranging from 1 hertz to 10^{25} hertz. The EM radiation is generated due to the acceleration of atomic particles such as electrons or ions. The motion of particles leads to the oscillation of the electric and magnetic fields that propagate perpendicular to each other [1]. Quantum mechanically, the radiation involves flow of quanta of light i.e., photons which move universally with the speed of light. The parameters that characterize a wave are frequency, wavelength and energy.

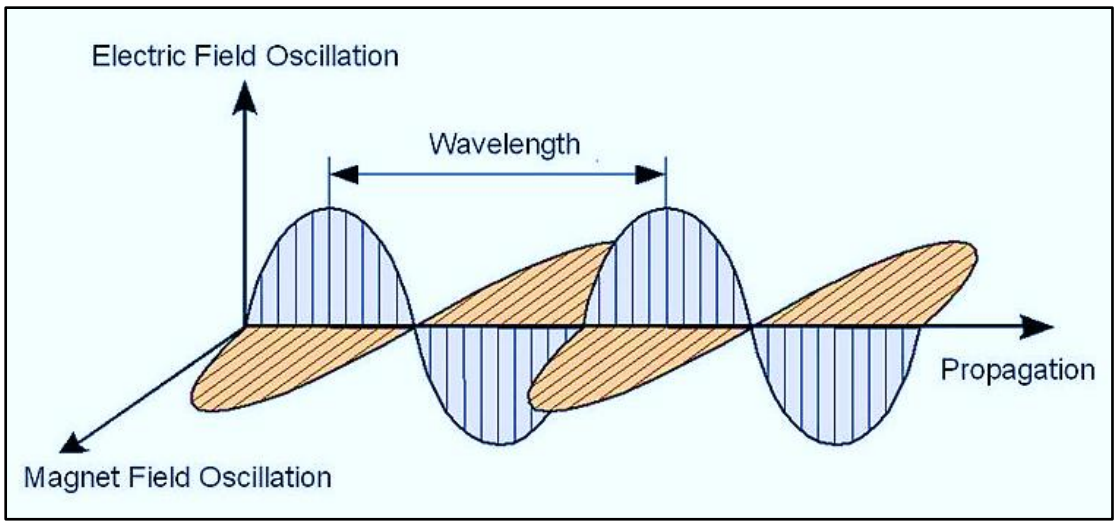

Fig 1.1. Illustration of propagation of electromagnetic wave [2].

The EM spectra is divided into seven regions in series of increasing frequency and energy, and decreasing wavelength. The intensity of the radiation is defined by the density of photons [3]. The EM radiation possess neither charge nor mass and is the

movement of energy across the space or any other medium in the form of electric and magnetic fields. The energy stored in the sun in the form of coal, gas and oil is obtained in the form of electromagnetic radiation [4].

The distance after which the wave position is repeated determines the wavelength of the wave and the frequency scales as inverse of the wavelength which is defined as the number of waves passing through a specified point in unit time. The electric and magnetic fields are generated due to the electrically charged particles.

The region of brilliant and intense THz has remained unexplored until 1970s due to the lack of appropriate sources for the generation and detection of THz radiation. Any substance with temperature above 10 *K* emits THz radiation. The clouds of gas and dust at temperatures of 10 to 100 *K* show weak thermal emission at THz frequencies [5].

The gap in the electromagnetic spectra between the frequency range of microwave and infrared radiation is filled by the terahertz radiation. The region has been called as "THz gap" due to the lack of suitable tools to explore it. The terahertz radiation falls in between the microwave region and the infrared region with frequency radiation ranging from 0.3 to 3 *THz* and the wavelength corresponding to the region lies in between 1 to 0.1 *mm*. As the wavelength of the THz radiation generally lies below 1mm, therefore it is also known as sub-millimeter radiation. The energy of the radiation is of the order of *meV*. This region of electromagnetic spectra have remained unexplored for long time but presently it has become an area of fascinating research due to its existing tremendous properties and applications. THz radiation poses behavior of non-ionization and high penetration through non conducting objects. The THz band holds uniqueness as it holds the useful characteristics of both the radio waves and the infrared waves [6].

The THz wave can be transmitted through non conducting materials such as clothes, paper, plastics, packing materials, leather, wood etc. and, therefore the THz pulses can be opted for the identification, imaging and analysis of these materials. These waves cannot penetrate through metals and are highly attenuated in water. The radiation is non-destructive and safe and, thus helps in chemical and internal analysis of different materials.

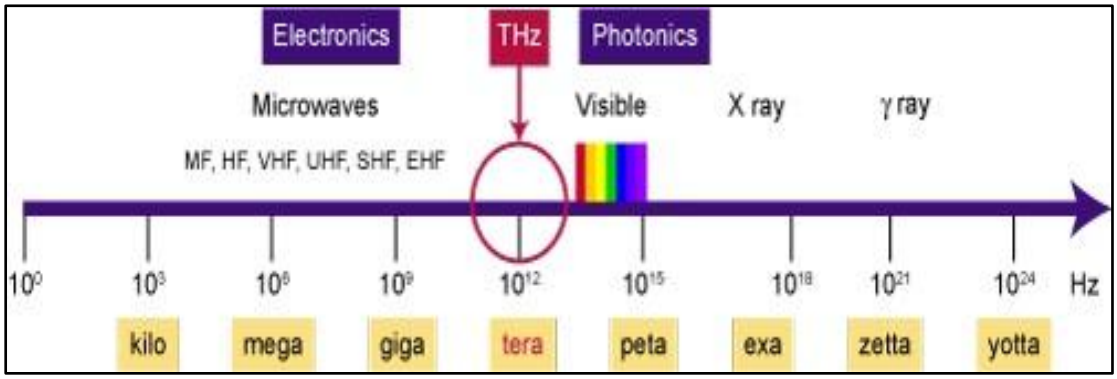

Fig 1.2. Electromagnetic spectra depicting the THz region [7].

Due to exclusive frequency and energy range of THz radiation, several approaches have been followed by incorporating both electronics and optics to study its generation and detection.

1.1 Methods for the Emission of Terahertz Radiation

The fascinating properties and applications of THz radiation have led this unexplored region of electromagnetic spectra to become an area of research after early nineties. THz poses its utility in various fields such as medical, spectroscopy, communication, imaging and others. Therefore, efforts have been put to develop better sources for generation and detection of the THz radiation. Numerous techniques that have been employed to study the generation of THz radiation involves optical rectification in semiconductors, dielectrics and plasmas [8-10], photoconductive antennas [11-13], quantum cascade lasers [14, 15], interaction of high power lasers with plasma [16, 17], free electron lasers [18, 19].

1.2 Optical Sources

1.2.1 Optical Rectification

In optical rectification, a time dependent polarization change is induced when a laser pulse travels through the nonlinear crystal which acts as a source for the emission of radiation [20-22]. This scheme for the generation of radiation was first revealed by K. H. Yang [23] by using $LiNbO_3$ as the electro-optic material. The incident and refracted THz pulse travels at the same speed due to the same refractive indices of the optical and THz pulse in a non-dispersive medium. The phase of the induced polarization matches with the amplitude of the THz radiation as a result of which it grows linearly. But practically, nonlinear crystals are dispersive which leads to the polarization to be out of phase after some distance. For the condition of phase matching to be satisfied, the group velocity of the optical pulse should be analogous to the phase velocity of the THz radiation [5].

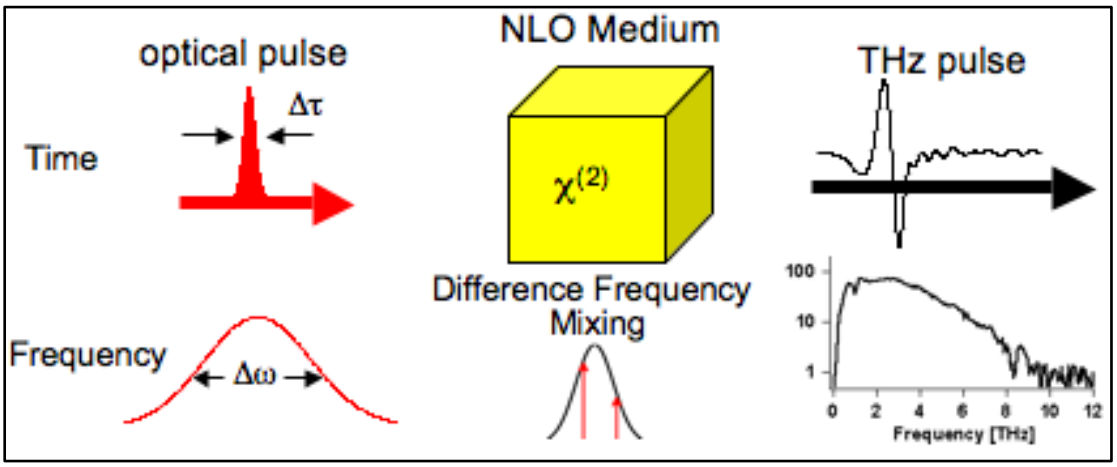

Fig 1.3. Generation of THz radiation via optical rectification. [24].

1.2.2 Frequency Difference Generation (DFG)

Two coherent radiation beams of frequencies ω_I and ω_{II} lying in the THz range on interacting with nonlinear medium of second order susceptibility $\left(\chi^2_{NL}\right)$ leads to the emission of radiation at the frequency difference i.e., $\omega_I - \omega_{II}$ [5, 25, 26]. The

bound electrons start oscillating when the field is incident on the medium. For the linear region, the applied electric field $\left(E_b(t)\right)$ scales linearly proportional to the dielectric polarisation $\left(P_d(t)\right)$ i.e.,

$$P_d(t) = \varepsilon_0 \chi^1_{NL} E_b(t), \tag{1.1}$$

where ε_0 is the free space permittivity. The strong input field leads to the polarisation as a series of terms:

$$P_d(t) = \varepsilon_0 \chi^1_{NL} E_b(t) + \varepsilon_0 \chi^2_{NL} E_b(t) + \varepsilon_0 \chi^3_{NL} E_b(t) + \ldots., \tag{1.2}$$

where this second order term contributes to the DFG scheme.

Cascaded DFG technique is a proficient way to enhance the efficiency of the DFG for the generation of the THz radiation [27]. Optical rectification and difference frequency generation are the techniques based on frequency down conversion.

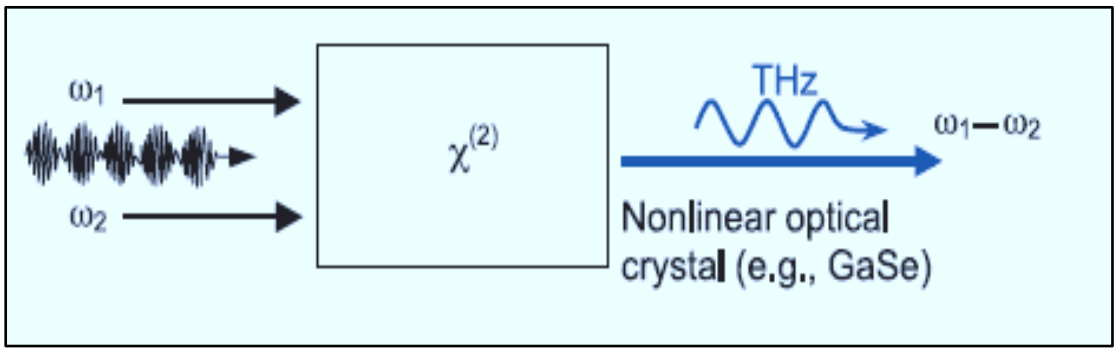

Fig 1.4. THz radiation generation via frequency difference technique [5].

1.2.3 Photomixing

This scheme implicates the overlapping of two lasers in the frequency range of infrared or visible region for the emission of radiation within the frequency difference of two lasers. The radiation can be detected via photoconductive switching.

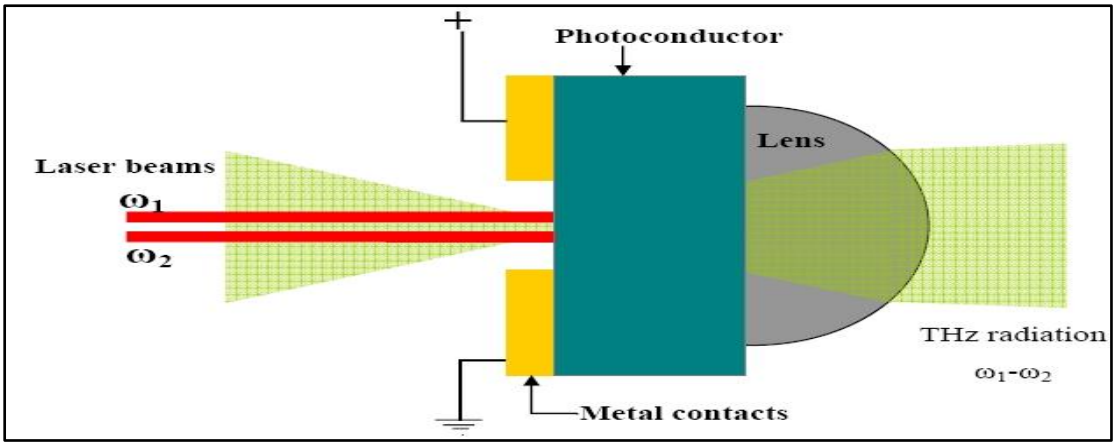

Fig 1.5. Emission of THz radiation via photomixing. [28]

1.2.4 Photoconductive Antennas

Photoconductive (PC) antennas comprises of two parallel metallic electrodes that are placed on semiconductor substrate with gap of micro scale between them. The electrodes are generally in the shape of antennas. A laser beam whose energy is greater than the band gap energy of the semiconductor material is incident on the gap between the PC antennas which leads to the excitation of electrons and holes in the substrate. The generated electrons and holes induce photocurrent due to the bias voltage. The THz radiations are thus driven by the time varying current [29, 30].

1.3 Electron based Sources

The basic principle for the electron beam based sources used for the generation of coherent radiation involves the translation of energy of the electron beam to the field energy of the electromagnetic radiation [31].The solid state electronic devices (SSEDs) such as diodes and transistors involves semiconductor as a medium for the electron transport through conduction The vacuum electronic devices (VEDs) that implements vacuum as a medium for achieving the high frequency range of the microwave region includes travelling wave tubes (TWT_S), backward wave oscillators (BWO_S), Gyrotrons, Klystrons [32-34]. For high power devices in order to sustain high beam currents VEDs are favoured.

1.3.1 Backward Wave Oscillator

Backward wave oscillator (BWO) is a slow wave device in which the electrons focused by the magnetic fields are drawn towards the anode through a decelerating structure which leads to the excitation of the electromagnetic wave that travels in the opposite direction and, thus the oscillations are sustained [35, 36]. Dobroiu *et al.* [36] first reported that BWO as a source is preferable for imaging application due to synchronous detection, high resolution and focusing ability.

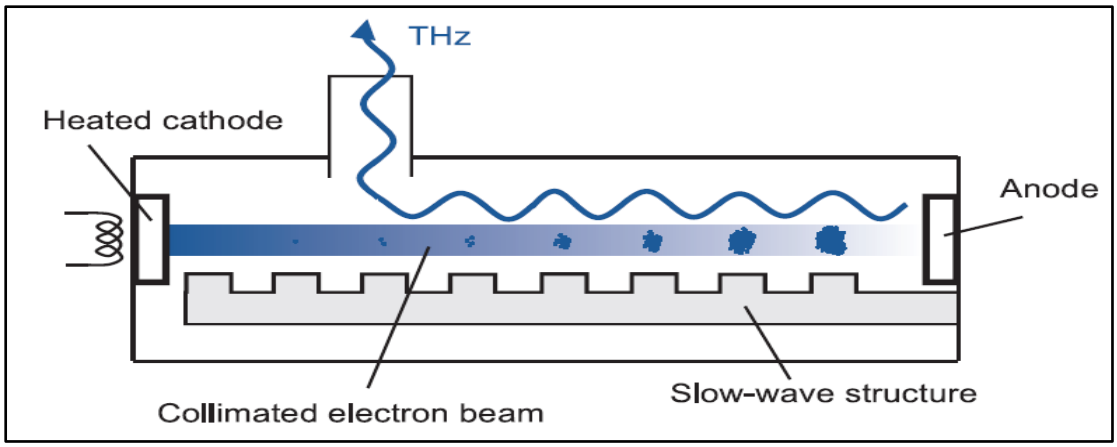

Fig 1.6. Backward wave oscillator employed for THz radiation emission [5].

1.3.2 Gyrotrons

Gyrotrons are fast wave devices that are capable of generating high average power in the range of millimeter and sub-millimeter wavelengths.

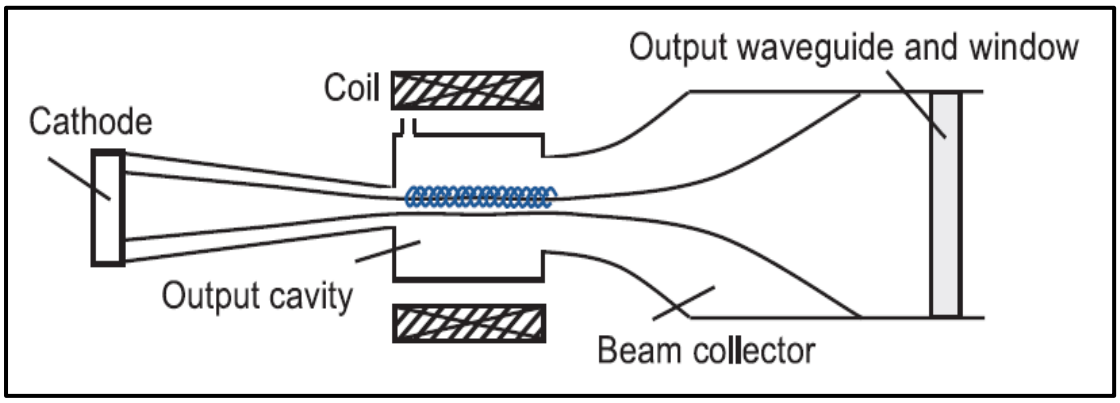

Fig 1.7. Gyrotron as a source for THz radiation emission [5].

It involves the transfer of energy between the electrons spiraling under the effect of magnetic field and the electromagnetic radiation at electron cyclotron frequency. The amplification of the radiation is maximum at the highest field strength position [37].

1.3.3 Travelling Wave Tube

Travelling Wave Tube (TWT) comprises of an electron gun as an electron beam source, a slow wave tube where the interaction between the beam electrons and the RF electromagnetic wave occurs and the amplification of the RF field turns up due to the energy transfer from the electrons of the beam. The beam electrons are focused by providing an external magnetic field around the tube. Generally, folded TWTs are used for the THz generation in which regenerative oscillations are forced via the circulation of output back to the input end [38, 39]. Although, the helical TWT have more bandwidth and are highly efficient but are restricted for obtaining the THz radiation due to fabrication difficulties of helix in small circuits by conventional techniques [31].

For a fast wave device, the physical dimensions of the interaction region is much greater than the radiation wavelength while for a slow wave device the interaction region dimensions and the radiation wavelength are comparable.

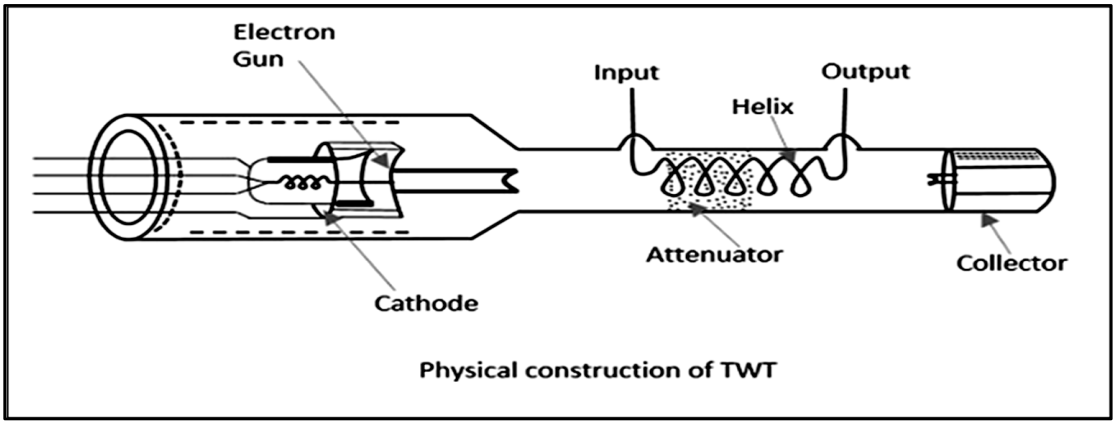

Fig 1.8. Schematic of TWT [31]

1.3.4 Free Electron Lasers

Free electron laser (FEL) is a classical tunable device for the emission of coherent terahertz radiation. The first FEL was invented in mid 1970s by John Madey [40] with first experiment performed at Stanford University. For the past few decades it has gained great attraction due to its wide tunability and high intensity.

FEL comprises of an electron beam, an accelerator and an oscillatory field that is known as undulator or wiggler. As compared to the conventional laser, the electron beam serves as the lasing medium. The term undulator is used generally for the periodic magnetic field in synchrotron light sources that are incoherent while wiggler refers to the field that provides oscillatory motion to the beam for free electron lasers such that the electrons and the radiation field couple with each other [41]. The electrons are accelerated to velocities comparable to the velocity of light to obtain a relativistic electron beam (REB). The wiggler field and the electromagnetic seed signal exerts a nonlinear ponderomotive force on the electrons of the REB that drives the exchange of energy by the electrons due to which the electrons that gain energy move fast while the electrons on losing the energy slows down w.r.t to the reference electrons. This makes the electrons to finally acquire a common velocity leading to the bunching of the beam at the scale length of the wavelength of the radiation wave. The electron bunches then move collectively to emit coherent radiation.

The possible regimes in which FEL can operate depending on the energy of the beam and current density are (a) Raman regime which operates at high beam current and low beam energy (b) Compton regime that operates at low beam current and high beam energies [42].

The electron beam can be confined into the interaction region either by applying an axial magnetic field [43, 44] or by ion channel guiding [45-47]. Usually, the

magnetic field is provided by using solenoids wrapped around the wiggler space where the beam has to be focused for effective interaction to occur. The applied static magnetic field provides electron cyclotron frequency. The gain and efficiency attained for the radiation generation becomes maximum when the frequency of the pump wave, and the electron cyclotron frequency becomes equivalent. An ion channel is formed when the high field strength electron beam driven into the plasma medium expels out the plasma electrons due to the repulsive force between the beam and plasma electrons, leaving behind the ions being massive. This channel acts as a path for the propagation of the beam by focusing and confining it in the axial direction due to the space charge force exerted due to the ions of the positive charge [48]. It results in effective hike in the FEL gain. For the ion channel to be formed, the density of the plasma electrons should be lower than the beam density [49].

The main mode of operation for high gain FEL is self-amplified spontaneous emission (SASE). SASE results in the creation of radiation wave from an electron beam of high energy. The process does not require an external seed signal and the spontaneous radiation produced due to the prior interaction with the wiggler region acts a seed signal in further interaction [50].

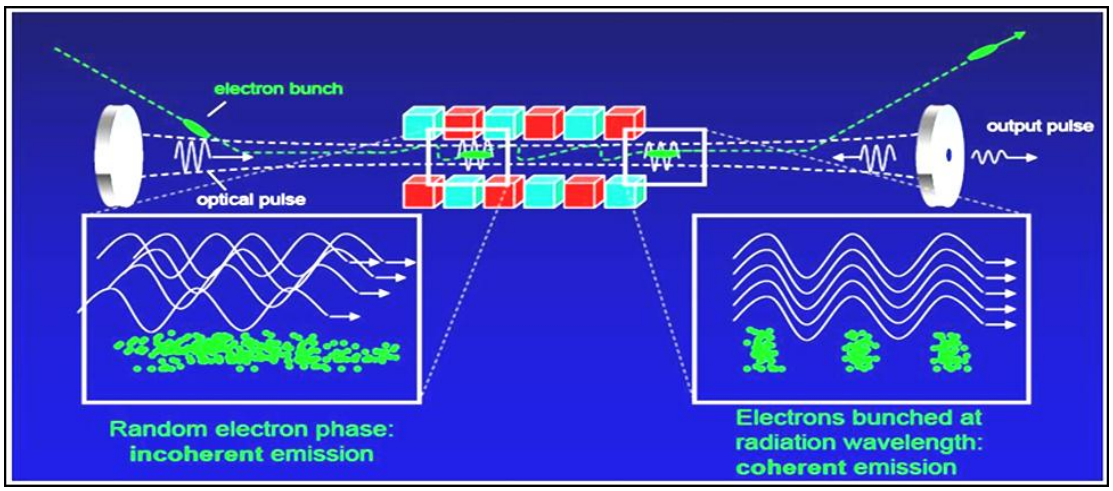

Fig 1.9. Schematic representation of free electron laser [51]

1.4 Wiggler

The wiggler employed can be electromagnetic, magnetic or electric. For the electron frame these appear to be different but in the lab frame all behave to be as electromagnetic waves. The frequency component of the purely magnetic wiggler is zero while the wave vector vanishes for the purely electric wiggler [52].

The wavelength of the radiation wave can be tuned by the energy of the electron beam and the wiggler period as

$$\lambda_R \cong \frac{\lambda_W}{2\gamma^2},$$

where λ_R is the wavelength of the radiation wave, λ_W is the wiggler wavelength and γ is the relativistic gamma factor. The radiation wavelength varies directly with the wavelength of the wiggler i.e., wiggler period and inversely with the square of the gamma factor.

The wavelength of the radiation wave for magnetostatic wiggler is given as $\lambda_R \cong \frac{\lambda_W}{2\gamma^2}$, while for the electromagnetic (EM) wiggler, the radiation wavelength scales as $\lambda_R \cong \frac{\lambda_W}{4\gamma^2}$.

The beam energy requirement can be comparatively reduced by using electromagnetic wave wigglers of short wavelength. Further, the radiation frequency induced by EM wiggler is estimated to be about double the frequency due to magnetostatic wiggler. Magnetostatic wiggler has advantage due to reproducible and well determined wiggler period. Helical wiggler comprises of magnetic field with components in both the axial and transverse direction that results in the spiral motion of the beam.

In a FEL when an electron loses momentum, then a part of it is absorbed by the photon and remaining by the wiggler. Therefore, wiggler plays an important role in the conservation of momentum which is an essential condition for the emission of radiation.

1.5 Plasma

The universe comprises of matter in the form of four states depending on the component particles and the bond strength namely: solid, liquid, gas and plasma. The state is determined by the equilibrium between the binding force and thermal energy of the particles. Plasma is the fourth state of matter which was first suggested by Irving Langmuir in 1922 [53]. Plasma is obtained due to ionization of gas which satisfies the criteria of quasineutrality, collective behavior and strong ionization [54]. Quasineutrality refers to the plasma as an overall neutral medium with equal number of ions and electrons. The debye length λ_D should be less as compared to the dimensions of the system L. Debye length determines the distance upto which the system is able to shield the applied electric potential. Collective behavior implies that plasma particles experience long range Coulomb force and each particle shows an interaction with large number of other particles. Plasma frequency is a significant parameter that characterizes the response of plasma to the external electric and magnetic fields. Plasma frequency is the frequency at which the electrons oscillate and the plasma acts as an arrangement of coupled oscillator. It is considered that electrons are subjected to external perturbations whereas ions behaves as background and counteracts the unperturbed plasma due to their heavier mass.

Plasma as a natural source is present in the interplanetary and interstellar region although at low densities. The upper layer of Earth's atmosphere i.e., ionosphere is ionized by the high frequency waves. The density of plasma is high in the ionosphere and increases on moving to the higher layers. In the magnetosphere, a

barrier is formed between the planets and plasma particles via solar wind. The presence of plasma interrupts the power lines and radio waves by causing the accumulation of charge only on one side of the spacecraft which results in an electric discharge [55]. Plasma also finds use in plasma display, arc welding, neon and fluorescent lamps.

One of the method implemented for the formation of plasma in lab is by applying a high electric field to the gas. The strength of the field depends on the geometry of the system enclosing the gas and the gas pressure. The source for the electric field can be electrodes or transformers [56]. In case of atoms of alkalies such as cesium, sodium, and potassium, plasma can be obtained by the direct heating of these elements above 3000K due to their low ionization energies.

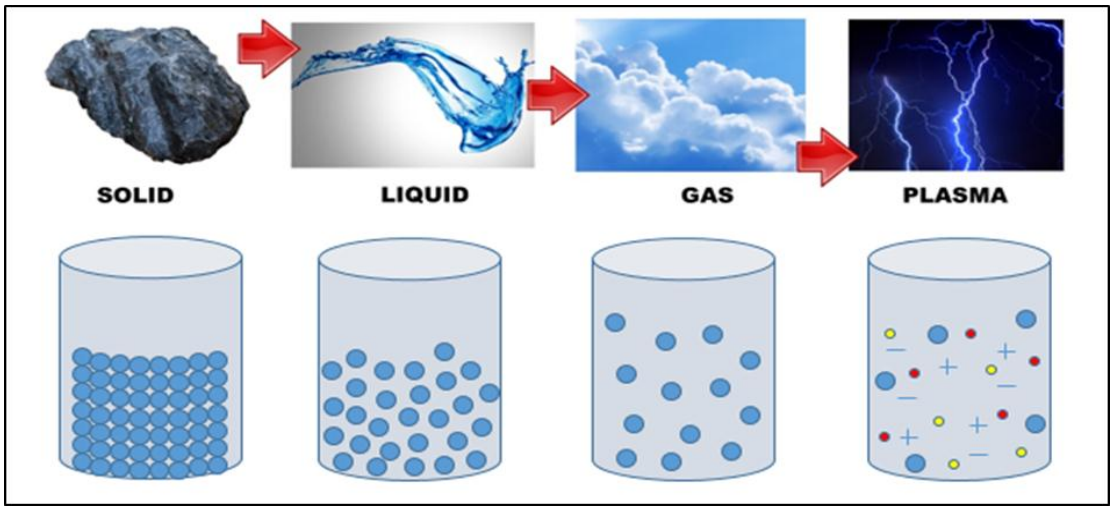

Fig 1.10. Plasma depicted as the fourth state of matter [57].

1.6 Role of Plasma in FEL

Plasma is a nonlinear medium which is dispersive and is capable of withstanding high field strengths. Plasma introduced in the presence of an external magnetic field offers the reduction in the energy of the beam by slowing down of the radiation phase velocity. The introduction of highly magnetized plasma offers neutralization

of charge and current which makes it to sustain high beam currents [58, 59]. The plasma medium promotes the bunching of the beam and leads to the generation of high power radiation when the frequency of the radiation wave and the plasma frequency becomes comparable. Plasma background provides drift to the electron motion in the transverse direction which results in better guiding of the radiation wave [60]. Rippled density plasma acts as a slow wave structure which supports the excitation of radiation wave by satisfying the phase matching condition. Plasma frequency also contributes to the tunability of FEL. Therefore, the FEL with shorter wavelength and high power can be operated by introducing background plasma.

Plasma being affluent in the wave phenomena supports plasma waves to play a role of wiggler in FEL. High frequency plasma waves can be employed as short wavelength wigglers in FEL. The electrostatic plasma waves that are used as wigglers includes Langmuir wave [61, 62], Upper hybrid wave [63, 64], Lower hybrid wave [65], and Ion Acoustic wave [66, 67].

Langmuir wave is an electron plasma wave which is due to the oscillations of the electrons around their equilibrium points oscillating at characteristic electron plasma frequency. This is due to the plasma characteristic to maintain charge neutrality under equilibrium over a large scale [68]. The oscillations poses high frequency. For the Langmuir wave as a wiggler, the medium should be either unmagnetized or the magnetic field should be in the axial direction. Upper hybrid wave is due to electron oscillation in magnetized plasma with the magnetic field in the direction perpendicular to the beam propagation. Surface plasma wave (SPW) is an electromagnetic wave that propagates at the interface between two media e.g., plasma and dielectric material or vacuum with phase velocity nearly equal to the speed of light. The amplitude of the wave shows an exponential decay on moving away from the interface. The SPW can be driven by the parallel propagating electron beam as the phase velocity of the wave is less than velocity of light.

1.7 Cerenkov Free Electron Laser (CFEL)

It is a slow wave FEL that reduces the velocity of the electromagnetic radiation wave below the speed of light so that it becomes comparable to the electron beam. The wave is slowed down by introducing a dielectric medium in the waveguide. The waveguide can be either filled completely with the dielectric or it is filled near the boundaries. The electric field of the electromagnetic wave is taken to be in the longitudinal direction (transverse magnetic mode) such that the beam travelling in the axial direction is retarded and transfers its energy to the transverse magnetic (TM) mode until the velocity of the beam reduces and becomes equivalent to the phase velocity of the radiation wave. The electron beam can be confined in close proximity to the dielectric material by applying an external magnetic field so that it interacts effectively with the EM mode.

If the phase velocity of wave and the beam velocity becomes comparable then, equal number of electrons are present in the positive and the negative cycle of the field of the wave. Therefore, in order to attain higher growth, the phase velocity of the wave should be slightly less than the velocity of the electron beam such that more electrons are present in the retarding phase to form bunches and transfer their energy to the wave [69]. Several TM modes can be supported by the waveguide leading to discrete frequencies. The modes having fields with phase velocity smaller than the light velocity lies in the dielectric medium and falls off swiftly on moving away from the medium. The decay of the wave increases with the increase in mode number.

1.8 Propagation of REB in Plasma

The following Maxwell's equations can be employed to study the propagation of a REB or an EM wave:

$$\nabla.\vec{E} = \frac{\rho}{\varepsilon_0}, \tag{1.3}$$

$$\nabla.\vec{B} = 0, \tag{1.4}$$

$$\nabla \times \vec{E} = -\frac{\partial \vec{B}}{\partial t}, \tag{1.5}$$

$$\nabla \times \vec{B} = \mu_0 \varepsilon_0 \frac{\partial \vec{E}}{\partial t} + \mu_0 \vec{J}, \tag{1.6}$$

where μ_0, ε_0 are the permeability and permittivity of the vacuum, respectively. E, B denotes the electric and magnetic fields, respectively that can be written in terms of scalar potential ϕ and vector potential A as:

$$\vec{E} = -\nabla\phi - \frac{\partial \vec{A}}{\partial t}, \tag{1.7}$$

$$\vec{B} = \nabla \times \vec{A}. \tag{1.8}$$

The wave equation for the radiation wave can be obtained by taking the curl of Eq. (1.5) and then using it in Eq. (1.6)

$$\nabla^2 \vec{E} - \nabla\left(\nabla.\vec{E}\right) + \frac{\omega^2}{c^2}\varepsilon_p \vec{E} = \frac{4\pi i\omega}{c^2}\vec{J}, \tag{1.9}$$

where $\varepsilon_p \left(= 1 - \frac{\omega_p^2}{\omega^2} \right)$ is the dielectric constant for the plasma medium and ω, ω_p are the frequency of the electron beam and the plasma, respectively.

The dynamical character of plasma medium is directed by the interaction of electron beam with the particles of the plasma. Various approaches such as single and two fluid theory, kinetic theory have been followed for describing the plasma theoretically.

The fluid theory describes the bulk characteristics of the medium. Statistical approach has been preferred as it becomes very complicated to take response of each individual particle. The electric and magnetic field for the plasma state are determined by the Maxwell's equation. The response of plasma to the fields can be examined by the fluid approximation.

The dynamics of single particle is described by the equation of motion and for the conservation of charge, equation of continuity is employed as:

$$m_k\left(\frac{\partial\vec{v_k}}{\partial t}+\left(\vec{v_k}.\nabla\right)\vec{v_k}\right)=q_k\left(\vec{E}+\vec{v_k}\times\vec{B}\right), \tag{1.10}$$

$$\frac{\partial n_k}{\partial t}+\nabla.\left(n_k\vec{v_k}\right)=0, \tag{1.11}$$

where n_k, m_k, q_k and v_k denotes the number density, mass, charge and velocity of the kth species ($k=e,\ i$ for electrons and ions, respectively), respectively. Further, the set of Maxwell's equation is also employed along with the equation of motion and equation of continuity for complete description of the system.

1.9 Ponderomotive Force

Ponderomotive force is a nonlinear force that is exerted on the charged particles due to the non-uniform oscillating fields of the high intensity electromagnetic waves. The distribution of the density of plasma electrons can be affected by the ponderomotive force which helps in describing the plasma acceleration analytically [70].

The electron motion in the presence of electric (E) and magnetic (B) field can be described by using linearized equation of motion as

$$\frac{dp}{dt} = m_e\left[\frac{\partial \vec{v}}{\partial t} + \left(\vec{v}.\nabla\right)\vec{v}\right] = -e\left(\vec{E} + \frac{1}{c}\vec{v}\times\vec{B}\right) \tag{1.12}$$

The electric field of an electromagnetic wave is considered as $E = A_0 \exp\left[-i\left(\omega t - kz\right)\right]$, where A_0 is the field amplitude of the wave, $\left(\omega,\ k\right)$ is the electromagnetic wave frequency and wave number, respectively. The electrons acquire an oscillatory velocity $\left(v_0\right)$ given as $v_0 = \frac{eE}{im_e\omega}$.

The electrons of the plasma medium experience a ponderomotive force $\left(\overrightarrow{F_p}\right)$ given as $\overrightarrow{F_p} = -e\nabla\phi_p$, where ϕ_p is the potential of the ponderomotive wave which can be expressed as $\phi_p = -\frac{e^2}{4m_e\omega^2}|E|^2$. The electrons are treated as fluids and their outcome to square of the electric field is computed.

The ponderomotive potential leads to the acceleration or deceleration of the beam electrons which contributes to the bunching of the electron beam and therefore drives the output radiation wave.

1.10 Electron Beam Prebunching

Prebunched electron beams refers to the formation of electron bunches of the relativistic electron beam prior to the interaction of beam with the wiggler and the electromagnetic wave. For the density modulation of the electron beam such that the current pulses are shorter than the wavelength of the radiation wave before interacting with the wiggler, the beam electrons radiate in phase which results in coherent emission of the radiation at the frequency of the bunched beam [71, 72].

The beam electrons gets accelerated or decelerated due to the nonlinear ponderomotive force exerted by the electromagnetic wave and the wiggler wave on the beam

electrons which results in the velocity or energy modulation of the beam. If the velocity modulated beam travels through the drift space, then the fast and slow moving electrons catch each other resulting in the formation of electron bunches. This leads to the density bunching of the electron beam.

The prebunched beams helps in the reduction of the size of the free electron laser with enhancement in the performance [73]. Several devices employed for the prebunching of the electron beam includes klystron, travelling wave tube, gyrotrons [74-76]. The working of klystron is based on the principle of modulation of velocity and density which can be explained using two cavity klystron as follows. The electrons are ejected from cathode which move with uniform velocities. On passing through the first cavity that acts as a buncher cavity, the electrons in the positive half cycle of the rf speeds up, those traveling through the negative half cycle slows down and those moving through the zero voltage passes with unaltered velocities. As a consequence on leaving the buncher cavity, all the electrons attains a common velocity which results in velocity modulation of the beam electrons which further on travelling through the drift region results in the formation of bunches leading to density or current modulation.

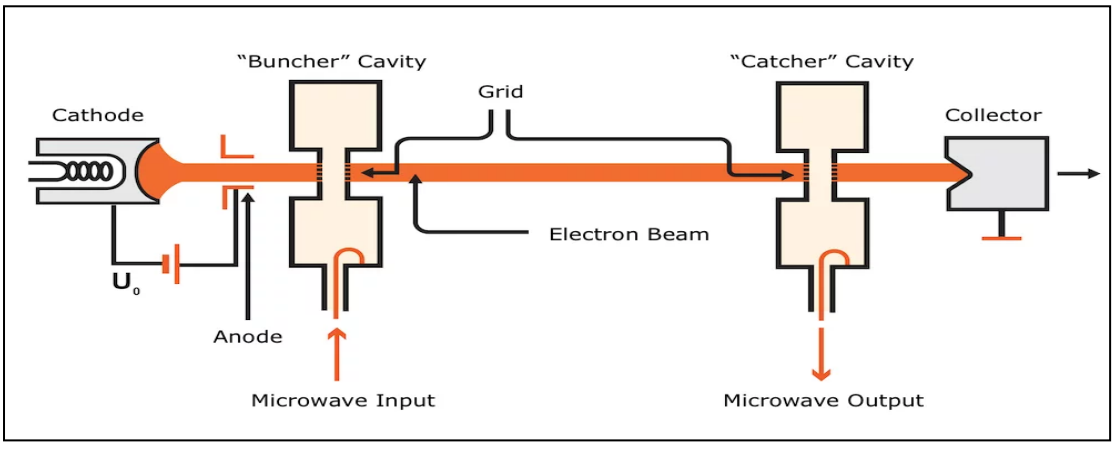

Fig. 1.11. Two cavity klystron representation [77].

The length of the drift space is decided such that bunching occurs optimum at the catcher cavity. For efficient bunching process, the phase of the voltage across the

catcher cavity should be such that the electrons passing through that cavity experience retardation so that maximum energy transfer from the electrons to the field of the cavity takes place [78].

1.11 Cerenkov Radiation

The EM radiation that is emitted when the electrons travels with energy greater than the phase velocity of the wave in the medium (i.e., the refractive index of the medium is greater than unity) is termed as the Cerenkov radiation. The condition for the Cerenkov resonance is fulfilled when the amplification of the radiation wave saturates and the reduced velocity of the electrons become comparable to the phase velocity of the radiation wave.

When the electrons experience drift, then the condition satisfying the conservation of energy and momentum for the generation of radiation determines the electrons to be in resonance with the ponderomotive force, which arises due to the electromagnetic wave and the field of the wiggler wave.

1.12 Growth of the EM Wave

When the electromagnetic wave interacts with the electron beam, the wave extracts the energy from the beam electrons thus leading to instability. The instability caused results in growth of the amplitude of the wave which is defined as the growth rate of the radiation wave. The instability saturates at a point when the beam reduces energy to an extent such that the velocity of the beam becomes equal to the phase velocity of the electromagnetic radiation wave. The growth rate is maximized if the condition of resonance interaction is satisfied. The efficiency of the process can thus be defined as the fraction of loss of electron energy to the initial energy of the electrons and can be evaluated from the growth rate of the radiation wave.

1.13 Terahertz Applications

1.13.1 Biomedical Imaging

This is an invasive technique due to low photon energy of THz radiation. THz imaging helps in obtaining spectroscopic images with phase sensitivity and thus, holds importance for identification of materials and functional imaging [79]. As the rotational and vibrational transition energies of components of tissue falls in the terahertz frequency range, the rich spectral fingerprints of the tissue are recognized. The complete THz band is absorbed strongly by the water or any other polar liquid which limits the radiation to penetrate through the tissues with large moisture content. The radiation has proved to be an efficient tool for diagnosing cancer. The images of the tissues and cells with variation in optical properties including the water content, increase in cell and protein density helps in detecting cancer.

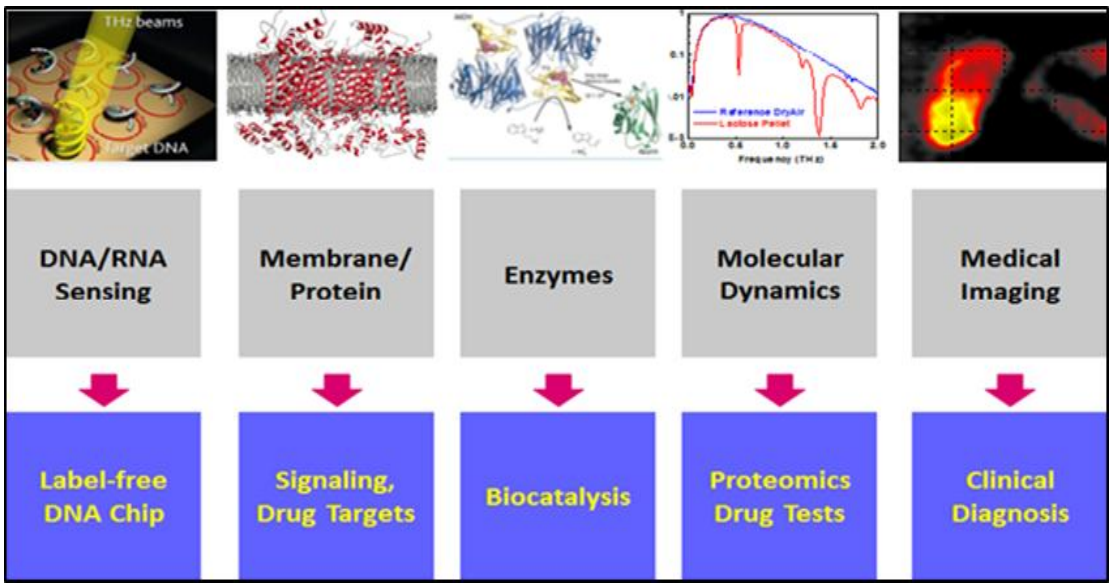

Fig 1.12. Representation of THz usage in biomedical science [80].

THz imagining helps in analysing the extent and depth of burn due to accumulation of fluid and swelling around the wound in burn injuries [81]. It also finds potentiality in dentistry by early detection of caries by obtaining the 3-D image obtained due to reflection through dielectric layers in the tooth [82-85].

1.13.2 Telecommunications

The shorter wavelength of the THz radiation allows the transmission of data at higher bandwidth. The signal provided is more focused which decreases the consumption of power at the mobile towers and therefore enhances the efficiency [86]. The wireless transmission of data with 20 times greater data rate than commonly used wi-fi was first reported in 2012 [87].

It also shows potentiality in communication at high altitudes where low absorption due to water vapor occurs including inter satellite communication and aircraft to satellite communication [88].

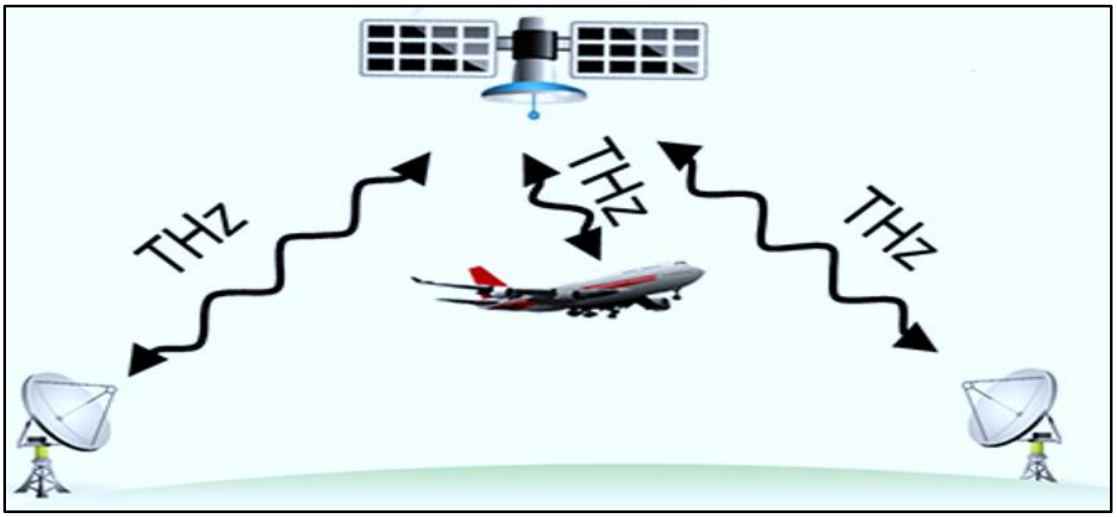

Fig 1.13. Use of THz radiation in communication [89].

1.13.3 Security Analysis

The THz radiation can be used to detect the hidden weapons and other explosives as the radiation is non-ionizing and can penetrate through plastics and fabrics while the privacy of the body is avoided [90]. Metallic substances such as sharp knife, gun etc. exhibit high reflective property at the THz frequency because of high electrical conductivity. The radiation thus holds importance in security checks and defense.

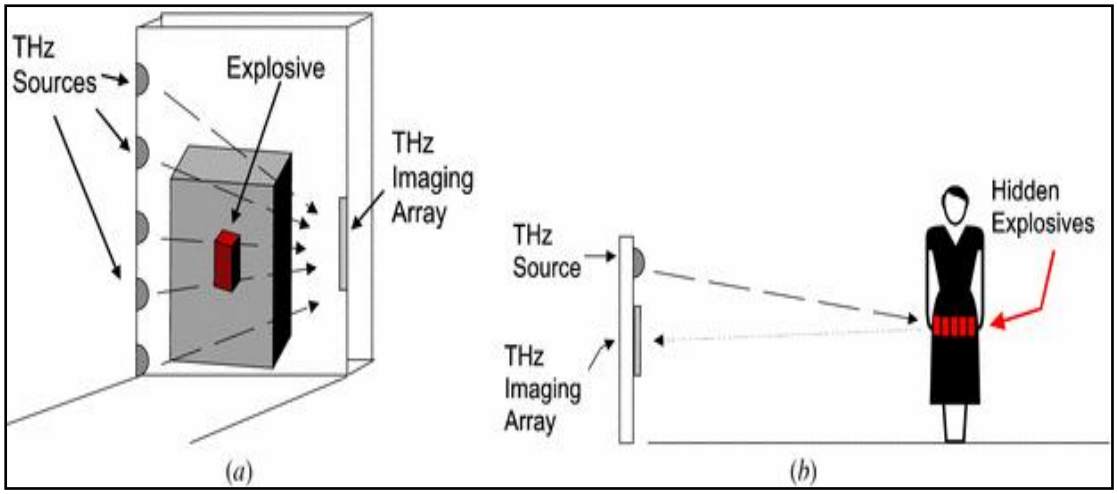

Fig 1.14. Illustration of THz radiation in security analysis [91].

1.13.4 Quality Check

The radiation holds potentiality in the food industry and used for checking the quality of sealed and packed foods by sensing the materials of low density [92]. The radiation being sensitive to water can be used for detecting the moisture content of dried food products. The THz has been reported to account for determining the thickness and moisture control of leather and therefore can be used for tanning process in industries [93].

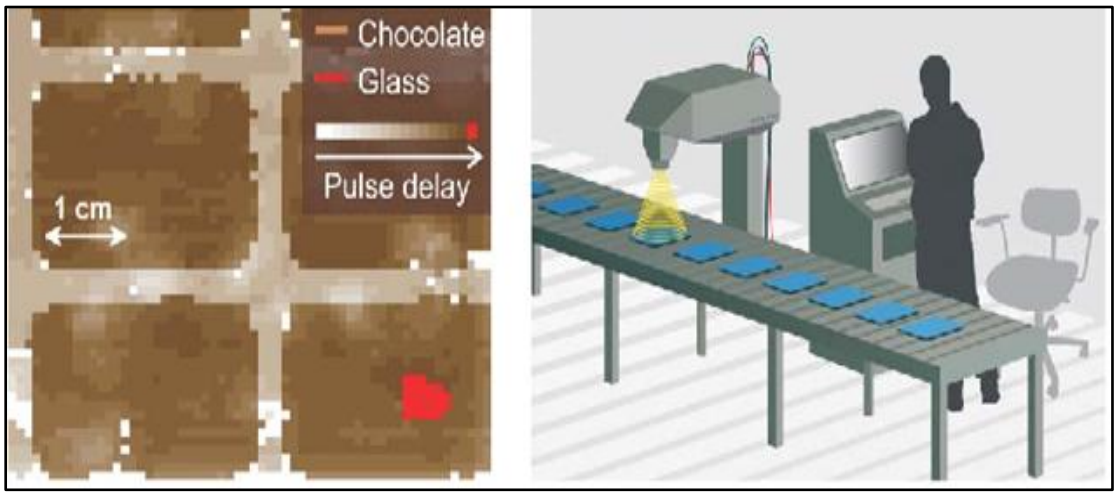

Fig 1.15. Representation of a chocolate bar THz image with buried glass splinter and future inspection system using THz, respectively [94].

1.13.5 Imaging and Material Characterization

This application includes the analysis of the structural image of the material along with spectroscopic study and identification. The energy of the photons of THz radiations is comparable to the energy range of the transitions between molecular energy levels which provides the spectroscopic fingerprint of the material. It helps in determining the mobility and concentration of carriers in semiconductors [95, 96]. THz spectroscopy also contributes in the study of parameters of superconducting thin films like energy gap and magnetic penetration intensity.

Fig 1.16. Demonstrating from left to right: Image of Goya's painting, The Sacrifice to Vesta; 50% THz view; 100% THz view, respectively of the painting [97].

1.14 Outline of Thesis

The motivation behind the thesis is to examine the emission of high power THz radiation using FEL by employing different plasma based wigglers for the sake of interaction with the REB. Our work mainly focuses to study the outcome of the THz radiation by using analytical treatment. For the numerical calculations of results the tools used are MATLAB and MATHEMATICA.

Chapter 1: The chapter owes to the theoretical explanation of the magnificent region of the electromagnetic spectra i.e, THz radiation. The incentive lying behind the work carried out is discussed. The properties and features of the radiation that have fascinated this as a research area are well described. Various techniques that

have been employed to explore the THz frequency region have been elaborated. The significance of the role of plasma and prebunched electron beams in free electron lasers is mentioned. The applications of the THz radiation in different fields are also discussed.

Chapter 2: In this chapter, the emission of THz radiation is proposed by taking a premodulated REB and the Langmuir plasma pump wave interaction. Langmuir plasma wave is a high frequency electrostatic plasma wave that plays a significant role of wiggler. The premodulation of the REB is accounted by using two laser beams propagating obliquely. The Cerenkov resonance due to the REB interaction with the plasma medium drives the electrostatic plasma wave. The application of static magnetic field results in axial guiding of the beam and providing an electron cyclotron frequency for satisfying the resonance condition. The growth rate and efficiency of the radiation wave emission have been examined for both finite and infinite boundaries of the plasma occupied region. This analytical study could be useful for realizing the dimensions of the system to be preferred for achieving comparatively high efficiency.

Chapter 3: In this chapter, a waveguide with dielectric lined along its boundaries acts as a slow wave structure. This chapter incorporates a plasma filled waveguide with dielectric boundaries that supports a transverse magnetic (TM) mode as a pump wave. An externally applied magnetic field is considered for guiding the electron beam. The radiation emission occurs when laser premodulated REB interacts with the electromagnetic pump wave. The beam propagation is suggested to be in close proximity of the dielectric lining for maximum energy transfer to the wave. The study indicates that low energy beams helps in obtaining efficient growth rate of the radiation wave.

Chapter 4: In this chapter, the interaction of premodulatd REB with the surface plasma wave (SPW), propagating at the interface of vacuum-plasma for the generation of

THz radiation has been discussed in this chapter by taking an analytical model. The ponderomotive force exerted on the beam electrons by the laser beams accounts for the modulation of the REB which takes place prior to the interaction with the SPW. The SPW is excited by the REB and it acts as a wiggler wave. The outcome of the parameters of the electron beam and the wiggler has been realized on the power and amplitude of the radiation wave. This work may be useful in obtaining high frequency radiation by decreasing the period of the wiggler wave.

Chapter 5: In this chapter, the radiation generation is studied by using an electromagnetic pump wave interacting with two laser premodulated REB in the plasma slab in the presence of static magnetic field. The radiation power and amplitude are evaluated and the effect of beam and plasma parameters on the tunability of the output THz radiation is examined. The optimum power is found to be achieved at the condition of resonance due to the electron frequency and the pump wave.

Chapter 6: This chapter includes the surface plasma wave (SPW) to be driven to instability by density modulated REB. The modulation of the beam density is mentioned by assuming a modulation index which varies from zero to unity. The pondermotive force exerted by the SPW and the radiation wave on the beam electrons further enhances the beam bunching. The wave growth rate and the amplitude are found to be enhanced with the modulation index. Further, the requirement for the beam energy can be reduced by using plasma.

Chapter 7: The outcomes of the work carried out during the thesis work has been concluded in this chapter. In addition, the future perspective of the present work has also been given.

References

[1] https://www.livescience.com/38169-electromagnetism.

[2] http://photonicswiki.org.

[3] https://chem.libretexts.org.

[4] https://www.britannica.com/science/electromagnetic-radiation.

[5] C. O'Sullivan and J. A. Murphy, *Field Guide to Terahertz Sources, Detectors, and Optics* (Society of Photo-Optical Instrumentation Engineers (SPIE), 2012).

[6] https://www.ophiropt.com/blog/laser-measurement/laser-measurement-for-terahertz-thz-technology/.

[7] https://ru.wikinews.org.

[8] J. B. Khurgin, J. Opt. Soc. Am. B **11**, 2492-2501 (1994).

[9] G. L. Dakovski, B. Kubera, and J. Shan, J. Opt. Soc. Am. B **22**, 1667-1670 (2005).

[10] R. K. Singh, M. Singh, S. K. Rajouria, and R. P. Sharma, Phys. Plasmas **24**, 073114 (2017).

[11] Y. C. Shen, P. C. Upadhya, H. E. Beere, E. H. Linfield, A. G. Davies, I. S. Gregory, C. Baker, W. R. Tribe, and M. J. Evans, Appl. Phys. Lett. **85**, 164 (2004).

[12] J. Zhang, Y. Hong, S. L. Braunstein, and K. A. Shore, Optoelectronics, IEE Proceedings **151**, 98-101 (2004).

[13] I. Lepeshov, A. A. Gorodetsky, N. A. Toropov, T. A. Vartanyan, E. U. Rafailov, A. Krasnok, and P. A. Belov, IOP Conf. Series: Journal of Physics: Conf. Series **917**, 062060 (2017).

[14] P. Dean, A. Valavanis, J. Keeley, K. Bertling, Y. L. Lim, R. Alhathlool, A. D. Burnett, L. H. Li, S. P. Khanna, D. Indjin, T. Taimre, A. D. Rakic´, E. H. Linfield, and A. G. Davies, J. Phys. D: Appl. Phys. **47**, 374008 (2014).

[15] A. V. Ikonnikov, K. V. Marem'yanin, S. V. Morozov, V. I. Gavrilenko, A. Yu. Pavlov, N. V. Shchavruk, R. A. Khabibullin, R. R. Reznik, G. E. Cirlin, F. I. Zubov, A. E. Zhukov, Zh. I. Alferov, Tech. Phys. Lett. **43**, 362-365 (2017).

[16] T. M. Antonsen, J. Palastro, and H. M. Milchberg, Phys. Plasmas **14**, 033107 (2007).

[17] L. Yu-Tong, W. Wei-Min, L. Chun, and S. Zheng-Ming, Chin. Phys. B **21**, 095203 (2012).

[18] T. Ping, H. Jiang, L. K. Feng, X. Y. Qian, and F. M. Wu, Sci. China Inf. Sci. **55**, 1-15 (2012).

[19] M. Kumar and V. K. Tripathi, Phys. Plasmas **19**, 073109 (2012).

[20] F. Blanchard, G. Sharma, L. Razzari, X. Ropagnol, H. C. Bandulet, F. Vidal, IEEE Journal of Selected Topics in Quantum Electronics **17**, 5-16 (2011).

[21] Z. Wang, IEEE Transactions on Geoscience and Remote Sensing **1**, 1-5 (2005).

[22] S. V. Sazonov, JETP letters **96**, 263-274 (2012).

[23] K. H. Yang, P. L. Richards, and Y. R. Shen, Applied Physics Letters **19**, 320 (1971).

[24] http://photonicswiki.org.

[25] T. Chen, J. Sun, L. Li, and J. Tang, Journal of Lightwave Technology **30**, 2156-2162 (2012).

[26] Y. J. Ding, J. Opt. Soc. Am. B **31**, 2696-2711 (2014).

[27] Z. Li, S. Wang, M. Wang, and W. Wang, Optics and Laser Technology **96**, 65–69 (2017).

[28] http://www.photonics.phys.strath.ac.uk/nonlinear-photonics/thz-generation/.

[29] H. J. Song and T. Nagatsuma, *Handbook of Terahertz Technologies devices and applications* (Taylor & Francis Group, 2015).

[30] N. M. Burforda, and M. O. El-Shenaweeb, Optical Engineering **56**, 010901 (2017).

[31] J. H. Booske, R. J. Dobbs, C. D. Joye, C. L. Kory, G. R. Neil, Gun-Sik Park, J. Park, and R. J. Temkin, IEEE Transactions on Terahertz Science and Technology **1**, 54-75 (2011).

[32] https://www.tutorialspoint.com/microwave_engineering/microwave_ engineering_travelling_wave_tube.html.

[33] A. Rostami, H. Rasooli, and H. Baghban, *Terahertz Technology Fundamentals and Applications*, (Springer-Verlag Berlin Heidelberg, 2011).

[34] G. P. Gallerano, and S. Biedron, Proceedings of the FEL Conference, 216-221 (2004).

[35] https://en.wikipedia.org/wiki/Backward-wave_oscillator.

[36] A. Dobroiu, M. Yamashita, Y. N. Ohshima, Y. Morita,C. Otani, and K. Kawase, APPLIED OPTICS **43**, 5637- 5646 (2004).

[37] https://ireap.umd.edu/sites/default/files/documents/ruifengpu-ms.pdf.

[38] S. Bhattacharjee, J. H. Booske, C. L. Kory, D. W. van der Weide, S. Limbach, S. Gallagher, J. D. Welter, M. R. Lopez, R. M. Gilgenbach, R. L. Ives, M. E. Read, R. Divan, and D. C. Mancini, IEEE Transactions on Plasma Science **32**, 1002-1014 (2004).

[39] P. Gao and J. H. Booske, IEEE International Vacuum Electronics Conference (IVEC) (2011).

[40] E. L. Saldin, E. A. Schneidmiller, and M. V. Yurkov, *The Physics of Free Electron Lasers* (Springer-Verlag Berlin Heidelberg, 2000).

[41] H. P. Freund, and T. M. Antonsen Jr, *Principles of Free-electron Lasers* (Chapman and Hall, 1992).

[42] T. C. Marshall, *Free electron lasers* (Macmillan Publishing Company, 1985).

[43] H. P. Freund and P. Sprangle, Phys. Rev. A **24**, 1965-1979 (1981).

[44] N. S. Ginzburg and N. Yu. Peskov, Phys. Rev. ST Accel. Beams **16**, 090701 (2013).

[45] Z. Ouyang and Shi-Chang Zhang, Physics of Plasmas **22**, 043111 (2015).

[46] K. Tskayama and S. Hiramstsu, Phys. Rev. A **37**, 173-177 (1988).

[47] A. Hasanbeigi, H. Mehdian, and P. Gomar, Phys. Plasmas **22**, 123116 (2015).

[48] H. Kurino, K. Ebihara, S. Hiramatsu,Y. Kimura, J. Kishiro, T. M. Ka, T. Ozaki and K. Takayama, Particle Accelerators **31**, 89-95 (1990).

[49] S. Jafari, F. Jafarinia, and H. Mehdian, Laser Phys. **23**, 085005 (2013).

[50] P. Schmüser, M. Dohlus, and J. Rossbach, *Ultraviolet and Soft X-Ray Free-Electron Lasers: Introduction to Physical Principles, Experimental Results, Technological Challenges* (Springer, Berlin Heidelberg, 2008).

[51] https://www.astec.stfc.ac.uk/Pages/ALICE-free-electron-laser.aspx

[52] C. Joshi, T. Katsouleas, J. M. Dawson, Y. T. Yan, and J. M. Slater, IEEE J. of Quantum Electronics **23**, 1571-1577 (1987).

[53] P. M. Bellan, *Fundamentals of Plasma Physics* (Cambridge University Press, 2004).

[54] F. F. Chen, *Introduction to Plasma Physics* (Plenum Press, New York, 1974).

[55] https://science.nasa.gov.

[56] https://www.britannica.com.

[57] https://www.advancedplasmasolutions.com/what-is-plasma/

[58] C. S. Liu and V. K. Tripathi, *Interaction of electromagnetic waves with electron beams and plasmas* (World Scientific Publishing Co. Pte. Ltd., 1994).

[59] R. B. Miller, An Introduction to the Physics of Intense Charged Particle Beams (Plenum Press, New York, 1982).

[60] S. H. Zolghadr, S. Jafari, A. Raghavi, Phys. Plasmas **23**, 053104 (2016).

[61] Lalita, V. K. Tripathi, and P. C. Agarwal, IEEE Trans. on Plasma Science **19**, 9-11 (1991).

[62] J. Panwar, and S. C. Sharma, Phys. Plasmas **24**, 083101 (2017).

[63] S. C. Sharma and V. K. Tripathi, IEEE Trans. on Plasma Science **23**, 792-797 (1995).

[64] M. Singh, S. Kumar, and R. P. Sharma, Phys. Plasmas **18**, 022304 (2011).

[65] A. Sharma and V. K. Tripathi, Phys. Fluids B **2**, 2787 (1990).

[66] R. N. Agarwal and V. K. Tripath, IEEE Trans. on Plasma Science **23**, 788-791 (1995).

[67] Y. Tyagi, D.Tripathi, K. Walia, and D. Garg, Phys. Plasmas **25**, 043118 (2018).

[68] B. Ghosh, *Basic Plasma Physics* (Alpha Science International Ltd. Oxford, U.K., 2014).

[69] http://physics-help.blogspot.com/2006/01/cherenkov-free-electron-laser.html

[70] R. Lundin, and A. Guglielmi, Space Sci. Rev. **127**, 1-116 (2006).

[71] A. Doria, R. Bartolini, J. Feinstein, G. P. Gallerano, IEEE J. of Quantum Electronics **29**, 1428-1436 (1993).

[72] G. Dattoli, L. Giannessi, P.L. Ottaviani, A. Segreto, Nuclear Instruments and Methods in Physics Research A **393**, 339-342 (1997).

[73] R. H. Pantell, I. V. Konoplev, and A. D. R. Phelps, Phys. Plasmas **7**, 4280 (2000).

[74] A. L. Eichenbaum, A. Abramovich, M. Arbel, M. Cohen, L. Gilutin, A. Gover, H. Kleinman, Y. Pinhasi, S. Volkovich, I. M. Yakover, Nucl. Instr. and Meth. in Phys. Res. A **393**, 361-365 (1997).

[75] A. L. Eichenbaum, IEEE Trans. on Plasma Science **27**, 568-574 (1999).

[76] M. Shrader, D. Preist, and B. Gaiser, reprinted from IDEM meet (1985).

[77] https://www.allaboutcircuits.com/technical-articles/introduction-to-the-two-cavity-klystron-amplifier/

[78] S. Y. Liao, *Microwave Devices and Circuits* (Prentice Hall, Englewood Cliffs, New Jersey, 3rd edition).

[79] B. Ferguson and Xi-Cheng Zhang, Nature materials **1**, 26-33 (2002).

[80] http://phome.postech.ac.kr/.

[81] Yun-Shik Lee, *Principles of Terahertz Science and Technology* (Springer Science Business Media, LLC, 2009).

[82] K. Kamburoğlu and N. O. Yetimoĝlu, OMICS J. Radiology **3**, 1000e127 (2014).

[83] A. Rostami, H. Rasooli, and H. Baghban, *Terahertz Technology Fundamentals and Applications* (Springer-Verlag Berlin Heidelberg, 2011).

[84] X. Yang, X. Zhao, K. Yang, Y. Liu, Y. Liu, W. Fu, and Y. Luo, Trends in Biotechnology **34**, 810-824 (2016).

[85] A. J. Fitzgerald, E. Berry, N. N. Zinovev, G. C. Walker, M. A. Smith, and J. M. Chamberlain, Phys. Med. Biol. **47**, R67–R84 (2002).

[86] S. Atakaramians, I. V. Shadrivov, A. E. Miroshnichenko, A. Stefani, H. E. Heidepriem, T. M. Monro, and V. S. Afshar, APL Photonics **3**, 051701 (2018).

[87] https://www.bbc.com/news/science-environment-18072618

[88] https://en.wikipedia.org/wiki/Terahertz_radiation

[89] https://www.zdnet.com/article/superfast-broadband-everywhere-terahertz-breakthrough-could-make-satellite-as-fast-as-fiber/

[90] https://www.i4u.com/19200/thruvision-t5000-t-ray-camera-sees-through-clothes.

[91] J. F. Federici, B. Schulkin, F. Huang, D. Gary, R. Barat, F. Oliveira, and D. Zimdars, Semicond. Sci. Technol. **20**, S266–S280 (2005).

[92] G. Ok, K. Park, H. J. Kim, H. S. Chun, and Sung-Wook Choi, Applied Optics **53**, 1406-1412 (2014).

[93] A. I. Hernandez-Serrano, S. C. Corzo-Garcia, E. Garcia-Sanchez, M. Alfaro, and E. Castro-Camus, Applied Optics **53**, 7872-7876 (2014).

[94] M. Tonouchi, Nat. Photonics **1**, 97–105 (2007).

[95] A. J. Huber, F. Keilmann, J. Wittborn, J. Aizpurua, and R. Hillenbrand, Nano Lett., **8**, 3766-3770 (2008).

[96] M. C. Hoffmann and J. A. Fülöp, J. Phys. D: Appl. Phys. **44**, 083001(2011).

[97] https://ideas.ted.com/is-the-world-ready-for-t-rays/.

Chapter 2

MODELING OF TERAHERTZ RADIATION EMISSION FROM A FREE ELECTRON LASER

2.1 Brief Outline of the Chapter

The formalism for the emission of high power radiation, using a relativistic electron beam pre-bunched by the two laser beams has been developed. A pre-bunched electron beam interacts with the Surface Plasma Wave (SPW), which is acting as wiggler counter-propagating to the surface wave in the vacuum region and Compton backscatters the surface wave into a high frequency terahertz (THz) radiation. The oscillatory velocity due to the wiggler couples with the laser modulated beam density which gives rise to non-linear current density that acts as an antenna to produce coherent THz radiation. This non-linear current density helps in evaluating the normalized power and field amplitude of the generated THz wave. The normalized power of the THz wave scales as the square of the electron beam current, electron bunch length and fourth power of the electron bunch radius. It is observed that the normalized field amplitude of the THz wave increases with the beam currents. In addition, the short wavelength THz radiation can be generated by reducing the wiggler period in the present scheme.

2.2 Introduction

The emission of radiation from Free Electron Laser (FEL) using pre-bunched electron beam has been a field of interest for several years [1-9] due to its potential applications in diverse areas including spectroscopy, medicine, security, and defense [10-13]. Prebunching of the beam leads to coherent emission of the radiation with enhanced power and efficiency [14-19].

The pre-bunching of the electron beam at the photocathode by using a drive laser as a THz switch was studied experimentally by Neuman *et al.* [1]. They observed that the modulation can be affected by the longitudinal space charge forces and tuned either by changing the initial profile of the drive laser or by changing the phase while entering in the accelerator.

FEL is employed as an efficient source for the generation of the THz radiation due to its wide tunability and high power. The output radiation can be tuned by varying the parameters of the electron beam and wiggler. Freund and O'Shea [2] demonstrated the incorporation of a pre-bunched electron beam model into a three-dimensional, polychromatic FEL simulation code MEDUSA and observed that the pre-bunched beams have substantial advantages on FEL operation and permit higher saturated powers for density modulated beams, shorter saturation lengths and rapid start-up from noise.

The possibility of pre-bunching using free electron laser with two parallel, relativistic electron streams in a static, magnetic wiggler was studied by Bekefi and Jacobs [3]. In this case, they observed that the tuning of the beam velocities lead to the resonant enhancement of the output radiation intensity. The amplitude of the radiation is affected by the two stream instability while the growth rate of the instability remains unaffected. Leemans *et al.* [14] have examined experimentally and theoretically the coherent THz emission by the relativistic electron beams (REB), pre-bunched by a laser at the vacuum-plasma interface. The emitted radiation

at the interface scales quadratically with charge for long wavelengths compared to the bunch length and the source performance, therefore, increases by maximizing the amount of charge. The experimentally measured energy fraction in the ranges 0.3-2.9 THz and 2.9-19 THz was 22% and 78%, respectively and this depends on the transverse plasma profile and bunch length.

Bhasin and Tripathi [20] have studied the generation of THz radiation by using an amplitude modulated surface plasma wave over a rippled metal free space interface. They observed that the efficiency of the THz power generation increases due to weak linear damping.

The effect of a pre-bunched REB propagating through a parallel plane guiding system on the excitation of THz plasmons was studied by Sharma and Malik [21]. They observed that the amplitude and efficiency of the unstable mode of the SPW show considerable enhancement with the modulation index and attain maximum values when the phase velocity of the THz radiation wave is comparable to the electron beam velocity. Sharma *et al.* [22] examined the growth rate and efficiency of the radiation by employing an interaction of an energy modulated electron beam with the surface plasma wave as wiggler at vacuum plasma interface. They observed that the phase velocity of the radiation can be reduced by plasma which helps in the decrease of beam energy required for generating the radiation.

Kumar *et al.* [23] explored the role of a self-generated plasma wave in enhancing the efficiency of the excitation of THz radiation by beating two laser beams in a hot plasma with a step density profile and observed that the THz power increases with the angle of incidence up to an optimum value but vanishes at normal laser incidence. Malik *et al.* [24] employed the superposition of laser fields for the emission of THz radiation of high power and observed that the frequency of the output radiation can be tuned by the size of the plasma that is created by the tunnel ionization of the gas, and the directionality can be controlled by the initial phase

difference between the two lasers. Singh *et al.* [25] studied the excitation of SPW by using a laser incident obliquely on the free space interface and observed that the power of the output radiation can be increased monotonically by increasing the frequencies of the laser and the SPW field.

Xiang and Stupakov [26] proposed a method for the generation of an intense, tunable narrow-band THz radiation through laser–electron interactions and observed that the central frequency of the radiation can be tuned by varying the wavelength of the two lasers and the energy of the electron beam. Malik *et al.* [27] proposed the generation of THz radiation by using two co-propagating lasers with Gaussian profile in a spatially periodic plasma in the presence of a transverse static magnetic field and observed that the frequency of the emitted radiation can be tuned by optimizing the magnetic field, amplitude, and periodicity of the density ripples. Sheng *et al.* [28] found, using the PIC simulations and model calculations, that the emission frequency, bandwidth, and pulse duration of the powerful THz radiation emitted using laser wakefield acceleration can be controlled by the laser pulse duration and plasma density profiles.

In this chapter, we study the emission of high power terahertz radiations when a relativistic electron beam (REB), pre-bunched by the two laser beams in the modulator and then travelling in the drift space, interacts with a surface plasma wave (SPW) which is acting as wiggler. The mechanism of the process is as follows: The two laser beams with frequency difference in the range of THz wave exert a pondermotive force on the electron beam, which leads to velocity modulation in the modulator. This velocity modulation translates into density modulation as the beam travels in the drift space, which gives a pre-bunched electron beam. This pre-bunched beam interacts with surface plasma wave as wiggler, in which the oscillatory velocity due to wiggler couples to the modulated beam density, giving rise to the non-linear current density at $\left(\omega_1^{'},\ \overrightarrow{k_1^{'}}\right)$, where $\omega_1^{'} = \omega' + \omega_0$ and $\overrightarrow{k_1^{'}} = \overrightarrow{k'} + \overrightarrow{k_0}$, ω' and k' are the

beat wave frequency and wave vector of the ponderomotive force on the beam of electrons, ω_0 and k_0 are the wiggler frequency and wave vector of SPW, respectively which leads to the emission of high power THz radiation. A surface plasma wave (SPW) is the wave that propagates at the interface between the two medium. The excitation of the SPW is studied in Sec. 2.3. In Sec. 2.4, we study the pre-bunching of the electron beam using two laser beams. In Sec. 2.5, we discuss the interaction of the density modulated electron beam, generated in the drift space with the SPW which is acting as wiggler. In Sec. 2.6, we have analyzed the results obtained and the conclusion part is given in Sec. 2.7.

2.3 SPW Excitation and Dispersion Relation

Following Prakash and Sharma [29], we consider a vacuum-plasma interface at $x=0$. The plasma occupies half of the space $x<0$ with permittivity $\varepsilon' = 1-\frac{\omega_{pe}^2}{\omega_0^2}$, where $\omega_{pe}\left(=\left(\frac{4\pi n_p e^2}{m_e}\right)^{1/2}\right)$ is the electron plasma frequency, n_p is the plasma density, m_e is the mass of electron and e is the electronic charge.

The vacuum of permittivity unity lies in $x>0$. A relativistic electron beam (REB) of velocity $v_b^0 z$, density n_b^0 and radius r_b is launched into the plasma. The electric field associated with the SPW is given by

$$\vec{E} = \overrightarrow{E_0} e^{-i(\omega_0 t - k_0 z)}, \tag{2.1}$$

where ω_0 and $\overrightarrow{k_0}$ are the frequency and wave vector of the SPW, respectively and $\overrightarrow{E_0}$ is the electric field amplitude of the SPW. We consider electric field to be polarised in the x-z plane.

The response of REB to the field of the SPW can be obtained by solving the equation of motion

$$\frac{\partial\left(\gamma_0\vec{v}\right)}{\partial t}+\left(\vec{v}.\nabla\right)\left(\gamma_0\vec{v}\right)=-\frac{e\vec{E}}{m_e}, \tag{2.2}$$

where $\vec{v}=v_b^0\hat{z}+\vec{v_0}$, $\vec{v_0}$ is the oscillatory velocity of the REB due to the SPW and $\gamma_0\left(=\frac{1}{\sqrt{1-\frac{v_b^{02}}{c^2}}}\right)$ is the relativistic gamma factor, c is the speed of light.

The oscillatory electron velocity in $x-$ and $z-$ directions after linearization of Eq. (2.2) are obtained as

$$v_{0x}=\frac{eE_{0x}e^{-i(\omega_0 t-k_0 z)}}{im_e\gamma_0^3(\omega_0-k_0v_b^0)}, \tag{2.3}$$

$$v_{0z}=\frac{eE_{0z}e^{-i(\omega_0 t-k_0 z)}}{im_e\gamma_0^3(\omega_0-k_0v_b^0)}, \tag{2.4}$$

where E_{0x} and E_{0z} are the electric field amplitude in $x-$ and $z-$ directions, respectively.

The perturbed beam density, n_{1b} due to the SPW can be obtained from the equation of continuity $\frac{\partial n}{\partial t}+\nabla.(n\vec{v})=0$, where $n=n_b^0+n_{1b}$.

$$n_{1b}=\frac{n_b^0e}{m_e\gamma_0^3}\left[\frac{k_IE_{0x}}{(\omega_0-k_0v_b^0)^2}-\frac{ik_0E_{0z}}{(\omega_0-k_0v_b^0)^2}\right], \tag{2.5}$$

where $k_I = \left(k_0^2 - \frac{\omega_0^2}{c^2}\right)^{1/2}$.

The perturbed current density is

$$\vec{J_1} = -e(n_b^0 \vec{v_0} + n_{1b} v_{b\,z}^0).$$

The perturbed current density in z - direction by taking only those terms which varies as $(\omega_0 - k_0 v_b^0)^{-2}$ is given as

$$J_{1z} = -\frac{e^2 v_b^0 n_b^0}{m_e \gamma_0^3}\left[\frac{k_I E_{0x}}{(\omega_0 - k_0 v_b^0)^2} - \frac{ik_0 E_{0z}}{(\omega_0 - k_0 v_b^0)^2}\right]. \tag{2.6}$$

Using the above value in the z - component of the wave equation

$\nabla^2 \vec{E} - \nabla(\nabla.\vec{E}) + \frac{\omega_0^2}{c^2}\vec{E} = -\frac{4\pi i \omega_0}{c^2}\vec{J}$, we obtain

$$\left(k_I^2 - k_0^2 + \frac{\omega_0^2}{c^2}\right)E_{0z} = -\frac{\omega_0 v_b^0 \omega_{pb}^2 k_0 E_{0z}}{c^2(\omega_0 - k_0 v_b^0)^2}, \tag{2.7}$$

where $\omega_{pb}^2 = \frac{4\pi n_b^0 e^2}{m_e}$ is the beam frequency.

On multiplying by E_{0z}^* and integrating from $x = 0$ to $x = \infty$, and taking $\int_0^\infty E_{0z} E_{0z}^* dx = 1$, Eq. (2.7) can be re-written as

$$\omega_0^4 - k_0^2 c^2\left(\frac{\varepsilon'+1}{\varepsilon'}\right)\omega_0^2 = \frac{\omega_{pb}^2 k_0 \omega_0^3 v_b^0\left(\frac{\varepsilon'+1}{\varepsilon'}\right)}{(\omega_0 - k_0 v_b^0)^2} \tag{2.8}$$

In the absence of the REB i.e., $\omega_{pb}^2 = 0,$ the standard dispersion relation for SPW$_s$ [31] can be obtained from Eq. (2.8) as

$$\omega_0^2\left(\frac{\varepsilon'}{\varepsilon'+1}\right) = k_0^2 c^2. \tag{2.9}$$

This dispersion relation is used for further calculations in Sec. IV. Eq. (2.8) can be rewritten as

$$\left(\omega_0^2 - \alpha_1^2\right)\left(\omega_0 - k_0 v_b^0\right)^2 = \omega_{pb}^2 k_0 \omega_0 v_b^0\left(\frac{\varepsilon'+1}{\varepsilon'}\right), \tag{2.10}$$

where $\alpha_1 = k_0 c\left(\frac{\varepsilon'+1}{\varepsilon'}\right)^{1/2}$

In the absence of beam, $\omega_{pb}^2 = 0$. On equating the factors of left hand side to zero, we obtain, $\omega_0 \sim \alpha_1$ as the SPW mode and $\omega_0 \sim k_0 v_b^0$ as the beam mode.

To solve Eq. (2.10) in the presence of beam, we assume that $\omega_0 = \alpha_1 + \delta$ $= k_0 v_b^0 + \delta$, where δ is the small frequency mismatch.

$$\delta = \left[\frac{\omega_{pb}^2 k_0 v_b^0}{2}\left(\frac{\varepsilon'+1}{\varepsilon'}\right)\right]^{1/3} e^{i\frac{2n\pi}{3}},$$

For n=1, Growth rate Γ, defined as the imaginary part of small frequency mismatch δ, given as

$$\Gamma = \mathrm{Im}\,\delta = \left[\frac{\omega_{pb}^2 k_0 v_b^0}{2}\left(\frac{\varepsilon'+1}{\varepsilon'}\right)\right]^{1/3} \frac{\sqrt{3}}{2}$$

From the equation of motion,

$$\frac{d^2z}{dt^2} \simeq -\frac{eE_z}{\gamma_0 m_e} \simeq -\frac{eE_{0z}}{m_e\gamma_0} e^{-k_I x} \cos(\omega_0 t - k_0 z),$$

where E_{0z} is the amplitude of the SPW. The above equation can be further written as

$$\frac{d^2z}{dt^2} \simeq -\frac{eE_{0z}}{m_e\gamma_0} e^{-k_0 z} = -\omega_b^2 z,$$

where $\omega_b = \left(\frac{eE_{0z}k_0}{m_e\gamma_0}\right)^{1/2}$ is the bounce frequency of electrons and the growth rate can be simplified to

$$\Gamma = \omega_b = \left(\frac{eE_{0z}k_0}{m_e\gamma_0}\right)^{1/2}.$$

Therefore, the amplitude of SPW=

$$\frac{\Gamma^2 m_e\gamma_0}{ek_0} = \frac{3m_e\gamma_0}{4ek_0}\left[\frac{\omega_{pb}^2 k_0 v_b^0}{2}\left(\frac{\varepsilon'+1}{\varepsilon'}\right)\right]^{2/3} \tag{2.11}$$

From Eq. (2.11) it can be seen that the amplitude of the SPW is a function of known parameters i.e., electron beam velocity, beam density and plasma density.

2.4 Beam Prebunching using Two Laser Beams

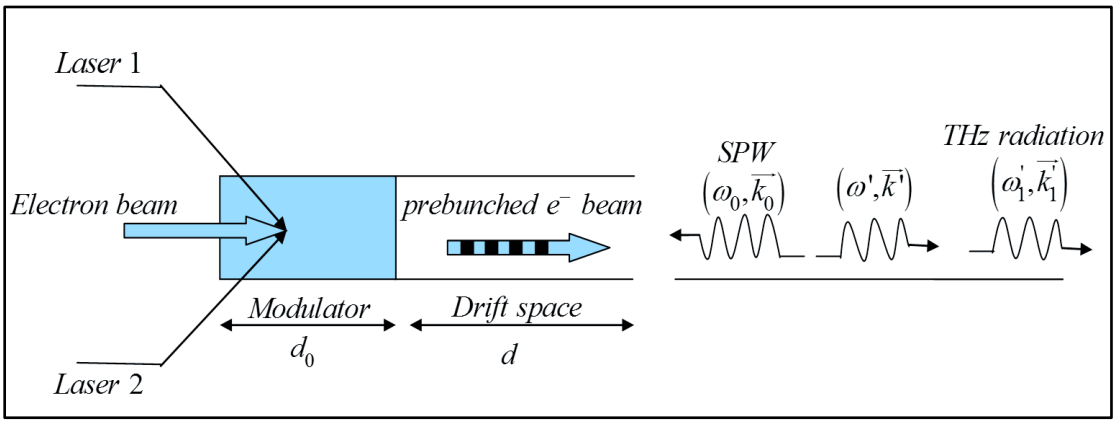

Fig 2.1. Schematic diagram showing the pre-bunching of the electron beam and its coupling with the Surface Plasma Wave (SPW) as wiggler.

Following the treatment of Kumar and Tripathi [7], the two laser beams with frequencies ω_1 and ω_2 , such that $\omega'(=\omega_1-\omega_2)$, interact with the relativistic electron beam (REB) of velocity $v_b^0\hat{z}$, density n_b^0 and cross-section a_b in the modulator. The electric fields for the two laser beams are given by

$$\vec{E_1} = \vec{a_1} e^{-i(\omega_1 t - k_1 z)}. \tag{2.12}$$

$$\vec{E_2} = \vec{a_2} e^{-i(\omega_2 t - k_2 z)}. \tag{2.13}$$

The lasers exert a ponderomotive force at (ω', k') on the beam electrons in the modulator region of width d_0.

$$\vec{F_p}(\omega', k') = -\frac{e}{2c}(\vec{v_1} \times \vec{B_2^*} + \vec{v_2^*} \times \vec{B_1}), \tag{2.14}$$

where $\vec{v_1} = \frac{e\vec{E_1}}{im_e\omega_1\gamma_0}$, $\vec{v_2} = \frac{e\vec{E_2}}{im_e\omega_2\gamma_0}$ are the oscillatory velocities of the electron beam.

Using the above values, Equation (2.14) can be simplified to

$$\overrightarrow{F_p} = \frac{e^2 k' a_1 a_2^*}{2 i m_e \gamma_0 \omega_1 \omega_2} e^{-i(\omega' t - k' z)} \hat{z}, \tag{2.15}$$

where ω' is the beat wave frequency in the THz range and $\vec{k}'$ is the beat wave vector. * denotes the complex conjugate of the mentioned quantity. The ponderomotive potential $\left(\phi_p\right)$ will then become

$$\phi_p = -\frac{e a_1 a_2^*}{2 m_e \gamma_0 \omega_1 \omega_2} e^{-i(\omega' t - k' z)}. \tag{2.16}$$

The longitudinal pondermotive force may accelerate or decelerate the injected electrons (velocity modulation) depending upon their initial phase and energy leading to density modulation, which results in a beam space charge potential (ϕ). In the present analysis, we have considered ponderomotive potential to be greater than the beam space charge potential, thus

$$\overrightarrow{F_p} = m_e \frac{d}{dt}(\gamma \vec{v}) = e \nabla \phi_p, \tag{2.17}$$

where $\vec{v} = \overrightarrow{v_b^0} + \overrightarrow{v_b^1}$ and $\gamma = \gamma_0 + \frac{\gamma_0^3 v_b^0 v_b^1}{c^2}$. On linearization of Equation (2.17), we obtain

$$\frac{d}{dt}(\gamma_0^3 \overrightarrow{v_b^1}) = \frac{e(\nabla \phi_p)}{m_e}. \tag{2.18}$$

The electron beam enters the modulator at time τ_0 and leaves it at time $\tau_1 \left(= \frac{d_0}{v_b^0} \right)$ after travelling a distance d_0, then it travels a distance d through the drift space

and reaches the wiggler at time $\tau_2 \left(= \frac{d}{v_b^0 + v_b^1} \right)$ (cf. Fig. 2.1). Equation (2.18) can be integrated to yield the perturbed beam velocity as

$$\overrightarrow{v_b^1} = \frac{iek'\phi_p d_0 \sin\theta_p e^{-i(\omega'\tau_0+\theta_p)} e^{-i(\omega'-k'v_b^0)\tau_0}}{2m_e\gamma_0^3 v_b^0 \theta_p} \hat{z}, \qquad (2.19)$$

where $\theta_p = (\omega' - k'v_b^0)\frac{d_0}{2v_b^0}$ is the modulator phase angle. On substituting the values of ϕ_p in Eq. (2.19) and taking the real part, we obtain

$$\overrightarrow{v_b^1} = -\eta v_b^0 \sin(\omega'\tau_0 + \theta_p) z, \qquad (2.20)$$

with

$$\eta = \frac{k'd_0}{2\gamma_0^4}\frac{c^2}{v_b^{02}}\frac{ea_1}{m_e\omega_1 c}\frac{ea_2^*}{m_e\omega_2 c}\frac{\sin\theta_p}{\theta_p}\cos(\omega' - k'v_b^0)\tau_0 .$$

We assume that the prebunched beam enters the wiggler at time τ_3, that is

$$\tau_3 = \tau_0 + \frac{d_0}{v_b^0} + \frac{d}{v_b^0 + v_b^1} = \tau_0 + \frac{d_0 + d}{v_b^0} + \frac{d\eta\sin(\omega'\tau_0 + \theta_p)}{v_b^0}. \qquad (2.21)$$

To get an expression of modulated beam density, we take I_2 as beam current entering the wiggler and, being a periodic function of time, expand it using Fourier series as

$$I_2(\tau_3) = \alpha_0 + \alpha_1\cos\omega'\tau_3 + \alpha_2\cos 2\omega'\tau_3 + ... + \beta_1\sin\omega'\tau_3 + \beta_2\sin 2\omega'\tau_3 ..... \qquad (2.22)$$

where the coefficients are

$$\alpha_1 = \frac{\omega'}{\pi}\int_0^{2\pi/\omega'} I_2 \cos\omega'\tau_3 d\tau_3 \text{ and } \beta_1 = \frac{\omega'}{\pi}\int_0^{2\pi/\omega'} I_2 \sin\omega'\tau_3 d\tau_3 . \quad (2.23)$$

Using the value of τ_3 from Equation (2.21) and on employing $I_2 d\tau_3 = I_0 d\tau_0$, we get

$$\alpha_1 = \frac{\omega' I_0}{\pi}\int_0^{2\pi/\omega'} \cos[\omega'\tau_0 + \frac{\omega'(d_0+d)}{v_b^0} + \frac{\omega' d\eta \sin(\omega'\tau_0+\theta_p)}{v_b^0}].$$

$$\beta_1 = \frac{\omega' I_0}{\pi}\int_0^{2\pi/\omega'} \sin\left[\omega'\tau_0 + \frac{\omega'(d_0+d)}{v_b^0} + \frac{\omega' d\eta \sin(\omega'\tau_0+\theta_p)}{v_b^0}\right]. \quad (2.24)$$

Assuming

$$\xi = \frac{\omega' I_0}{\pi}\int_0^{2\pi/\omega'} \exp\left(i\omega'\left(\tau_0 + \frac{d_0+d}{v_b^0}\right)\right) \times \exp\left(\frac{i\omega' d\eta \sin\left(\omega'\tau_0+\theta_p\right)}{v_b^0}\right). \quad (2.25)$$

And using the Bessel's function identities, Equation (2.25) can be rewritten as

$$\xi = -2I_0 J_1\left(\frac{\omega' d\eta}{v_b^0}\right) e^{-i\left(\frac{\omega'(d_0+d)}{v_b^0} - \theta_p\right)}, \quad (2.26)$$

where $\alpha_1 = \mathrm{Re}\ (\xi)$ and $\beta_1 = \mathrm{Im}(\xi)$. The component of current as a function of the beat wave frequency in the THz range is given as $I_2(\omega') = \alpha_1 \cos\omega'\tau_3 + \beta_1 \sin\omega'\tau_3$. On substituting the values of α_1 and β_1, we obtain

$$I_2(\omega') = -2I_0 J_1\left(\frac{\omega' d\eta}{v_b^0}\right)\cos(\omega'\tau_3 - \delta), \quad (2.27)$$

where $\delta = \frac{\omega'(d_0 + d)}{v_b^0} - \theta_p$, $I_0 = n_b^0 e v_b^0 a_b$.

The laser modulated beam density is given by

$$n_b^m(\omega', k') = -\frac{I_2(\omega')}{e v_b^0 a_b} = -2n_b^0 J_1\left(\frac{\omega' d\eta}{v_b^0}\right)\cos(\omega'\tau_3 - \delta). \qquad (2.28)$$

2.5 Beam Wiggler Interaction

The oscillatory velocity acquired by the beam electrons due to surface plasma wave as wiggler is $\vec{v}_0 = \frac{e\overrightarrow{E_0}e^{-i(\omega_0 t - k_0 z)}}{im_e\gamma_0^3\left(\omega_0 - k_0 v_b^0\right)}$, which when coupled with the modulated beam density leads to the nonlinear current density at $(\omega_1', \overrightarrow{k_1'})$, given as

$$\overrightarrow{J_{NL}}(\omega_1', \overrightarrow{k_1'}) = -n_b^m e\overrightarrow{v_0} = \frac{2n_b^0 e^2 \overrightarrow{E_0} J_1\left(\frac{\omega' d\eta}{v_b^0}\right)\cos(\omega'\tau_3 - \delta)e^{-i(\omega_0 t - k_0 z)}}{im_e\gamma_0^3\left(\omega_0 - k_0 v_b^0\right)}, \qquad (2.29)$$

where $\omega_1' = \omega' + \omega_0$ and $\overrightarrow{k_1'} = \overrightarrow{k'} + \overrightarrow{k_0}$. The current density helps in evaluating the power and amplitude of the THz wave. In the present case, we have considered a homogeneous plasma due to sharp vacuum–plasma interface boundary; in addition, we have taken the length of the wiggler to be less than the drift space length.

Case I: Evaluation of the Power of the THz Radiation

The retarded vector potential is given as

$$\vec{A}(\vec{r}, t) = \frac{\mu_0}{4\pi}\frac{\int J(\vec{r}, t - R/c)}{R} d^3 r' = \frac{\mu_0 n_b^0 r_b^2 e^2 \overrightarrow{E_0} J_1\left(\frac{\omega' d\eta}{v_b^0}\right)e^{-i(\omega_0 t - \delta)}e^{-i(\omega'(t - r/c))} I_1}{2im_e\gamma_0^3 r\omega_0\left(1 - \frac{k_0 v_b^0}{\omega_0}\right)}, \qquad (2.30)$$

where

$$I_1 = \int_0^{l_b} \exp\left[i\left(\frac{\omega'}{c}\left(\frac{c}{v_b^0} - \cos\theta \right) + k_0 \right) z' \right] dz' = \frac{\exp\left(i\frac{\omega' l_b}{c}\left(\frac{c}{v_b^0} - \cos\theta + \frac{ck_0}{\omega'} \right) \right) - 1}{i\left(\frac{\omega'}{c}\left(\frac{c}{v_b^0} - \cos\theta \right) + k_0 \right)},$$

l_b is the bunch length of the beam and r_b is the electron beam bunch radius. Using Equation (2.30) in $\vec{B} = \nabla \times \vec{A} = i\frac{\omega_1'}{c} r \times \vec{A}$, we get

$$\vec{B} = \frac{r \times x n_b^0 e^2 r_b^2 E_0 \omega_1' J_1\left(\frac{\omega' d\eta}{v_b^0} \right) e^{-i(\omega_0 t - \delta)} e^{-i\left(\omega'\left(t - r/c\right)\right)} \exp(i\theta') \frac{\sin\theta'}{\theta'} l_b}{2 m_e \gamma_0^3 r c^3 \varepsilon_0 \omega_0 \left(1 - \frac{k_0 v_b^0}{\omega_0} \right)}, \quad (2.31)$$

where $\theta' = \frac{\omega' l_b}{2c}\left(\frac{c}{v_b^0} - \cos\theta + \frac{ck_0}{\omega'} \right)$.

Time averaged power is $r^2 \int \vec{S}_{av} d\Omega$ and the maximum power over the wiggler length l_b is $l_w^2 \int S_{\max} d\Omega$, where $\vec{S}_{av}$ is the average poynting vector given by

$$\vec{S}_{av} = r \frac{c}{2\mu_0} |B|^2.$$

The average power is given as

$$4\pi r^2 \vec{S}_{av} = \frac{\omega_{pb}^4 r_b^4 l_b^2 E_0^2}{32\pi \gamma_0^6 c^3 \varepsilon_0 \left(1 - \frac{k_0 v_b^0}{\omega_0} \right)^2} \frac{\omega_1'^2}{\omega_0^2} J_1^2\left(\frac{A\omega'^2}{\omega_0^2} \right) r, \quad (2.32)$$

which can be normalized to

$$\frac{r^2\vec{S}_{av}}{l_w^2\frac{E_0^2}{2c\mu_0}}=\frac{\omega_{pb}^4 r_b^4 l_b^2 \omega_1^{'2}}{64\pi^2\gamma_0^6\varepsilon_0^2 c^4 l_w^2\omega_0^2\left(1-\frac{k_0 v_b^0}{\omega_0}\right)^2}J_1^2(\frac{A\omega^{'2}}{\omega_0^{\ 2}})r, \qquad (2.33)$$

with $A=\frac{1}{2\gamma_0^4}\frac{\omega_0 d_0}{c}\frac{\omega_0 d}{c}\frac{c^3}{v_b^{03}}\frac{ea_1}{m_e\omega_1 c}\frac{ea_2^*}{m_e\omega_2 c}$. It can be seen from Equation (2.33) that the radiated power is tunable depending on the beam and wiggler parameters that in the Cerenkov interaction case, that is $\omega_0 \approx k_0 v_b^0$, the normalized THz power reaches the maximum value.

Case II: Evolution of THz Electric Field

The wave equation for THz wave is

$$-\nabla^2\overrightarrow{E_T}+\frac{1}{c^2}\frac{\partial^2\overrightarrow{E_T}}{\partial t^2}=\frac{4\pi i\omega_1^{'}}{c^2}\overrightarrow{J_{NL}(\omega_1^{'},\vec{k}_1^{'})}, \qquad (2.34)$$

with $\overrightarrow{E_T}=A_T(z)e^{-i(\omega_1^{'}t-k_1^{'}z)}x$, $\vec{k}_1^{'}=\overrightarrow{k'}+\overrightarrow{k_0}$, $\omega_1^{'}=\omega'+\omega_0$, and we get

$$-2ik_1^{'}\frac{\partial A_T}{\partial z}-\frac{2ik_1^{'}}{v_{gT}}\frac{\partial A_T}{\partial t}+(k_1^{'2}-\frac{\omega_1^{'2}}{c^2})A_T=\frac{8\pi\omega_1^{'}n_b^0e^2E_0e^{-i(\omega_0 t-\delta)}J_1(\frac{\omega' d\eta}{v_b^0})}{m_e c^2\gamma_0^3\left(\omega_0-k_0v_b^0\right)}, \qquad (2.35)$$

where $v_{gT}\left(=\frac{c^2k}{\omega_1^{'}}\right)$ is the group velocity of the THz radiation wave, and $k_1^{'2}=\frac{\omega_1^{'2}}{c^2}$ at perfect phase matching condition. To understand Equation (2.35), we use a new set of variables, $\psi'=t-\frac{z}{v_{gT}}$ and $\lambda=v_{gT}\psi'$, and we obtain

$$\frac{\partial A_T}{\partial\lambda}=-\frac{\omega_1^{'}\omega_{pb}^2E_0e^{-i(\omega_0 t-\delta)}J_1(\frac{\omega' d\eta}{v_b^0})}{ik_T c^2\gamma_0^3\left(\omega_0-k_0v_b^0\right)}. \qquad (2.36)$$

On integration and taking the real part, the amplitude of THz wave is obtained as

$$A_T = \frac{\omega_1^{'}\omega_{pb}^2 l_w E_0 \sin(\omega_0 t-\delta) J_1(\frac{\omega' d\eta}{v_b^0})}{k_T c^2 \gamma_0^3 \left(\omega_0 - k_0 v_b^0\right)}, \qquad (2.37)$$

which can be normalized as

$$\left|\frac{A_T}{A_{T\max}}\right|^2 = \left|\frac{eA_T}{m_e \omega_1^{'} c}\right|^2 = \frac{\omega_{pb}^4 e^2 E_0^2 l_w^2 v_b^{02}}{\omega_0^4 c^6 \gamma_0^6 m_e^2 \left(1-\frac{k_0 v_b^0}{\omega_0}\right)^2} \frac{\omega_0^2}{\omega_1^{'2}} (1+\frac{k_0 v_b^0}{\omega_0}\frac{\omega_0}{\omega_1^{'}})^{-2} J_1^2(\frac{A\omega'^2}{\omega_0^2}). \qquad (2.38)$$

From Equation (2.38), it can be seen that in the Cerenkov resonance case, that is, $\omega_0 \sim k_0 v_b^0$, the beam velocity is comparable to the phase velocity of the SPW (wiggler wave), the amplitude of the THz wave reaches the maximum value.

2.6 Results and Discussion

We use the following typical parameters to examine the behaviour of the normalized power and amplitude of the emitted THz radiation: beam energy $E_b (=1.29MeV)$, beam velocity $v_b^0 (=0.96c)$, relativistic gamma factor $\gamma_0 (=3.57)$, beam current $I_b (=20kA)$, beam radius $r_b \left(=15\times10^{-3}cm\right)$, electron beam density $n_b^0 \left(=6.1\times10^{15}cm^{-3}\right)$, length of the modulator $d_0 (=0.5cm)$, length of the drift space $d (=1.5cm)$, length of the wiggler $l_w \left(=0.75cm\right)$, electron bunch length $l_b (=3cm)$, $\frac{ea_1}{m_e\omega_1 c}=0.06$, $\frac{ea_2^*}{m_e\omega_2 c}=0.06$, $\frac{\sin\theta_p}{\theta_p}=1$, plasma density $n_p \left(=5\times10^{18}cm^{-3}\right)$ and field amplitude $E_0 \left(=48.6\times10^5 statvolt/cm\right)$.

Using Eq. (2.33), we have plotted Figure 2.2, which shows the variation of the normalized THz power $\left(\frac{r^2 \vec{S}_{av}}{l_w^2 \frac{E_0^2}{2c\mu_0}} \right)$ with $\frac{\omega_1^{'2}}{\omega_0^2}$ for $v_b^0 = 0.94c$ and $0.96c$. The effect of electron beam energy on the normalized power of the radiation has been studied. It can be seen that the normalized THz power initially increases with the radiation frequency, attains a maximum value of 1.1×10^{-4} at a frequency of $\simeq \mathbf{11}$ THz for $v_b^0 = 0.96c$. For $v_b^0 = 0.94c$, the maximum normalized power achieved is 0.7×10^{-4} at frequency $\simeq 4$ THz with the same behaviour. This behaviour is observed due to the Bessel's function character of the density modulation of the relativistic electron beam. The peak shifts to a higher value of THz frequency with increase in the beam velocity from $0.94c$ to $0.96c$ .That is by increasing the electron beam energy, the normalized power of the THz radiation enhances. Our results (cf. Fig. 2.2) are in compliance with the theoretical findings of Xiang and Stupakov [26].

Using Eq. (2.38), we have plotted Fig. 2.3 which shows the variation of the normalized THz field amplitude $\left(\frac{eA_T}{m\omega_1^{'}c} \right)^2$ with the normalized radiation frequencies $\frac{\omega_1^{'2}}{\omega_0^2}$ for different plasma densities $n_p = 3\times10^{18} cm^{-3}$, $5\times10^{18} cm^{-3}$ and $7\times10^{18} cm^{-3}$. From the figure it can be seen that the field amplitude of the THz wave, first increases with the radiation frequency, attains a maximum value and then falls off. Moreover, the field amplitude decreases with increase in the plasma density.

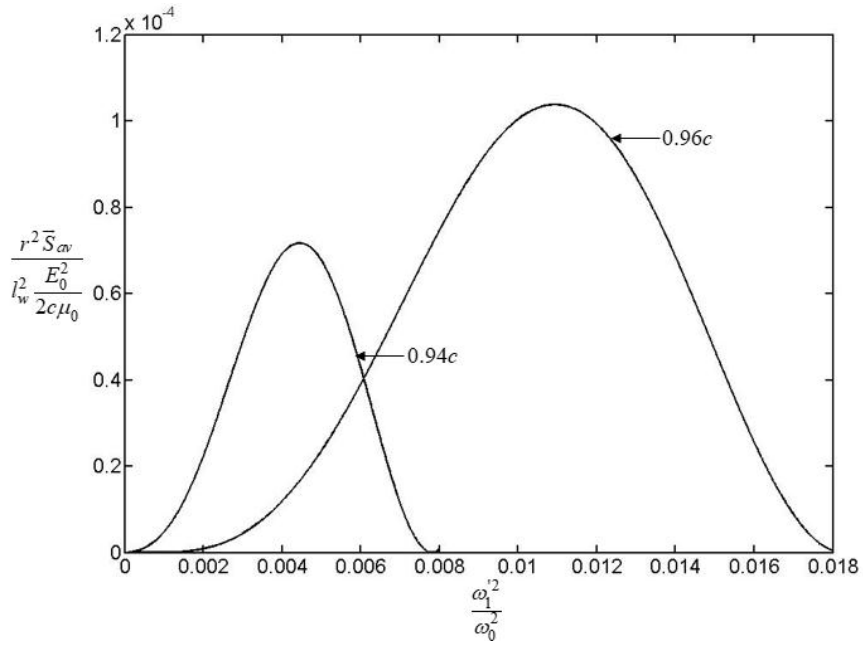

Fig 2.2. Variation of the normalized THz power with $\frac{\omega_1'^2}{\omega_0^2}$ *for beam velocities* $v_b^0 = 0.94c$ and $0.96c$.

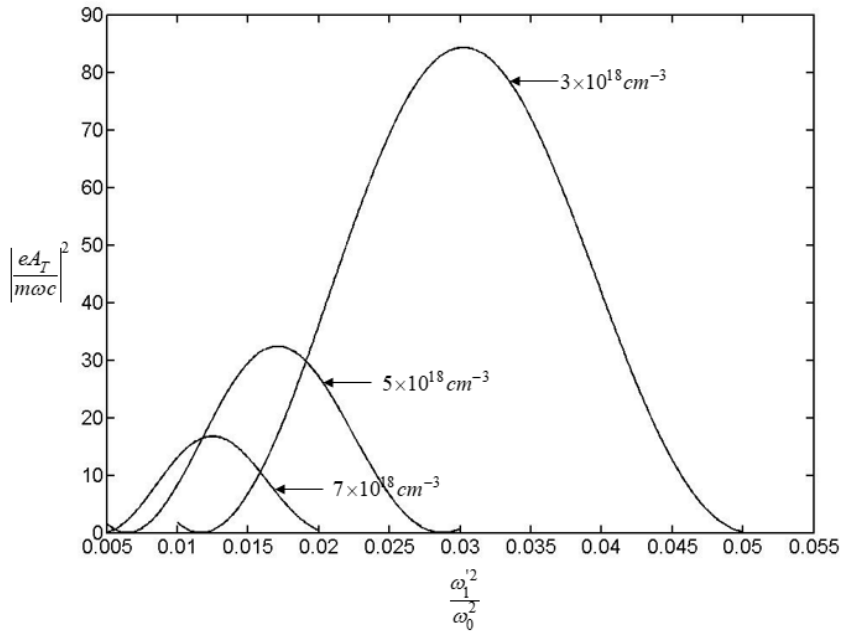

Fig 2.3. Illustration of the variation of the normalized THz field amplitude with $\frac{\omega_1'^2}{\omega_0^2}$ *for different plasma densities.*

Figure 2.4 shows that the average power of the THz radiation increases with the frequency of the radiation. The power varies as square of both the pump electric field and the output frequency of the radiation. At lower values of frequency, the pump amplitude is not noticeable, but as the frequency increases the power increases with the increase in the amplitude of the pump field. This result is in line with the theoretical investigation of Singh *et al.* [25].

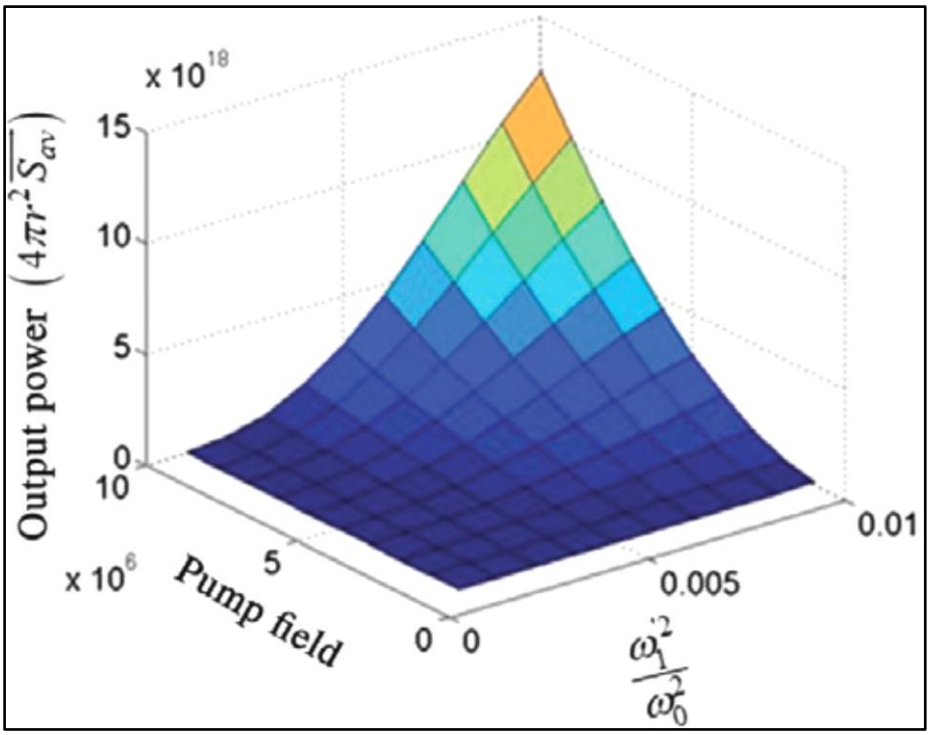

Fig 2.4. Variation of average power with normalized frequency and pump field.

Figure 2.5., shows that the frequency of the emitted THz radiation increases with the wiggler wave vector (k_0) and from the relations $k_0 = \frac{2\pi}{\lambda_0}$ and $\lambda_1 = \frac{\lambda_0}{2\gamma_0^2}$ (λ_0 is the wiggler period and λ_1 is the emitted radiation wavelength), the wiggler period decreases with the increase in wiggler wave vector and consequently the frequency of the output radiation can be increased by reducing the wiggler period.

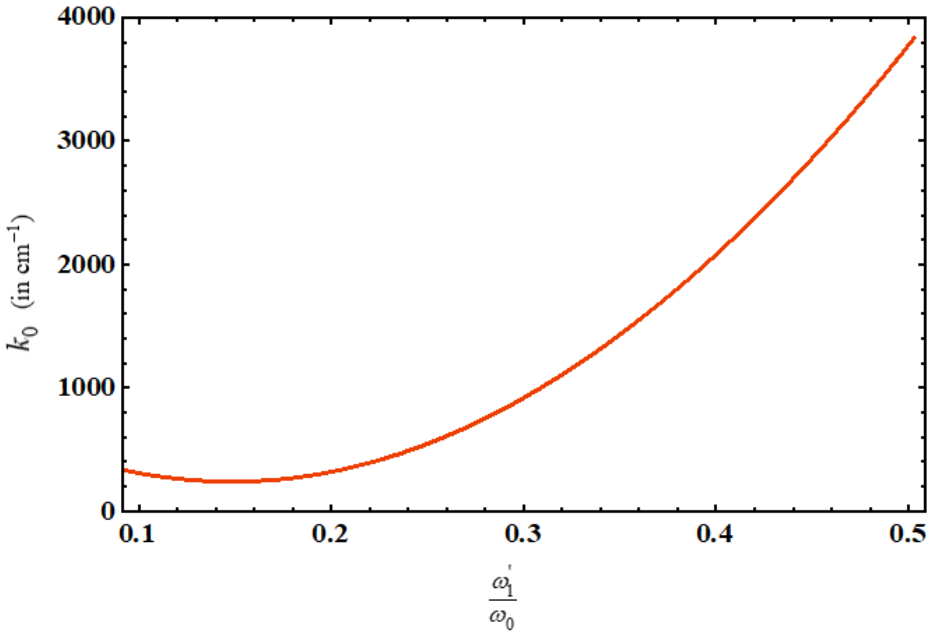

Fig. 2.5. Dependence of wiggler wave vector on the normalized THz frequency for $v_b^0 = 0.96c$.

2.7 Conclusion

Laser pre-bunched electron beam coupling to surface plasma wave as wiggler appears to be a potential candidate for the terahertz radiation generation. The normalized power of the THz radiation wave scales as the square of the electron beam density, square of the electron bunch length and fourth power of the beam bunch radius. In addition, the peak for the normalized THz power shifts to higher value of THz frequency with increase in the beam velocity. The shift is $\cong 1.5$ times higher with beam velocity $v_b^0 = 0.96c$. It also increases with beam density. The normalized THz field amplitude varies linearly with the length of the wiggler and inversely with the wave vector of the THz radiation. The normalized THz amplitude decreases with the plasma density and increases with the increase of the beam current and hence the beam density. The average power of the THz radiation increases with the pump electric field amplitude. The frequency of the radiation increases with the wiggler wave vector. The normalized power and amplitude of the

THz radiation first increases with normalized THz radiation frequency, attains a maximum value and then falls off. This behaviour is due to the Bessel's function character of the density modulation. We have considered the Cerenkov interaction, i.e., $\omega_0 \sim k_0 v_b^0$ and at this condition the normalized THz power and the normalized THz field amplitude reaches the maximum value. The amplitude of the SPW varies as two-third power of the electron beam velocity and beam density. The output radiation can be improved by increasing the beam density and decreasing the wiggler period. The scheme seems to be very attractive for the generation of high power THz radiation at shorter wavelengths.

References

[1] J. G. Neumann, R. B. Fiorito, P. G. O'Shea, H. Loos, B. Sheehy, Y. Shen and Z. Wu, J. Appl. Phys. **105**, 053304 (2009).

[2] H. P. Freund, P. G. O'Shea, J. Neumann, Nucl. Instrum. Methods Phys. Res.A **507**, 400 (2003).

[3] G. Bekefi and K. D. Jacobs, J. Appl. Phys. **53**, 4113 (1982).

[4] M. Arbel, A. Gover, A. L. Eichenbaum and H. Kleinman, Phys. Rev. ST Accel. Beams **17**, 020705 (2014).

[5] M. Cohen, A. L.Eichenbaum, M. Arbel, D. Ben-Haim, H. Kleinman, M. Draznin, A. Kugel, I. M. Yacover, and A. Gover, Phys.Rev.Lett. **74**, 3812 (1995).

[6] Y. Shibata, K. Ishi, S. Ono, Y. Inoue, S. Sasaki, M. Ikezawa, T. Takahashi, T. Matsuyama, K. Kobayashi, Y. Fujita and E. G. Bessonov, Phys. Rev. Letter **78**, 2740 (1997).

[7] M. Kumar and V. K. Tripathi, Phys. Plasmas **19**, 073109 (2012).

[8] A. Gover, Phys. Rev. ST Accel. Beams **8**, 030701 (2005).

[9] S. Liu and Yen-Chieh Huang, Nucl. Instrum. Methods Phys. Res.A **637,** S172 (2011).

[10] E. Pickwell, V. P. Wallace, J. Phys. D: Appl. Phys. **39**, R 301 (2006).

[11] J. F. Federici, B. Schulkin, F. Huang, D. Gary, R. Barat, F. Oliveira, D. Zimdars, Semicond. Sci. Technol. **20**, S266 (2005).

[12] M. Tonouchi, Nat. Photonics **1**, 97 (2007).

[13] P. H. Siege, IEEE Trans. Microw. Theory Tech. **52**, 2438 (2004).

[14] W.P. Leemans, J. Van Tilborg, J. Faure, C.G.R. Geddes, Cs. Toth, C.B. Schroeder, E.Esarey and G. Fubiani, G. Dugan, Phys. Plasmas **11**, 2899 (2004).

[15] H. S. Uhm, Phys. Plasmas **4**, 3684 (1997).

[16] S. C. Sharma and A. Bhasin, Phys. Plasmas **14**, 053101 (2007).

[17] I. V. Konoplev and A. D. R. Phelpsa, Phys. Plasmas **7**, 4280 (2000).

[18] A. Doria, R. Bartolini, J. Feinstein, G. P. Gallerano, R. H. Pantell, Phys. Plasmas, **29**, 1428 (1993).

[19] A. Bhasin, S. C. Sharma, Phys. Plasmas **14**, 073102 (2007).

[20] L. Bhasin and V. K. Tripathi, IEEE J. Quantum Electronics **46**, 965 (2010).

[21] S. C. Sharma, P. Malik, Phys. Plasmas **22**, 043301 (2015).

[22] S. C. Sharma, J. Sharma, A. Bhasin, R. Walia, Phys. Plasmas **78**, 635 (2012).

[23] M. Kumar, V. K. Tripathi and Y. U. Jeong, Phys. Plasmas **22,** 063106 (2015).

[24] A. K. Malik, H. K. Malik and U. Stroth, Phys. Rev. E **85**, 016401 (2012).

[25] D. B. Singh, G. Kumar, V. K. Tripathi, J. Appl. Phys. **101**, 043306 (2007).

[26] D. Xiang, G. Stupakov, Phys. Rev. ST: Accel. Beams **12**, 080701 (2009).

[27] A. K. Malik, H. K. Malik, U. Stroth, Phys. Rev. ST: Accel. Beams **85**, 016401 (2012).

[28] Z. M. Sheng, K. Mima, J. Zhang, Phys. Plasmas **12**, 123103 (2005).

[29] V. Prakash, S. C. Sharma, Phys. Plasmas **16**, 093703 (2009).

[30] C. S. Liu and V. K. Tripathi, *Electromagnetic Theory for Telecommunications* (Cambridge University Press, Cambridge, 2007).

[31] C. S. Liu, V. K. Tripathi, *Interaction of Electromagnetic Waves with Electron Beams and Plasmas* (World Scientific Publishing, Singapore 1994).

[32] C. Joshi, J. M. Dawson, Y. T. Yan, J. M. Slater, IEEE J. Quant. Electron. **9**, 1571 (1987).

Chapter 3

MODELING THE EMISSION OF HIGH POWER TERAHERTZ RADIATION USING LANGMUIR WAVE AS A WIGGLER

3.1 Brief Outline of the Chapter

The emission of high power terahertz (THz) radiation lying in the range of millimeter to sub-millimeter wavelengths has been studied analytically using Langmuir wave as an electrostatic pump wave in the presence of static magnetic field for both the finite and infinite geometry. The interaction of two laser beams with the relativistic electron beam (REB) leads to velocity modulation of the beam, which then translates into density modulation on traveling through the drift space. The premodulated beam on interacting with the pump wave acquires an oscillatory velocity that couples with the perturbed and modulated beam densities to result in nonlinear current density which helps in evaluating the growth rate and efficiency of the output THz radiation. The beam and plasma wave wiggler parameters are found to influence the growth rate and efficiency of the emitted THz radiation.

3.2 Introduction

Terahertz (THz) radiation poses a great scope of research in various potential fields [1-5] due to its high penetration and non-ionization characteristics. Several schemes have been proposed for the generation of these high power radiation including mainly optical rectification [6-8] in dielectrics, plasmas and semiconductors, interaction of high power lasers with electro-optic crystals or by employing prebunched electron beams [9-11] using free electron lasers.

Welsh and Wynne [6] have analyzed the emission of radiation pulses by the incoherent optical rectification on metallic nanostructured surfaces via excitation of surface plasmons. The emission of terahertz radiation by optical rectification of amplitude modulated surface plasma, excited on rippled metal surface by an obliquely incident laser beam has been studied by Bhasin and Tripathi [8]. They concluded that the amplitude of the wave scales as square root of the laser wavelength and laser spot size, and the efficiency of the wave is found to be high due to very weak linear damping. Sharma and Malik [12] have observed analytically the effect of prebunched relativistic electron beam (REB) on the excitation of surface plasmons lying in the terahertz range using semiconductors and observed that the efficiency and amplitude of the plasmons can be tuned by the beam parameters and the spacing of the semiconductor plates.

The effective schemes employed for the generation of THz radiation can be interaction of relativistic electron beams or short wavelength lasers with the plasma medium. Plasma eigen modes employed as an electrostatic wiggler helps in obtaining radiation of shorter wavelength with high wiggler strength [13]. Singh *et al.* [14] have investigated the emission of terahertz radiation by the non-linear decay of upper hybrid wave in the presence of static magnetic field into a high frequency laser wave and terahertz wave of low frequency. They observed that the power and growth rate of the terahertz radiation increases with the magnetic field. Sharma *et al.*

[15] have employed surface plasma wave as wiggler in the presence of prebunched REB for the generation of radiation in the range of sub-millimeter wavelength. They concluded that the plasma density helps in improving the gain and efficiency of the device. The growth rate was found to increase with the plasma density and varied as one third power of the beam density. Zolghadr *et al.* [16] have studied the effect of magnetized plasma on the output power and the saturation length using whistler wave wiggler. They observed that the output power increases and the saturation length decreases with the plasma frequency. Further, the power decreases and saturation length increases with the cyclotron frequency. More recently, Hussain *et al.* [17] have investigated that the terahertz radiation emitted using super Gaussian laser beams interaction with the plasma in the presence of static electric field is strongly affected by the plasma density, intensity of the laser beams and strength of the externally applied field. Radiation with frequencies upto 200 GHz generated from the Cerenkov interaction in the magnetized plasma have been experimentally detected by Yugami *et al.* [18]. They found that the intensity of the radiation to be proportional to the magnetic field intensity and power as square of the field strength. The results indicate that this is an efficient way to obtain tunable radiation with high power.

Plasma can withstand with high fields due to being in the ionized state and hence overcome the limitation of material breakdown. The plasma medium has thus proved to be the most suited medium for the generation of high power radiation. The introduction of plasma in the free electron lasers helps in reducing the beam energy requirement and acts as a slow wave structure. Tripathi and Liu [19] have addressed the effects on the radiation and the electron beam due to plasma introduced in a magnetic wiggler. They observed that the plasma and the strong magnetic field reduces the electron beam energy requirement and enhances the growth rate. The depression in the electron density of plasma due to the beam acts as an optical guiding medium when the beam and plasma densities are comparable.

The emission of high power tunable radiation by the interaction of relativistic electron beam with dusty plasma crystal has been studied by Mehdian *et al.* [20]. They observed that the crystal as a wiggler provides high output frequency, power and efficiency at comparatively low beam energy and quality. Hedayati *et al.* [21] have investigated that the plasma medium in the presence of static magnetic field helps in obtaining radiation of shorter wavelength by reducing the wiggler period and lowering the electron beam energy. They also concluded that the electron bunching enhances at the wave frequency comparable to the plasma frequency. The generation of terahertz radiation by employing rippled underdense plasma has been investigated by Pathak *et al.* [22]. In this case, the frequency was observed to be tuned by the beam energy and ripple wavelength, and the parameters affecting the growth rate were plasma density, depth and amplitude of density ripple. Kumar and Tripathi [23] have employed the beating of two collinear laser pulses in a clustered gas to study the emission of radiation. In this case, it was concluded that the power of the THz radiation varies linearly as square of the amplitude of laser, fourth power of the plasma frequency of cluster electrons and inversely as square of the laser frequency. Gildenburg and Vvedenskii [24] have demonstrated the terahertz radiation generation by the linear conversion of an ultrashort laser pulse. The power of the radiation was obtained in the range of gigawatt using optical intensity of about 10^{14}-10^{15} Wcm^{-2}.The conversion efficiency was realized to be comparatively quite high when the length of the laser pulse was not much greater than the period of the optical field.

In the present chapter, we have developed an analytical model to study the emission of terahertz radiation by the interaction of a density modulated electron beam with an electrostatic plasma pump wave wiggler. The mechanism for the analysis is as followed. The REB first gets energy modulated at the difference frequency of the two laser beams exerting non-linear ponderomotive force on the electron beam in the modulator. The beam on travelling through the drift space gets density

modulated. The density modulated beam interacts with the plasma region, where the Langmuir plasma wave is excited that acts as an electrostatic pump wave. The beam acquires an oscillatory velocity due to the pump wave. Further, the radiation wave and the pump leads to the perturbed beam density that couples with the oscillatory velocity to give nonlinear current density which behaves as an antenna for the emission of high power terahertz radiation. In sec 3.3, we have shown the modulation of the REB and its interaction with the pump wave in infinite and finite geometry to study the behavior of high power output radiation. Sec 3.4 includes the discussions for the obtained results and the investigations are concluded in Sec 3.5.

3.3 Physical Model

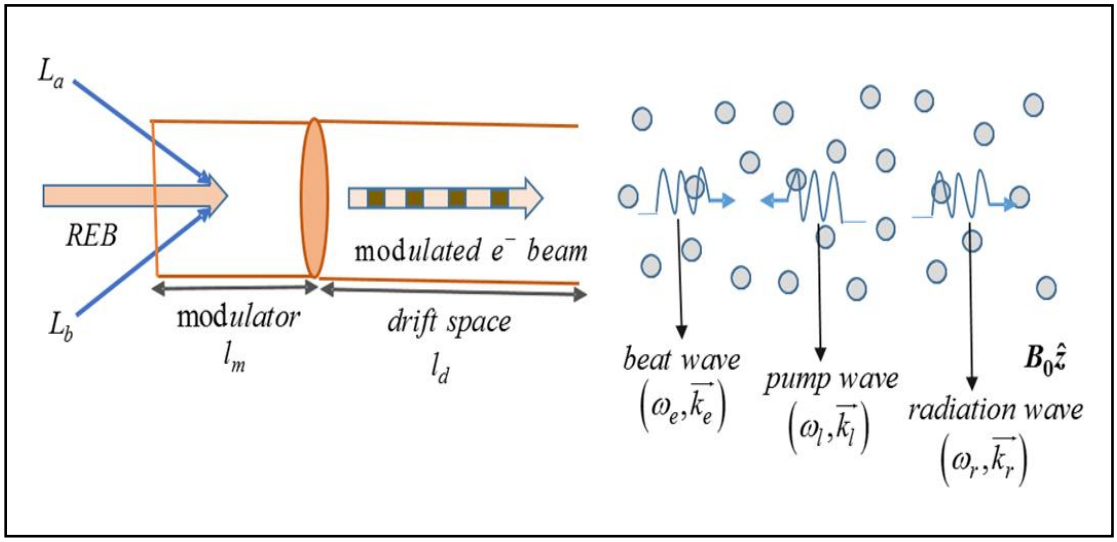

Fig 3.1. Schematic of interaction of premodulated REB (by two laser beams) with the Langmuir plasma pump wave (in unbound plasma).

In the present analysis, on taking into account the interaction of premodulated REB with the pump wave we investigate the emission of THz radiation. Preliminarily, we investigate the electron beam modulation by considering a REB of density n_e^0 moving in the axial direction with initial velocity $v_e^0 \hat{z}$ which is modulated by two lasers, laser L_a and laser L_b (cf. Fig. 3.1) polarized in $\hat{x}$- direction and co-

propagating in $\hat{z}$-direction with frequencies ω_a and ω_b, and wave vectors $\overrightarrow{k_a}$ and $\overrightarrow{k_b}$, respectively. The electric and magnetic fields of the laser beams propagating in the modulator are considered as

$\overrightarrow{E_{L_\xi}} = A_\xi e^{-i(\omega_\xi t - k_\xi z)}\,\hat{x}$ and $\overrightarrow{B_{L_\xi}} = \dfrac{c\left(\overrightarrow{k_\xi} \times \overrightarrow{E_{L_\xi}}\right)}{\omega_\xi}\hat{y}$, where $\xi = a,b$ for lasers L_a and L_b, respectively.

The two laser beams interact with REB in the modulator region as a result of which the beam electrons acquire an oscillatory velocity $\overrightarrow{v_{0_\xi}} = \dfrac{e\overrightarrow{E_{L_\xi}}}{im_e\omega_\xi\gamma_0}$ (where $\xi = a,b$ for lasers L_a and L_b, respectively); where m_e is the mass of electron and $\gamma_0 = \left(1 - \left(\dfrac{v_e^0}{c}\right)^2\right)^{-1/2}$ is the relativistic gamma factor. Due to the interaction of oscillatory velocity of the beam and the magnetic fields of the laser beams, an axial nonlinear ponderomotive force $\overrightarrow{f_{pe}}$ [25] is exerted on the beam electrons

$$\overrightarrow{f_{pe}} = f_0 \cos\left(\omega_e t - k_e z\right), \tag{3.1}$$

where $f_0 = \dfrac{e^2 k_e A_a A_b^*}{2im_e\gamma_0\omega_a\omega_b}$, $\omega_e\left(=\omega_a - \omega_b\right)$ is the frequency (lying in the terahertz range) and $k_e\left(=k_a - k_b\right)$ is the wave number of the velocity modulated REB, e is the electronic charge. The length of the overlap region (or modulator region) is $l_m(= \dfrac{2r_l}{\sin\left(\theta_l/2\right)} \simeq \dfrac{4r_l}{\theta_l}$, where θ_l is the angle of interaction and r_l is the radius of

laser spot). The angle of interaction is taken very small so as to have significant velocity modulation and only the frequency components (ω_e) relevant for the generation of THz radiation are considered while the other frequency components ($2\omega_a$, $2\omega_b$) are ignored. The electron beam response under the ponderomotive force is governed by the relativistic equation of motion,

$$\frac{\partial}{\partial t}\left(\gamma\vec{v}\right)=\frac{\overrightarrow{f_{pe}}}{m_e}, \tag{3.2}$$

where $\vec{v}=\overrightarrow{v_e^0}+\overrightarrow{v_e^m}$, $\gamma=\gamma_0+\frac{v_e^0 v_e^m \gamma_0^3}{c^2}$. On linearizing the Eq. (3.2), the modulated velocity (v_e^m) attained by the beam is obtained as

$$v_e^m=\frac{f_0 l_m}{m_e\gamma_0^3 v_e^0}\frac{\sin(\theta_l)}{\theta_l}e^{-i(\omega_e t_m+\theta_l)}=-\alpha_m v_e^0\sin(\omega_e t_m+\theta_l), \tag{3.3}$$

where $\alpha_m=\frac{k_e l_m c^2}{2\gamma_0^4 v_e^{02}}\frac{e^2 A_a A_b^*}{m_e^2\omega_a\omega_b c^2}\frac{\sin(\theta_l)}{\theta_l}$, t_m is the time at which beam arrives at the modulator and $\frac{\sin(\theta_l)}{\theta_l}\approx 1$ for appreciable velocity modulation. The beam thus gets velocity modulated in the modulator region where the initial slow moving electrons (late electrons) start moving fast and fast moving electrons (early electrons) slows down in order to attain a common velocity.

The beam then passes through the drift space, where due to acceleration and deceleration, the late electrons catch the early electrons, leading to the density modulation of the electron beam. The density (n_e^m) of the modulated REB can be written as [23]

$$n_e^m = -2n_e^0 J_1\left(\frac{\omega_e l_d \alpha_m}{v_e^0}\right)\cos(\omega_e t_m - \varphi), \tag{3.4}$$

where $t_p\left(= t_m + \frac{l_m}{v_e^0} + \frac{l_d\left(1+\alpha_m \sin(\omega_e t_m + \theta_l)\right)}{v_e^0}\right)$ is the time at which the beam electrons leave the drift space and enter the pump wave; l_d is the length of drift space.

In the next stage, we consider a system filled with an isothermal plasma of uniform density n_p^0 in which the premodulated REB excites an electrostatic plasma wave (pump wave) due to Cerenkov interaction which acts as a wiggler in the present analysis. Now, the interaction of the premodulated REB with the excited pump wave in the presence of external static magnetic field $\left(B_0 \,||\, \hat{z}\right)$ is studied. On taking the beam response in the electron frame moving with velocity $v_e^0\hat{z}$, where the beam is treated as non-relativistic, we obtain the oscillatory velocity component as $\overrightarrow{v_e^{l'}} = \frac{e\left[i\omega_l'\left(\nabla'\phi_l'\right) - \left(\omega_{ce}' \times \nabla'\phi_l'\right)\right]}{m_e\left(\omega_l'^2 - \omega_{ce}'^2\right)}$, where $'$ denotes the quantities in the electron frame, $\phi_l = A_l e^{-i(\omega_l t - k_l z)}$ is the electrostatic potential of the plasma wave, $\overrightarrow{E_l}\left(= -\nabla\phi_l\right)$ is the pump electric field which is polarized in the $x-z$ plane and $\omega_{ce}\left(= \frac{eB_0}{m_e c}\right)$ is the electron cyclotron frequency. The perturbation induced due to an electromagnetic radiation wave is given as $\overrightarrow{E_r} = \overrightarrow{A_r} e^{-i(\omega_r t - k_r z)}$, where $(\omega_r,\ \overrightarrow{k_r})$ is the frequency and wave number of the radiation wave, respectively. The radiation wave and the pump wave simultaneously exerts a nonlinear

pondermotive force [26-28] on the beam electrons, $\overrightarrow{F_p'} = e\nabla'\phi_p'$, where the ponderomotive potential $\left(\phi_p'\right)$ can be simplified to

$$\phi_p' = -\frac{e\left[i\omega_l'\left(\nabla'\phi_l'^{*}\right)+\left(\overrightarrow{\omega_{ce}'}\times\nabla'\phi_l'^{*}\right)\right]\overrightarrow{E_r'}}{2im_e\omega_r'\left(\omega_l'^2-\omega_{ce}'^2\right)}. \tag{3.5}$$

The response of beam electrons in terms of velocity ($\overrightarrow{v_e'}$) and density $\left(n_e'\right)$ due to the ponderomotive force and the self-consistent electric field is obtained as

$$\overrightarrow{v_e'} = -\frac{e\nabla'\left(\phi' + \phi_p'\right)}{im_e\omega_e'} \tag{3.6}$$

$$n_e' = -\frac{k_e'^2e^3n_e^{0'}\left[i\omega_l'\left(\nabla'\phi_l'\right)-\left(\omega_{ce}'\times\nabla'\phi_l'\right)\right]\left[1+\frac{n_e^{m'}}{n_e^{0'}}\right]\left(\phi' + \phi_p'\right)}{m_e\omega_e'^2\left(\omega_l'^2-\omega_{ce}'^2\right)}. \tag{3.7}$$

The nonlinear current density $\left(\overrightarrow{J_{NL}'}\right)$ being an important source for the emission of terahertz radiation arises by coupling of the perturbed beam density with the oscillatory beam velocity. Hence, the nonlinear current density at $\left(\omega_r, \overrightarrow{k_r}\right)$ is obtained as

$$\overrightarrow{J_{NL}'} = -n_e'e\overrightarrow{v_e^{l'}} = \frac{k_e'^2e^3A_l'(\phi' + \phi_p')n_e'^0\left[1+\frac{n_e^{m'}}{n_e^{0'}}\right]\left[i\omega_l'\left(\nabla'\phi_l'\right)-\left(\omega_{ce}'\times\nabla'\phi_l'\right)\right]e^{-i(\omega_r't-k_r'z)}}{im_e\omega_e'^2\left(\omega_l'^2-\omega_{ce}'^2\right)}, \tag{3.8}$$

where $\omega_r = \omega_e + \omega_l$ and $\overrightarrow{k_r} = \overrightarrow{k_e} + \overrightarrow{k_l}$.

Further to study the proficient generation of the high power THz radiation, the growth rate and efficiency radiation wave have been evaluated for the geometries with infinite [15] (local effects) and finite [28-30] (nonlocal effects) boundaries.

Case I: Effects of Infinite Boundary on THz Radiation Wave

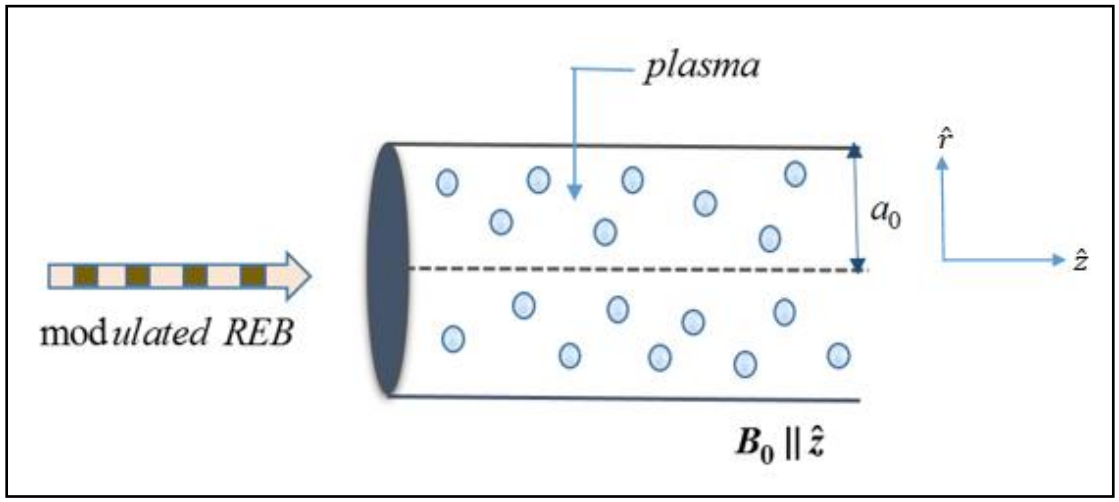

Fig 3.2. Schematic of interaction of REB with the plasma pump wave in a cylindrical column (bound plasma).

We consider the excited pump wave in plasma in a very large dimensional space such that it can be considered as an infinite system. In order to study the generation of terahertz radiation with the local effects of the wiggler wave, the wave equation is employed as

$$-\nabla^2 \overrightarrow{E_r} = \frac{4\pi i\omega_r}{c^2} \overrightarrow{J_{NL}} + \frac{i\omega_r}{c^2} \frac{\partial \overrightarrow{E_r}}{\partial t}. \tag{3.9}$$

The expression for non-linear current density that drives the radiation wave is substituted in the above wave equation after applying Lorentz transformation [31] on it in the lab frame to obtain

$$\left(\omega_r^2 - k_r^2 c^2\right)\left(\omega_e - k_e v_e^0\right)^2 = \frac{\omega_{pb}^2 e^2 \left(k_e - \frac{\omega_e v_e^0}{c^2}\right)^2 \left[i\gamma_0 \omega_l \left(\nabla \phi_l\right) - \left(\omega_{ce} \times \nabla \phi_l\right)\right]^2 \left(1 + \frac{n_e^m}{n_e^0}\right)\left(1 - \frac{\chi_e}{\varepsilon}\right)}{2m_e^2 \gamma_0 \left(\gamma_0^2 \omega_l^2 - \omega_{ce}^2\right)^2}, \quad (3.10)$$

where χ_e is the beam susceptibility, $\varepsilon = 1 + \chi_e$ and $\omega_{pb}\left[= \left(\frac{4\pi n_e^0 e^2}{m_e}\right)^{1/2}\right]$ is the electron beam plasma frequency. To simplify the above equation, we take $\omega_e = k_e v_e^0 + \delta_{ir}$ and $\omega_r = k_r c + \delta_{ir}$, where δ_{ir} is the small frequency mismatch.

$$\delta_{ir} = \left(\frac{\omega_{pb}^2 e^2 \left(k_e - \frac{\omega_e v_e^0}{c^2}\right)^2 \left[i\gamma_0 \omega_l \left(\nabla \phi_l\right) - \left(\omega_{ce} \times \nabla \phi_l\right)\right]^2 \left(1 + \frac{n_e^m}{n_e^0}\right)\left(1 - \frac{\chi_e}{\varepsilon}\right)}{4\omega_r m_e^2 \gamma_0 \left(\gamma_0^2 \omega_l^2 - \omega_{ce}^2\right)^2} \right)^{1/3} e^{i2n\pi/3}.$$

The growth rate of the radiation wave Γ_{ir} is obtained by taking the imaginary part of δ_{ir} with n=1.

$$\Gamma_{ir} = \mathrm{Im}\,\delta_{ir} = \frac{\sqrt{3}}{2} \left(\frac{\omega_{pb}^2 e^2 \left(k_e - \frac{\omega_e v_e^0}{c^2}\right)^2 E_l^2 \left(1 + \frac{n_e^m}{n_e^0}\right)\left(1 - \frac{\chi_e}{\varepsilon}\right)}{4\omega_r m_e^2 \gamma_0^3 \omega_l^2 \left(1 - \frac{\omega_{ce}^2}{\gamma^2 \omega_l^2}\right)^2} \right)^{1/3}. \quad (3.11)$$

The efficiency of the radiation [32] ($\eta_{ir} = \frac{\Gamma_{ir}}{\omega_r} \frac{\gamma_0^3}{\sqrt{3}\left(\gamma_0 - 1\right)}$) can be evaluated as

$$\eta_{ir}=\frac{1}{2}\left(\frac{\omega_{pb}^2 e^2\gamma_0^6\left(k_e-\frac{\omega_e v_e^0}{c^2}\right)^2 E_l^2\left(1+\frac{n_e^m}{n_e^0}\right)\left(1-\frac{\chi_e}{\varepsilon}\right)}{4\omega_r^4 m_e^2(\gamma_0-1)^3\omega_l^2\left(1-\frac{\omega_{ce}^2}{\gamma_0^2\omega_l^2}\right)^2}\right)^{1/3}. \tag{3.12}$$

Case II: Effects of Finite Boundary on THz Radiation Wave

The radiation wave has been considered for the same with the finite geometry. In order to study the nonlocal theory of the pump wave, we consider a uniform cylindrical plasma column of radius a_0 as shown in Fig. 3.2. Using the expression of Lorentz transformed nonlinear current density in the wave equation, we obtain

$$\frac{\partial^2 E_r}{\partial r^2}+\frac{1}{r}\frac{\partial E_r}{\partial r}+k^2E_r= -\frac{\omega_{pb}^2 e^2\left[i\gamma_0\omega_l\left(\nabla\phi_l\right)-\left(\omega_{ce}\times\nabla\phi_l\right)\right]^2\left(k_e-\frac{\omega_e v_e^0}{c^2}\right)\left(1+\frac{n_e^m}{n_e^0}\right)\left(1-\frac{\chi_e}{\varepsilon}\right)}{2c^2m_e^2\gamma_0\left(\omega_e-k_e v_e^0\right)^2\left(\gamma_0^2\omega_l^2-\omega_{ce}^2\right)^2}, \tag{3.13}$$

where $k^2=\frac{\omega_r^2}{c^2}-k_r^2$.

In the absence of beam $\left(\text{i.e., } \omega_{pb}=0\right)$, the equation reduces to

$$\frac{\partial^2 E_r}{\partial r^2}+\frac{1}{r}\frac{\partial E_r}{\partial r}+k^2E_r=0. \tag{3.14}$$

The solution of the above equation is of the Bessel's form which can be given as $E_r=A_nJ_0\left(k_nr\right)$, where $J_0(k_nr)$ is the zeroth order Bessel function of first kind. At $r=a_0$, the electric field should vanish i.e., $E_r=0$ and the solution reduces to

$J_0(k_n a_0) = 0$, i.e., $k_n = \dfrac{X_n}{a_0}\ (n = 1,2,3.....)$, X_n are the zeros of the Bessel function and n is the mode number.

In the presence of beam $\left(i.e., \omega_{pb} \neq 0\right)$, a series of orthogonal sets of wave functions can be used to express the solution of the wave function with $E_r = \sum_m A_m J_0(k_m r)$. We substitute this expression in Eq. (3.13) and multiply both sides of the equation by $rJ_0\left(k_n r\right)$ and then integrate it over r from 0 to a_0. On retaining only the dominant mode $\left(i.e., m = n\right)$, we obtain

$$\frac{\omega_r^2}{c^2} - k_{1r}^2 = \frac{\omega_{pb}^2 e^2 \left(k_e - \dfrac{\omega_e v_e^0}{c^2}\right)^2 \left[i\omega_l \gamma_0 \left(\nabla \phi_l\right) - \left(\omega_{ce} \times \nabla \phi_l\right)\right]^2 \left(1 + \dfrac{n_e^m}{n_e^0}\right)\left(1 - \dfrac{\chi_e}{\varepsilon}\right)\alpha_1}{2m_e^2 c^2 \gamma_0 \left(\omega_e - k_e v_e^0\right)^2 \left(\gamma_0^2 \omega_l^2 - \omega_{ce}^2\right)^2}, \quad (3.15)$$

where $k_{1r}^2 = k_r^2 + k_n^2$ and $\alpha_1 = \dfrac{\int_0^{r_e} rJ_0(k_m r)J_0(k_n r)dr}{\int_0^{a_0} rJ_0(k_m r)J_0(k_n r)dr}$, where r_e is the radius of the electron beam. At $r_e = a_0$, $\alpha_1 = 1$. Equation (3.15) can be simplified to

$$\left(\omega_r^2 - k_{1r}^2 c^2\right)\left(\omega_e - k_e v_e^0\right)^2 = \frac{\omega_{pb}^2 e^2 \left(k_e - \dfrac{\omega_e v_e^0}{c^2}\right)^2 \left[i\gamma_0 \omega_l \left(\nabla \phi_l\right) - \left(\omega_{ce} \times \nabla \phi_l\right)\right]^2 \left(1 + \dfrac{n_e^m}{n_e^0}\right)\left(1 - \dfrac{\chi_e}{\varepsilon}\right)\alpha_1}{2m_e^2 \gamma_0 \left(\gamma_0^2 \omega_l^2 - \omega_{ce}^2\right)^2} \quad (3.16)$$

Here, $\omega_r \simeq k_{1r} c$ agrees to the radiation mode and $\omega_e \simeq k_e v_e^0$ corresponds to the beam mode. The growth rate (Γ_{fr}) is obtained on solving the above expression by using $\omega_r = k_{1r} + \delta_{fr}$ and $\omega_e = k_e v_e^0 + \delta_{fr}$, where δ_{fr} is the small frequency mismatch and taking its imaginary part

$$\Gamma_{fr} = \frac{\sqrt{3}}{2}\left(\frac{\omega_{pb}^2 e^2 E_l^2 \left(k_e - \frac{\omega_e v_e^0}{c^2} \right)^2 \left(1 + \frac{n_e^m}{n_e^0} \right) \left(1 - \frac{\chi_e}{\varepsilon} \right) \alpha_1}{4\left[\left(\frac{X_n}{a_0} \right)^2 + k_r^2 \right]^{1/2} m_e^2 c \gamma_0^3 \omega_l^2 \left(1 - \frac{\omega_{ce}^2}{\gamma_0^2 \omega_l^2} \right)^2} \right)^{1/3} . \qquad (3.17)$$

In the case of finite geometry, the frequency of the output radiation depends on the modes and radius of the waveguide as

$$\omega_r = \left[\left(\frac{X_n}{a_0} \right)^2 + k_r^2 \right]^{1/2} c . \qquad (3.18)$$

The efficiency of the output radiation $\eta_{fr} \left(= \frac{\Gamma_{fr}}{\omega_r} \frac{\gamma_0^3}{\sqrt{3}\left(\gamma_0 - 1 \right)} \right)$ can be expressed as

$$\eta_{fr} = \frac{1}{2}\left(\frac{\omega_{pb}^2 e^2 E_l^2 \gamma_0^6 \left(k_e - \frac{\omega_e v_e^0}{c^2} \right)^2 \left(1 + \frac{n_e^m}{n_e^0} \right) \left(1 - \frac{\chi_e}{\varepsilon} \right) \alpha_1}{4\left[\left(\frac{X_n}{a_0} \right)^2 + k_r^2 \right]^2 m_e^2 c^4 \omega_l^2 \left(1 - \frac{\omega_{ce}^2}{\gamma_0^2 \omega_l^2} \right)^2 \left(\gamma_0 - 1 \right)^3} \right)^{1/3} . \qquad (3.19)$$

For the infinite and finite geometry, the growth rate and efficiency of the output radiation is found to be influenced by the parameters of the beam (scales as one third power of the beam density) and the pump wave (scales as two third power of the electric field). For both the cases, at $\omega_{ce} \simeq \gamma_0 \omega_l$, Cerenkov resonance occurs and the growth rate and efficiency of the THz radiation

attains the maximum value. The frequency of the output radiation depends on the radius and modes of the cylindrical column in case of finite boundaries while in case of infinite, the dimensions of the system does not affect the radiation.

3.4 Results and Discussion

The present analysis involves an analytical model for the study of the growth rate and efficiency of the terahertz radiation which is being radiated by the interaction of the laser premodulated relativistic electron beam with the Langmuir pump wave wiggler. The response of the beam and wiggler parameters on the output radiation has been studied by employing the following typical parameters, viz., electron beam velocity $v_e^0 = 0.95c$, relativistic gamma factor $\gamma_0 = 3.2$, beam energy $E_b = 1.12MeV$, beam density $n_e^0 = 4\times10^{15} cm^{-3}$, beam current $I_e = 6.2\times10^{14} gm^{1/2} cm^{3/2} \sec^{-2}$, radius of the electron beam $r_e = 0.06cm$, length of modulator $l_m = 0.75cm$, drift space length $l_d = 1.5cm$, pump wave frequency $\omega_l = 7\times10^{13} rad \sec^{-1}$, radius of the cylindrical waveguide $a_0 = 0.1cm$.

To investigate the effect of density modulation, the growth rate of the output radiation has been estimated in Fig. 3.3. From the figure it can be seen that for both the finite and infinite geometry, the growth rate decreases with the increase of output radiation frequency. The maximum value of the growth rate achieved for an unmodulated beam is $4.2\times10^9 \sec^{-1}$ while that for a density modulated beam, the growth rate attains the maximum value of $6\times10^9 \sec^{-1}$ which is nearly 43% higher than the unmodulated beam.

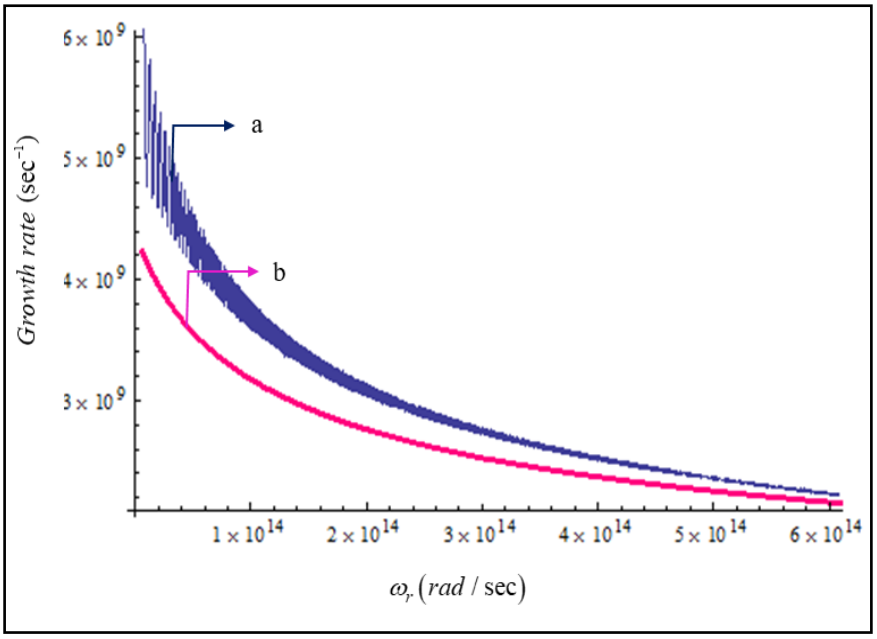

Fig 3.3. Growth rate of the unstable wave as a function of radiation frequency for (a) modulated REB and (b) unmodulated REB.

Fig. 3.4 illustrates the influence of pump field and radiation frequency on the growth rate of the output radiation for different electron beam densities (i.e., $4\times10^{15}cm^{-3}$, $8\times10^{15}cm^{-3}$ and $12\times10^{15}cm^{-3}$) in case of infinite geometry. The figure indicates that upon increasing the pump field and beam densities, the growth rate augments and scales as one-third of the beam density and two-third power of the pump field. The similar observation of increase of growth rate with beam density has been experimentally observed by Chang *et al.* [33] (cf. Fig. 4(b)). Furthermore, the growth rate decreases with increase of radiation frequency.

Fig. 3.5 shows the growth rate variation as a function of radiation frequency with the effect of applied magnetic field. The figure shows that in the presence of magnetic field the growth rate enhances to about19%which is maximum and is achieved when the electron cyclotron frequency is comparable to the pump wave frequency.

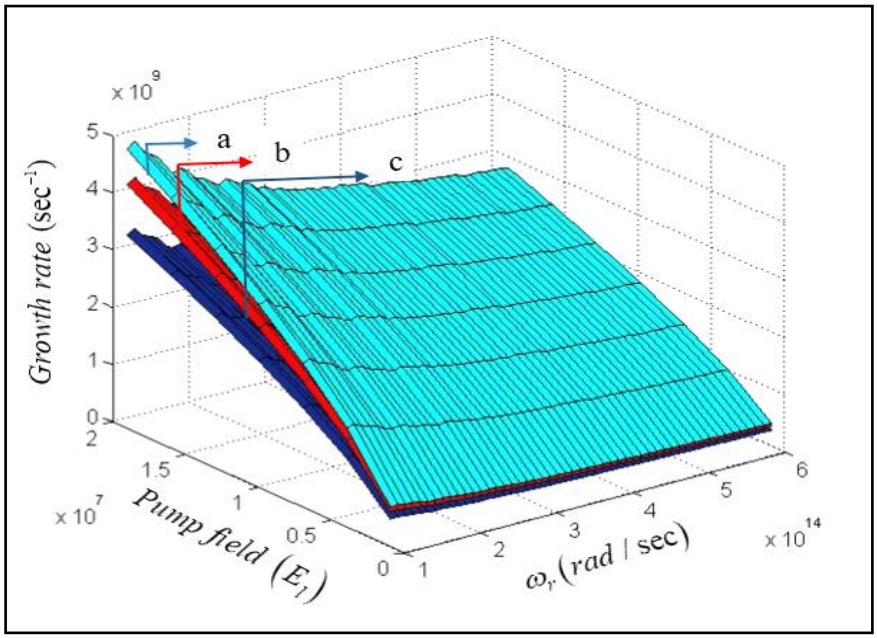

Fig 3.4. Variation of the growth rate with respect to field amplitude of the pump wave and radiation frequency at different values of beam densities for (a) $4\times10^{15}cm^{-3}$*, (b)* $8\times10^{15}cm^{-3}$ *and (c)* $12\times10^{15}cm^{-3}$.

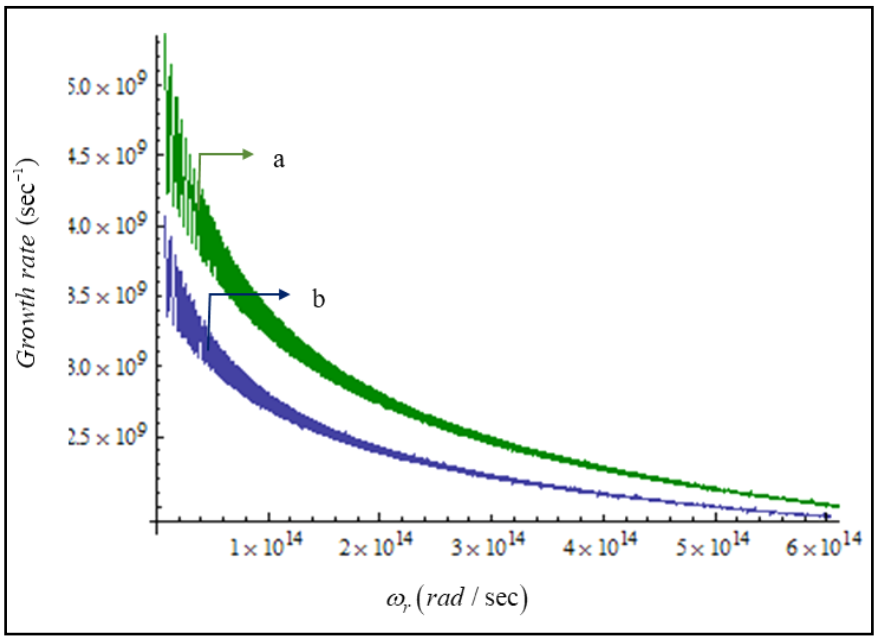

Fig 3.5. Growth rate versus radiation frequency (a) in the presence of external magnetic field and (b) in the absence of magnetic field.

In Fig. 3.6, we have illustrated the variation of the growth rate with the electron cyclotron frequency. Initially the growth rate increases with the magnetic field and then attains a maximum value at a point where the frequency of the pump wave becomes comparable to the electron cyclotron frequency and then starts decreasing with further increase of the magnetic field.

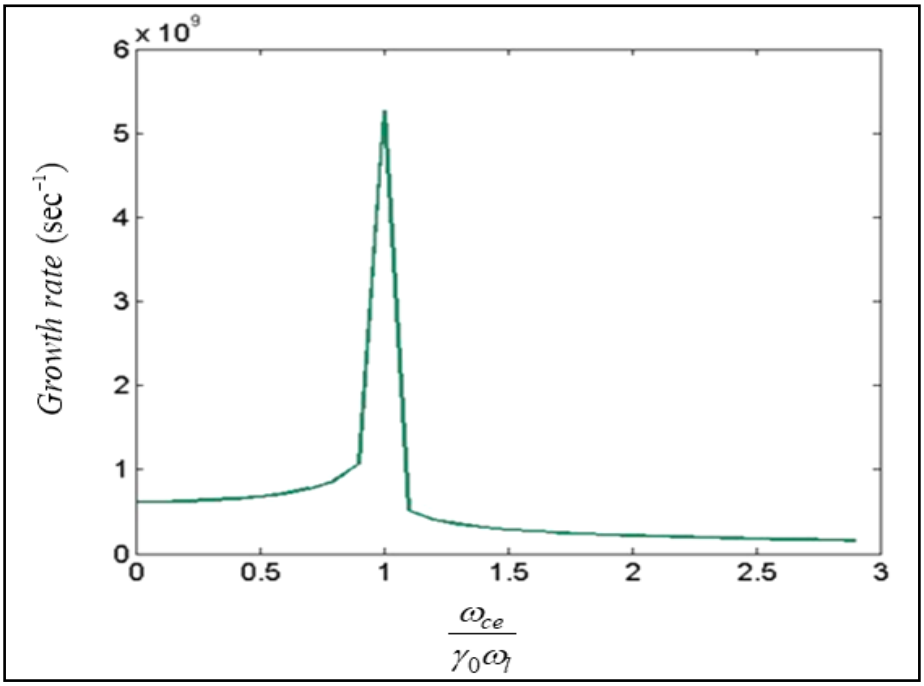

Fig 3.6. Variation of growth rate as a function of normalized electron cyclotron frequency.

Using Eq. (3.18), the dependence of output radiation frequency on the radius and modes of the cylindrical plasma column has been shown in Fig. 3.7. The figure shows that the frequency of the radiation increases with the modes of the wave and decreases with the radius of the waveguide. This behavior is similar to the findings of Malik *et al.* [34].

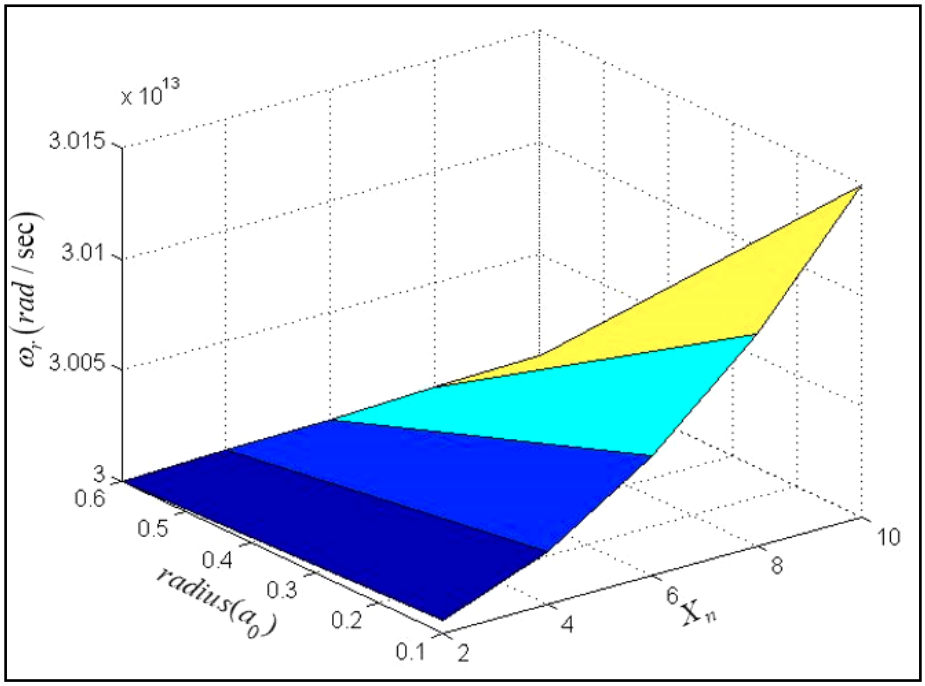

Fig 3.7. Radiation frequency as a function of radius of the cylindrical plasma column and modes of the wave.

Fig. 3.8 shows the variation of the growth rate with the radiation frequency for finite and infinite geometry. The decrease in growth rate is more in case of finite geometry in comparison to the infinite case (the same behavior has been observed by Bhasin and Sharma [30]. As seen from the Fig. 3.7 that the frequency of the radiation in case of finite geometry depends on the parameters of the geometry. Hence, the growth rate is bounded by the dimensions of the cylindrical plasma column and increases with increase in radius of the cylinder. Further, as the modes increases, the frequency increases and the growth rate decreases.

The efficiency of the emitted output radiation as a function of the radiation frequency has been plotted in Fig. 3.9. The efficiency falls off with the frequency and is low for the cylindrical plasma column as compared to the unbound plasma.

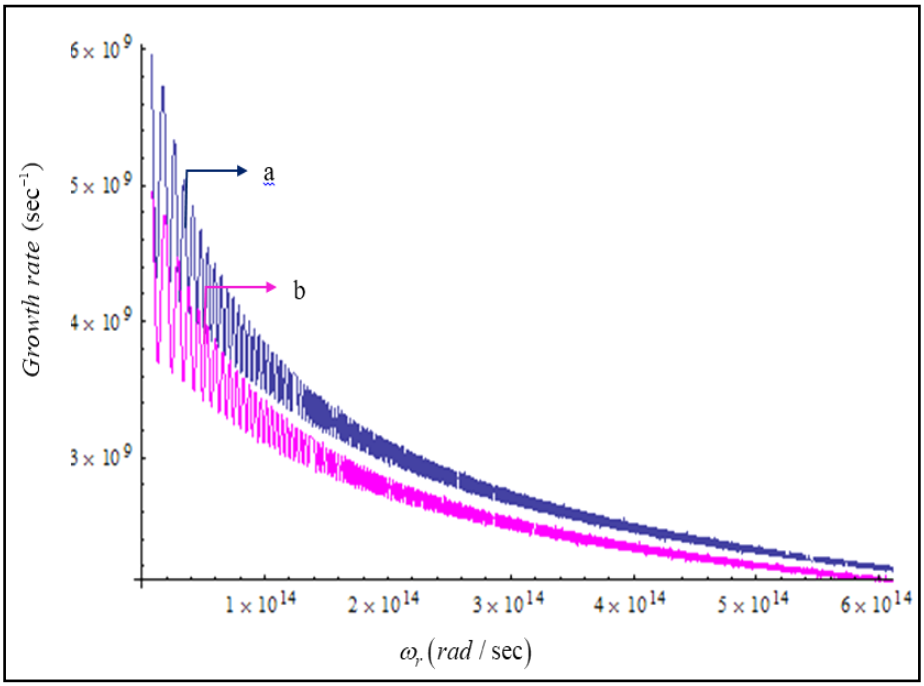

Fig 3.8. Growth rate as a function of radiation frequency for (a) infinite geometry and (b) finite geometry.

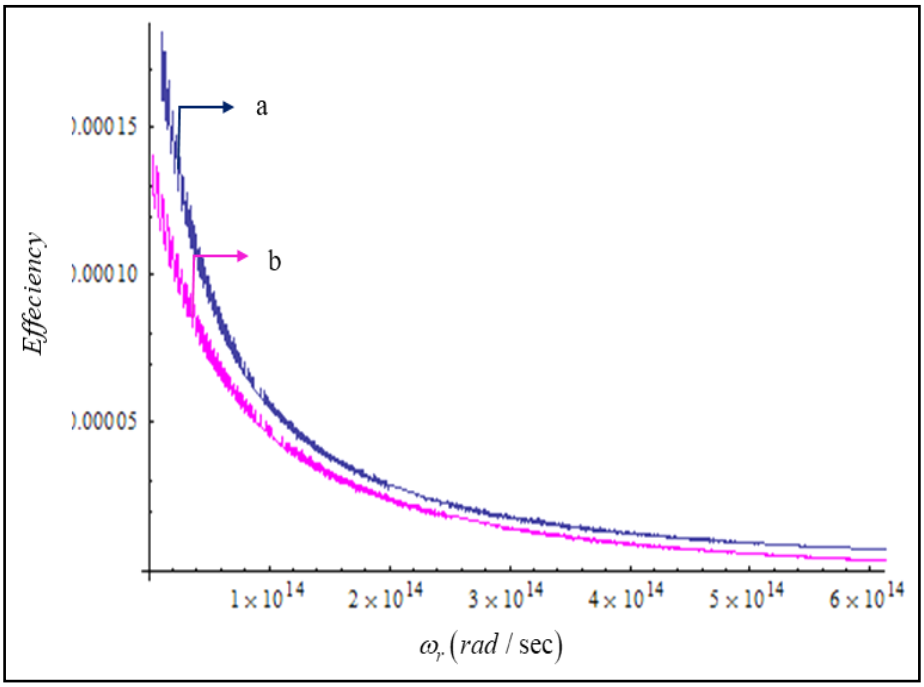

Fig 3.9. Efficiency as a function of radiation frequency for (a) infinite geometry and (b) finite geometry.

3.5 Conclusion

The emission of terahertz radiation has been studied with the effect of beam premodulation and in the presence of applied static magnetic field. The growth rate and efficiency of the radiation wave have been analyzed for both infinite and finite geometry. The growth rate decreases monotonically with the frequency of the output radiation. In case of finite geometry i.e., cylindrical plasma column the growth rate decreases as the modes increases and is bounded by the dimensions of the plasma column, thus the maximum value attained is less as compared to the infinite geometry. The modulation of the relativistic electron beam leads to an increase in the growth rate to about 43%. The growth of the radiation wave depends on the parameters of beam and the wiggler wave, and hence can be improved by increasing the density of the electron beam and amplitude of the pump wave. The applied static magnetic field leads to the enhancement of the growth rate until the electron cyclotron frequency becomes comparable to the pump wave frequency. The scheme thus holds importance in obtaining tunable radiation with high power.

References

[1] J. F. Federici, B. Schulkin, F. Huang, D. Gary, R. Barat, F. Oliveira and D. Zimdars, Semicond. Sci. Technol. **20,** S266 (2005).

[2] W. L. Chan, J. Deibel and D. M. Mittleman, Rep. Prog. Phys. **70,** 1325 (2007).

[3] M. Tonouchi, Nature Photonics **1**, 97 (2007).

[4] M.-A Brun, F. Formanek, A. Yasuda,M. Sekine, N. Ando and Y. Eishii, Phys. Med. Biol. **55,** 4615 (2010).

[5] A. R. Orlando, G. P. Gallerano, J Infrared Milli Terahz Waves **30**, 1308 (2009).

[6] G. H. Welsh and K. Wynne, Optics Express **17**, 2470 (2009).

[7] Y.-S. Lee, T. Meade, V. Perlin, H. Winful, T. B. Norris, and A. Galvanauskas, Appl. Phys. Lett. **76**, 2505 (2000).

[8] L. Bhasin and V. K. Tripathi, Phys. Plasmas **16**, 103105 (2009).

[9] S. C. Sharma, J. Panwar and R. Sharma, Contrib. Plasma Phys. **57**, 167 (2017).

[10] J. G. Neumann, R. B. Fiorito, P. G. O'Shea, H. Loos, B. Sheehy, Y. Shen, and Z. Wu, J. Appl. Phys. **105**, 053304 (2009).

[11] Avi Gover, Phys. Rev. ST Accel. Beams **8**, 030701 (2005).

[12] S. C. Sharma and P. Malik, Phys. Plasmas **22**, 043301 (2015).

[13] C. Joshi, T. Katsouleas, J. M. Dawson, Y. T. Yan and Jack M. Slater, IEEE J. Quantum Electronics **23**, 1571 (1987).

[14] M. Singh, S. Kumar and R. P. Sharma, Phys. Plasmas **18**, 022304 (2011).

[15] S. C. Sharma, J. Sharma, A. Bhasin and R. Walia, J. Plasma Physics **78**, 635 (2012).

[16] S. H. Zolghadr, S. Jafari, and A. Raghavi, Phys. Plasmas **23**, 053104 (2016).

[17] S. Hussain, R. K. Singh, and R. P. Sharma, Phys. Plasmas **23**, 073120 (2016).

[18] N. Yugami, T. Higashiguchi, H. Gao, S. Sakai, K. Takahashi, H. Ito, and Y. Nishida, Phys. Rev. Lett **89**, 065003 (2002).

[19] V. K. Tripathi and C. S. Liu, IEEE Trans. On Plasma Science **18**, 466 (1990).

[20] H. Mehdian, S. Jafari and A. Hasanbeigi, Plasma Phys. Control. Fusion **52**, 055005 (2010).

[21] R. Hedayati, S. Jafari and S. Batebi, Plasma Phys. Control. Fusion **57**, 085007 (2015).

[22] V. Bandhu Pathak, D. Dahiya and V. K. Tripathi, J. Appl. Phys. **105**, 013315 (2009).

[23] M. Kumar and V. K. Tripathi, Phys. Plasmas **18**, 053105 (2011).

[24] V. B. Gildenburg and N. V. Vvedenskii, Phys. Rev. Lett. **98**, 245002 (2007).

[25] M. Kumar and V. K. Tripathi, Phys. Plasmas **19**, 073109 (2012).

[26] W. L. Kruer, *The Physics of Laser Plasma Interactions* (Addison-Wesley Publishing, 1988).

[27] Basudev Ghosh, *Basic Plasma Physics* (Alpha Science International, 2014).

[28] V. K. Tripathi and C. S. Liu, IEEE Trans. On Plasma Science **17**, 583 (1989).

[29] D. Tripathi, R. Uma and V. K. Tripathi, Phys. Plasmas **19**, 093105 (2012).

[30] A. Bhasin and S. C. Sharma, Phys. Plasmas **14**, 073102 (2007).

[31] J. D. Jackson, *Classical Electrodynamics* (John Wiley & Sons, 1962).

[32] C. S. Liu and V. K. Tripathi, *Interaction of Electromagnetic Waves with Electron Beams and Plasmas* (World Scientific Publishing Co. Pvt. Ltd., Singapore, 1994).

[33] R. P. H. Chang, Phys. Rev. Lett. **35**, 285 (1975).

[34] Anil K. Malik, Hitendra K. Malik and Shigeo Kawata, J. Appl. Phys. **107**, 113105 (2010).

Chapter 4

TERAHERTZ RADIATION EMISSION FROM A SURFACE WAVE PUMPED FREE ELECTRON LASER

4.1 Brief Outline of the Chapter

We develop an analytical formalism for tunable coherent terahertz (THz) radiation generation from bunched relativistic electron beam (REB) counter –propagating to the surface wave in the vacuum region Compton backscatters the surface wave. Plasma supports the surface wave that acquires a large wave number around pump wave frequency. The surface wave extends into vacuum region and can be employed as a wiggler for the generation of terahertz radiation. As the beam bunches pass through the surface plasma wave wiggler, they acquire a transverse velocity, constituting a transverse current producing coherent THz radiation. It was found that the terahertz power increases with electric field as well as with the thermal velocity of electrons. It was also found that the growth rate and efficiency of the instability both increases with the modulation index of the density modulated beam.

4.2 Introduction

Recently, there has been a great deal of interest in generation of high power terahertz radiation due to its non-ionizing behavior and good penetrating power and hence its applications in wide areas including medical imaging, chemical and security identification, spectroscopy analysis, remote sensing[1-3]. The main aspects of generating terahertz radiation of high power lies in using a prebunched or a modulated electron beam interacting with the wiggler in a free electron laser where it exchanges the energy with the electromagnetic radiation. The beam transfers the energy to the radiation wave and the wave gets amplified [4-11].The kind of the wave excited due to beam-plasma interaction depends on the parameters of beam and plasma, mainly the three parameters: wiggler period, beam velocity and the phase velocity of the radiation [6].

Chen *et al.* [7] investigated the generation of the radiation by the interaction of relativistic circularly polarized laser pulses with overdense plasma which allows large plasma density and high pump laser intensity. Kumar and Tripathi [8] have studied that the coupling of a relativistic electron beam, modulated by two laser beams with a magnetic wiggler. They observed that THz power increases with the beam velocity and varies linearly with the bunch length and scales as square of the bunch radius. Neumann *et al.* [9] have experimentally demonstrated the generation of multiple sub picoseconds pulses repeated at the terahertz frequencies with a modified drive laser by creating the highly modulated electron beams at the photocathode. Sharma *et al.* [10] have examined the growth rate, efficiency of the radiation by employing an interaction of an energy modulated electron beam with the surface plasma wave as wiggler at vacuum plasma interface. They observed that the phase velocity of the radiation can be reduced by plasma which helps in the decrease of beam energy required for generating the radiation.

Yugami *et al.* [11] have experimentally demonstrated the generation of the radiation by the coupling of the wake field with the magnetic field and observed that the

relative power of the radiation varied with the square of the applied magnetic field strength and increases with the increase of the density. They also suggested that the frequency can be tuned by varying the pressure of the supersonic gas, used to create the vacuum-plasma interface. Singh *et al.* [12] observed the coupling of an oscillatory velocity of electron beam produced by the laser beam incident on the metal surface with the density perturbation produced by the surface plasma wave propagating along a metal-free space boundary via the generation of nonlinear current and observed that power of the radiated beam increases monotonically with the frequency of the probing laser and the SPW field. Kraft *et al*.[13] have studied the generation of the wave by injecting the beam at an angle to the magnetic field and concluded that the emission is very weak in case of parallel propagation and is not affected by the beam modulation whereas the emission is improved upto 50% if incident obliquely.

For the generation of the radiation by the upper hybrid wave FEL, the plasma density must be greater than the beam density, otherwise the frequency of the upper hybrid wave will approach the cyclotron frequency and hence it will lead to cyclotron damping, investigated by Sharma and Tripathi [14]. Pathak *et al.* [15] have reported the generation of terahertz radiation using free electron laser in rippled density plasma and observed that the growth rate is affected by the plasma density, amplitude, depth of density ripple and the transverse component of the ripple wave vector. Liu and Tripathi [16] employed a layered dielectric with periodic permittivity in space as a wiggler for the generation of the radiation and observed that the beam energy requirement is considerably as compared to one without dielectric. Sharma and Singh [17] investigated that the two cross focused lasers in the presence of collisional plasma were able to produce nonlinear current at the terahertz frequency. They observed that the amplitude and power of the wave increases with the amplitude of the static electric field. Leemans *et al.* [18] observed that the radiation is emitted at the plasma boundary when the pre-bunched beam is

highly dense and scales quadratically with the density for larger wavelengths as compared to the bunch length.

In this chapter, we study the Terahertz radiation emission from the surface wave pumped FEL and examine the growth rate and efficiency of the generated terahertz radiation by a density modulated relativistic electron beam counter-propagating surface plasma wave. The surface wave degrades as it moves away from the surface $\left(k_{0x} << k_{0z}\right)$ and hence they have large amplitude at low powers. The SPW is a guided electromagnetic wave which propagates between the two media with different conductivities and dielectric properties along the boundary [19, 20]. The dispersion relation for the surface plasma wave (SPW) is derived in Sec. 4.3. We have considered the vacuum-plasma interface and calculated the growth rate, power and efficiency of the generated wave in the Sec. 4.4. The results are discussed in Sec. 4.5 and the conclusion is given in Sec 4.6.

4.3 Theoretical Dispersion Relation

We consider a relativistic pre-bunched electron beam which is density modulated traveling in the $z-$ direction and a vacuum-plasma interface with SPW propagating above the interface. The interface is taken at $x=0$, with vacuum present above $x=0$ and plasma below $x=0$, both occupying half of the spaces. The vacuum has permittivity unity i.e., $\varepsilon_0=1$ and plasma with effective permittivity, $\varepsilon_{eff}=1-\frac{\omega_p^2}{\omega_0^{02}}$ with $\omega_p^2=\frac{4\pi n_0 e^2}{m_e}$, where ω_p is the plasma frequency and ω_0^0 is the SPW frequency. The plasma is characterized by lattice dielectric constant ε_L and conductivity as $\sigma=\frac{n_0 e^2}{m_e \omega_0^0}$, where n_0 is the plasma density, e is the electronic charge and m_e is the mass of the electron.

The electric field of the SPW propagating along the interface is given as

$$\vec{E} = Ee^{-i(\omega_0^0 t - k_{wz} z)}\hat{x}. \tag{4.1}$$

Electric field is polarized in the $x-z$ plane. Using the Maxwell's III and IV equations, we obtain

$$\nabla^2 \vec{E} + \omega_0^{02} / c^2 \in \vec{E} = 0, \tag{4.2}$$

which can be written as

$$\partial^2 E_z / \partial x^2 - k_p E_z = 0, \quad \text{for plasma} \tag{4.3}$$

and

$$\partial^2 E_z / \partial x^2 - k_v E_z = 0, \quad \text{for vacuum} \tag{4.4}$$

with $k_p^2 = k_{wz}^2 - \frac{\omega_0^{02}}{c^2}\varepsilon$ and $k_v{}^2 = k_{wz}{}^2 - \omega_0^{02}/c^2$, where c is the speed of light and k_p, k_v are the plasma wave vector and vacuum wave vector, respectively.

The solutions of above equations can be given as

$$\overrightarrow{E_z} = A_p e^{k_p x} e^{-i(\omega_0^0 t - k_{wz} z)}, \text{ for plasma} \tag{4.5}$$

and

$$\overrightarrow{E_z} = A_v e^{-k_v x_e} {}^{-i(\omega_0^0 t - k_{wz} z)}, \text{ for vacuum} \tag{4.6}$$

The dispersion relation for SPW can be obtained by applying the boundary conditions at $x = 0$ for E_z and εE_z continuous at the boundary

$$k_{wz}^{02} = \frac{\omega^2}{c^2}\left(\frac{\varepsilon}{1+\varepsilon}\right), \tag{4.7}$$

where $\varepsilon = k_p / k_v$.

In order to ensure that the surface wave is spatially damped away from the interface, we require $k_z^2 < 0$ i.e., $1+\varepsilon < 0$ or $\omega < \frac{\omega_p}{\sqrt{1+\varepsilon}} \simeq \omega < \frac{\omega_p}{\sqrt{2}}$ such that $k_p, k_v \to \infty$. Thus the waves are strongly localized near the surface.

4.4 Beam Wiggler Interaction

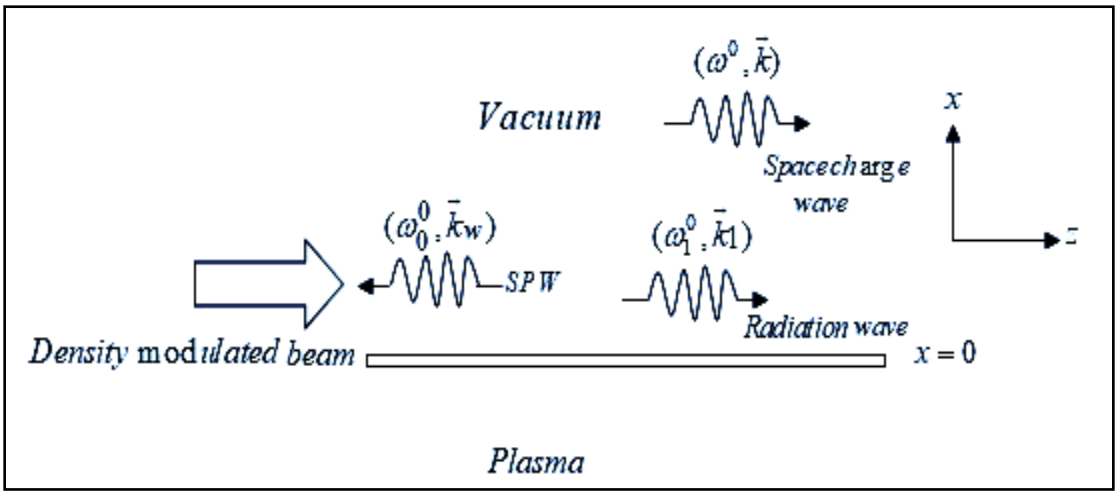

Fig. 4.1. Schematic diagram of SPW-pumped FEL.

The density modulated prebunched electron beam interacts with the surface plasma wave which acts as a wiggler in the present case. The initial parameters of the beam are: n_b^0 as the initial beam density and beam velocity v_b^0. In the free electron laser, we have considered the propagation of SPW as a wiggler wave. The electron beam when interacts with the SPW, acquires an oscillatory velocity $\overrightarrow{v_0^0}$ that can be obtained by using the equation of motion

$$m_e\left[\frac{\partial(\gamma\overrightarrow{v_0^0})}{\partial t}+(\overrightarrow{v_b^0}.\nabla)(\gamma\overrightarrow{v_0^0})\right]=-e\left(\vec{E}+\frac{1}{c}\overrightarrow{v_0^0}\times\vec{B}\right), \tag{4.8}$$

On solving this equation with $\vec{B}=\frac{c}{\omega_0^0}\left(\overrightarrow{k_w}\times\vec{E}\right)$ and taking different components of velocity, we obtain the x-component of oscillatory velocity as

$$v_{0x}^0=\frac{eE_{0z}}{m_e\omega_0^0\gamma_0}\left(\frac{k_{wz}}{k_{0v}}+\frac{k_{0v}v_b^0}{(\omega_0^0-k_{wz}v_b^0)}\right). \tag{4.9}$$

The equilibrium can be perturbed by applying the electromagnetic perturbation with perturbed values of electric field $\left(\overrightarrow{E_{1x}}\right)$, magnetic field $\left(\overrightarrow{B_1}\right)$ and beam velocity $\left(\overrightarrow{v_1^0}\right)$ as $\overrightarrow{E_{1x}}=\overrightarrow{A_1}e^{-i(\omega_1^0t-k_{1z}z)}$, $\overrightarrow{B_1}=\frac{c}{\omega_1^0}(\overrightarrow{k_1}\times\overrightarrow{E_1})$, and $\overrightarrow{v_1^0}=\frac{e\overrightarrow{E_1}}{im\omega_1^0\gamma_0}$, respectively.

Ponderomotive force is exerted by the FEL radiation and the SPW on the beam electrons with the equation of motion as

$$m\frac{\partial\vec{v}}{\partial t}=-e\vec{E}+\overrightarrow{F_p}-\frac{1}{n}\nabla(nT_e), \tag{4.10}$$

where $\overrightarrow{F_p}=-m(\vec{v}.\nabla)\vec{v}-\frac{e}{c}(\vec{v}\times\vec{B})$ is the ponderomotive force. The z-component of the ponderomotive force is given as $F_{pz}=e\nabla\phi_p$.

The ponderomotive force produces perturbed oscillatory velocity $\left(\overrightarrow{v_2^0}\right)$ of the electrons in the axial direction with density perturbation $\left(n_2\right)$ obtained using the equation of motion and equation of continuity, respectively as

$$v_{2b}^0 = -\frac{ek_z\phi_p}{m_e\gamma_0^3(\omega^0 - k_z v_b^0)}, \tag{4.11}$$

$$n_{2b} = \frac{k_z^2}{4\pi e}\chi_b\phi_p, \tag{4.12}$$

where $k_z\left(=k_{wz}+k_{1z}\right)$ and $\omega^0\left(=\omega_0^0+\omega_1^0\right)$ are the wave number and frequency of the space charge wave, respectively, $\phi_p\left(=-\frac{m_e\gamma_0}{2e}v_{1x}^0 v_{0x}^{0\,*}\right)$ is the ponderomotive potential and $\chi_b\left(=-\frac{\omega_{pb}^2}{\left(\omega^0 - k_z v_b^0\right)^2\gamma_0^3}\right)$ is the beam susceptibility.

In case of Compton regime, the potential of the beam mode is much less than the ponderomotive potential $\left(\phi << \phi_p\right)$ and hence can be neglected.

The beam density can be defined as $n_b^0 = n_b^0 + n_{1b}^0 + n_{bm}^0$, where n_{bm}^0 is the modulated beam density such that $n_{bm}^0 = \Delta n_b^0$, Δ being the modulation index.

On solving the equation of continuity, we get

$$n_{1b} = \frac{n_b^0\overrightarrow{v_{1b}^0}}{(\omega^0 - k_z v_{0b}^0)}\left[k_z(1+\Delta)+k_{wz}\Delta\right]. \tag{4.13}$$

The perturbed non-linear current density can be given as

$$\overrightarrow{J_1^{NL}} = -en_b^0\overrightarrow{v_{1b}^0} - en_{1b}^0\overrightarrow{v_b^0} - en_{bm}^0\overrightarrow{v_{1b}^0}. \tag{4.14}$$

which can be simplified to

$$\overrightarrow{J_1^{NL}} = \frac{ie^2 n_b^0 k_z v_{0x}^0 \overrightarrow{E_1}}{2m_e \omega_1^0 \gamma_0^3 (\omega^0 - v_b^0 k_z)} \left[(1+\Delta) + \frac{v_b^0}{(\omega^0 - v_b^0 k_z)} (k_z (1+\Delta) + k_{wz} \Delta) \right]. \quad (4.15)$$

On using Maxwell's III and IV equations

$\nabla \times \vec{E} = -\frac{1}{c} \frac{\partial \vec{B}}{\partial t}$ and $\nabla \times \vec{H} = \frac{4\pi}{c} \overrightarrow{J_1} + \frac{1}{c} \frac{\partial \overrightarrow{E_1}}{\partial t}$ as

$$\left(\omega_1^{02} - k_{1z}^2 c^2 \right) \left(\omega^0 - v_b^0 k_z \right)^2 = \frac{4\pi \omega_1^0 e^2 n_b^0 k_z v_{0x}^0 v_b^0}{2m_e \omega_1^0 \gamma_0^3} [k_z (1+\Delta) + k_{wz} \Delta], \quad (4.16)$$

On assuming that $\omega^0 = k_z v_b^0 + \delta$ and $\omega_1^0 = k_{1z} c + \delta$, we obtain

$$\delta = \left[\frac{\pi e^2 n_b^0 k_z v_{0x}^0 v_b^0}{\omega_1^0 m_e \gamma_0^3} (k_z (1+\Delta) + k_{wz} \Delta) \right]^{1/3} e^{\frac{2in\pi}{3}}, \quad (4.17)$$

where δ is the small frequency mismatch. The growth rate Γ of the instability is obtained by taking the imaginary part of δ i.e., $\Gamma = \mathrm{Im}\,\delta$, Hence, the growth rate is given as

$$\Gamma = \left[\frac{\omega_{pb}^2 v_{0x}^0 v_b^0}{c\gamma_0^3} \left((1+\Delta) \frac{\omega_1^0}{c} + k_{wz} \Delta \right) \right]^{1/3} \frac{\sqrt{3}}{2}, \quad (4.18)$$

where $\omega_{pb}^2 = \frac{4\pi n_{0b}^0 e^2}{m_e}$.

The power of the wave generated can be calculated using

$$P = \omega_0^0 \frac{\partial \varepsilon_0}{\partial \omega^0} \frac{E_0^2}{8\pi} v_g \pi r_b^2, \quad (4.19)$$

where $v_g \cong v_{th} = \sqrt{\frac{T_e}{m_e}}$ is the group velocity of the beam, v_{th} is the electron thermal velocity. T_e is the temperature of the plasma, and πr_b^2 is the cross section area of the beam.

The efficiency of the beam is given as $\eta = \frac{\Gamma}{\omega_1} \frac{\gamma_0^3}{\sqrt{3}(\gamma_0 - 1)}$,

On substituting the value of growth rate in the above expression, efficiency is obtained as

$$\eta = \left[\frac{\omega_{pb}^2 v_{0x}^0 v_b^0}{c} \left((1+\Delta) \frac{\omega_1^0}{c} + k_{wz} \Delta \right) \right]^{1/3} \frac{\gamma_0^2}{2\omega_1^0 (\gamma_0 - 1)}. \quad (4.20)$$

4.5 Results and Discussion

Standard parameters of THz radiation have been used for calculating the required parameters of the radiation which is obtained from the Surface Plasma wave pumped FEL. The typical parameters used for evaluating the growth and efficiency are: beam energy $E_b = 0.12 MeV$, beam current $I_b = 1.4 A$, beam radius $r_b = 2.4 cm$, electric field $E_0 = 100 esu$, and radiation frequency $\omega_1^0 = 3 \times 10^{12} rad \sec^{-1}$.

Figure 4.2 illustrates that the growth rate increases with the increase in the modulation index and has reached the largest value when $\Delta = 1$ and when the frequency and wave number of the generated radiation wave is of the order of the pre-bunched modulated electron beam. For the largest value of Δ i.e., $\Delta = 1$ the growth rate turns out to be $\Gamma = 1.85 \times 10^9 \sec^{-1}$. When $\Delta = 0$ i.e., without pre-modulated beam, the growth rate of the THz radiation is $\Gamma = 2.52 \times 10^9 \sec^{-1}$.

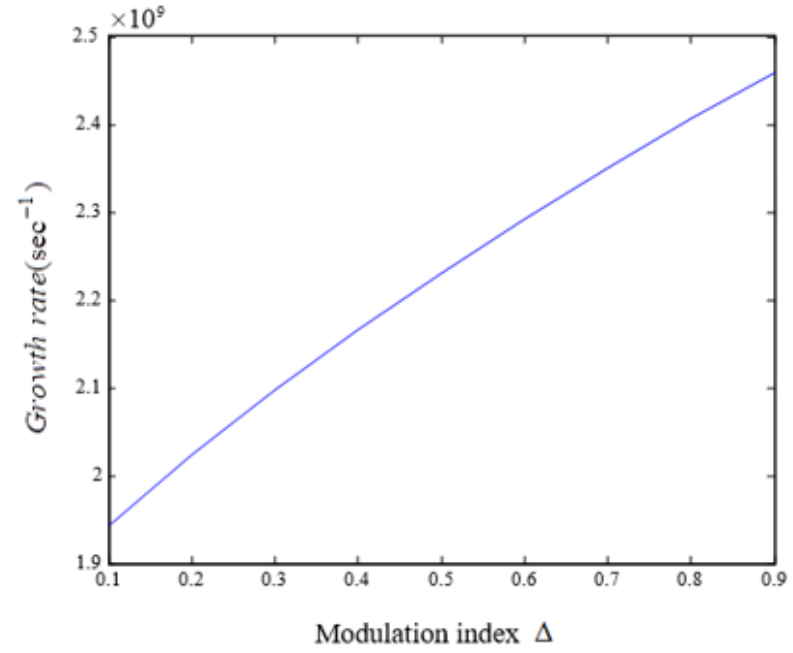

Fig 4.2. The figure shows the variation of growth rate as a function of the modulation index.

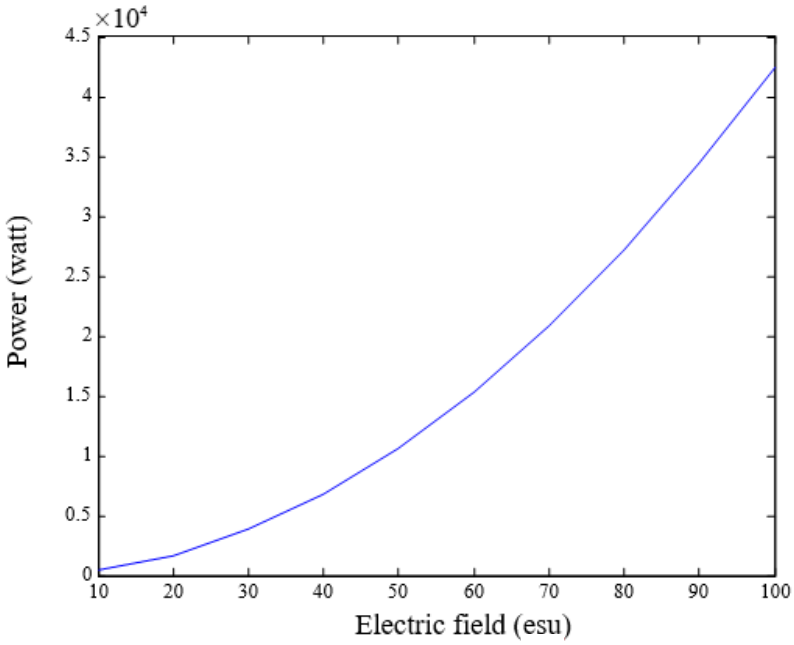

Fig 4.3. Variation of power of the radiated wave with the strength of the electric field.

Figure 4.3 shows that the power increases as we increase the electric field and comes out to be of the order of kilo watt. Hence by providing the suitable magnetic field, we can obtain an electric field of optimum value and therefore can be able to obtain the radiation of more high power, which is our motive.

Figure 4.4 shows that the power of the beam increases as the electron thermal velocity of electrons increases. The plot shows that the power increases linearly with the electron thermal velocity.

From Figure 4.5 it can be seen that the efficiency increases with the modulation index. The growth rate and efficiency scales as two-third power of the plasma frequency. Hence, it improves with an increase in plasma frequency, thus the plasma density.

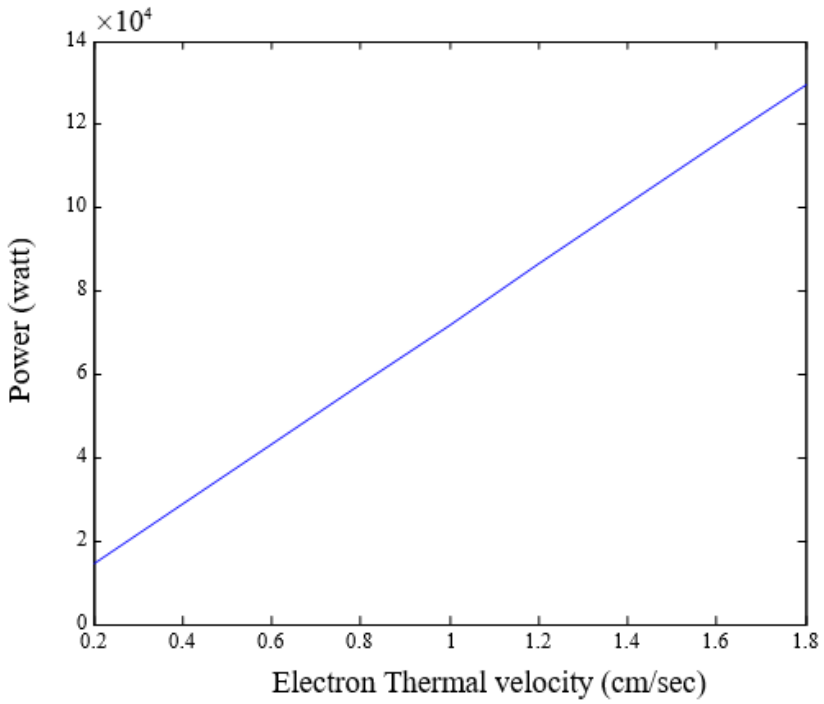

Fig 4.4. The figure illustrates variation of power with the thermal velocity of the electrons.

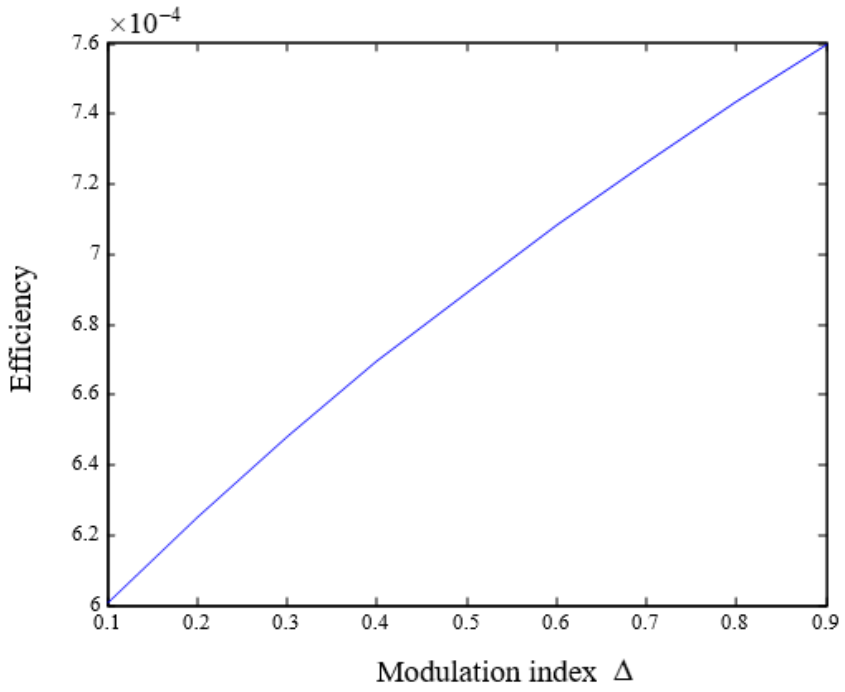

Fig 4.5. The figure shows the effect of modulation index on the efficiency of the radiation wave.

4.6 Conclusion

It can be concluded that the SPW are driven to instability by pre-bunched relativistic beam, which is density modulated leading to the increase in growth rate, amplitude and efficiency of the radiation wave with the modulation index and attained the largest value when it approached unity. The beam and plasma interaction leads to the growth of the radiation beam and the growth rate increases with the increase in plasma density. Using the SPW as a wiggler, it has been possible to generate high power radiation even at lower beam current. The density modulation has led to an improvement in the radiation generation of FEL instability and the radiation of desired frequency, and power can be obtained by varying the frequency and modulation index of the incident relativistic beam. Further plasma can help in reducing the phase velocity of the radiation wave significantly, thus helping in the decrease of beam energy required for generating THz radiation.

References

[1] M. Singh, S. Kumar and R. P. Sharma, Phys Plasmas **18**, 022304-1 (2011).

[2] V. B. Pathak, D. Dahiya and V. K. Tripathi, J. Appl. Phys. **105**, 013315-1 (2009).

[3] T. M. Antonsen, Jr. and John Palastro, H. M. Milchberg, Phys. Plasmas **14**, 033107-1 (2007).

[4] M. Cohen, A. Kugel, D. Chairman, M. Arbel, H. Kleinman, D. Ben-Haim, A. Eichenbaum, M. Draznin, Y. Pinhasi, I. Yakover, A. Grover, Nucl. Instr. and Meth. Phys. Res. **A**, 358 (1995).

[5] C. Kraft, G. Matthieussent, P. Thevenet, S. Bresson, Phys. Plasmas **1**, 2163 (1994).

[6] V. Beniwal, S. C.Sharma, and M. K. Sharma, Phys. Plasmas **11**, 5716 (2004).

[7] Zi-Yu Chen, Xiao-Ya Li and W. Yu, Phys. Plasmas **20**, 103115 (2013).

[8] M. Kumar and V. K. Tripathi, Phys. Plasmas **19**, 073109-1 (2012).

[9] J. G. Neumann, R. B. Fiorito, P. G. O'Shea, H. Loos, B. Sheehy, Y. Shen, and Z. Wu, J. Appl. Phys **105**, 053304 (2009).

[10] S. C. Sharma, J. Sharma, A. Bhasin and R. Walia, J. Plasma Physics **78**, 635 (2012).

[11] N. Yugami, T. Higashiguchi, H. Gao, S. Sakai, K. Takahashi, H. Ito, Y. Nishida, T. Katsouleas, Phys. Rev. Letter **89**, 065003-1 (2002).

[12] D. B. Singh, G. Kumar and V. K. Tripathi, J. Appl. Phys **101**, 043306-1 (2007).

[13] C. Kraft, G. Matthieussent, B. Lembege, Phys. Plasmas **1**, 4082 (1994).

[14] S. C. Sharma and V. K. Tripathi, IEEE Trans. Plasma Sci. **23**, 792 (1995).

[15] V. B. Pathak, D. Dahiya and V. K. Tripathi, J. Appl. Phys **105**, 013315-1 (2009).

[16] C. S. Liu and V. K. Tripathi, IEEE Trans. Plasma Sci. **23**, 459 (1995).

[17] R. P. Sharma and R. K. Singh, Phys Plasmas **21**, 073101-1 (2014).

[18] W. P. Leemans, J.van Tilborg, J. Faure, C. G. R. Geddes, Cs.Toth, C. B. Schroeder, E. Esarey, G. Fubiani, and G. Dugan, Phys. Plasmas **11**, 2899 (2004).

[19] C. S. Liu and V. K. Tripathi, *Electromagnetic Theory for Telecommunications, Foundation* (Delhi, 2007).

[20] C. S. Liu and V. K. Tripathi, *Interaction of Electromagnetic waves with Electron Beams and Plasmas* (World Scientific Singapore, 1994).

Chapter 5

TERAHERTZ RADIATION EMISSION USING PLASMA FILLED DIELECTRIC LINER WITH THE EFFECTS OF PREMODULATED RELATIVISTIC ELECTRON BEAM

5.1 Brief Outline of the Chapter

A theoretical model for the efficient emission of high power terahertz (THz) radiation has been proposed in this chapter. The premodulation of the beam is accounted by the interaction of the two laser beams with the relativistic electron beam (REB). The premodulated REB travels through a dielectric liner waveguide which is filled with isothermal plasma. The REB travels near the dielectric lining boundary and therefore transfers maximum energy to the electromagnetic radiation wave via Cerenkov interaction. The growth rate and efficiency of the radiation wave is examined and are found to be altered by the parameters of the REB and the dielectric medium. The growth rate varies as one-third power of the beam density and as two third power of the amplitude of the pump wave field. The proposed scheme seems to be an effective method for the generation of tunable THz radiation.

5.2 Introduction

For the past few decades, the area of emission of terahertz radiation has attracted researchers to explore new models to study its potentiality for various applications in the field of spectroscopy, biomedical imaging, security analysis and telecommunications [1-4]. Various schemes which involve the use of relativistic electron beam [5-7] and laser beams [8-9] have been employed to study the generation of THz radiation.

The emission of THz radiation by beating of two Gaussian laser pulse beams in rippled plasma with neutral-electron collision consideration has been proposed by Bakhtiari *et al*. [10]. They observed that by optimizing the parameters of the laser beams, collisional plasma and array structure, the efficiency of the radiation is enhanced to a considerable amount. Namiot *et al*. [11] have studied the generation and amplification of high frequency terahertz electromagnetic waves by employing a thin dielectric plate which does not behave as a slow wave structure but still the interaction is effective. The use of REBs employed in free-electron lasers results in a radiation with augmented growth and efficiency. The use of relativistic electrons in the emission of THz radiation via non-linear coupling with the plasma beat wave was proposed by Gupta *et al.* [12]. They found that the efficiency of the system improves with increase in the velocity of the beam.

Auger decay helps in the electronic structural analysis of solids, molecules, and atoms. Schütte *et al.* [13] studied the emission of Auger electrons due to the ionization of Xe and Kr in the strong oscillating field of THz radiation. Malik *et al*. [14] have proposed that the power and frequency of THz radiation, excited resonantly by the mixing of two Gaussian laser pulses in a periodic density rippled plasma in the presence of external magnetic field can be tuned by the magnetic field, periodicity and amplitude of the density ripples. The emission of terahertz radiation due to photoelectron current induced by the ionization of gas due to nonlinear

mixing of fundamental and second harmonic of the ultrashort laser pulses has been studied analytically by Kim *et al*. [15]. Recently, the excitation of electromagnetic wave by the interaction of self-modulated electron beam and overdense plasma has been studied by Yang *et al*. [16] by using PIC simulation. Due to the resonance between the plasma wakefield and electron beam, plasma oscillations are amplified to generate THz radiation. Wang *et al*. [17] have observed that the polarisation, frequency and amplitude of the electromagnetic wave can be altered by the bias applied to the plasma slab and the density of the plasma.

For the generation of THz radiation via Cerenkov interaction either use of a slow wave structure or a wiggler is employed. Cerenkov free electron laser acts as a slow wave structure by employing a dielectric lining in a waveguide and are proposed for the generation of millimetre and sub-millimetre wavelengths [18-20].The use of prebunched electron beam in free electron lasers leads to coherent emission with reduction in the accumulation time of the radiation [21, 22]. Sharma and Bhasin [23] have studied the effect of beam prebunching on Cerenkov free electron laser and found that significant improvement in gain and efficiency is observed if the frequency of the modulated electron beam becomes comparable to the radiation wave. Tripathi and Liu [24] have observed that for the generation of a particular frequency wave, the dielectric lining on the waveguide can withstand with high power densities and also reduces the constraint for beam voltage. Kibis *et al*. [25] have studied the emission of THz radiation by applying potential difference across the ends of a quasi-metallic carbon nanotube. The emission is found to be strongly influenced by the voltage applied in the ballistic regime.

A magnetized plasma medium which acts as nonlinear medium permits the propagation of electron beams with high current as it suppresses the space-charge effects. It also offers the possibility of using moderate energy electron beams for obtaining high frequency radiations [26, 27]. Antonsen *et al*. [28] have addressed that the propagation of laser pulses in miniature non uniform plasma channels, due

to the channel inhomogeneity and manifestation of guided waves, efficient excitation of radiation is achieved. Chauhan and Parashar [29] have analysed the emission of THz radiation for both homogenous and inhomogeneous plasma densities via the nonlinear mixing of lasers which are incident obliquely on the plasma slab. The generation of terahertz radiation by the direct conversion of an ultrashort laser pulse due to the excitation of oscillations of plasma has been suggested by Gildenburg and Vvedenskii [30]. Malik [31] has observed that the external magnetic field helps in obtaining collimated radiation with improved efficiency and tunability. The experimental investigations of Chen *et al*. [32] suggests that the use of multiple air plasmas leads to the efficient generation of terahertz radiation due to the superposition of individual fields. Singh and Malik [33] have analysed the contribution of collisional plasma under the influence of magnetic field on the efficiency and amplitude of the terahertz radiation.

As far as author's knowledge concern nobody has studied terahertz radiation emission by employing dielectric liner and premodulated REB. In this chapter, we have designed an analytical formalism to examine the generation of high frequency terahertz radiation wave by the interaction of density modulated REB with a dielectric lined waveguide in the presence of an external magnetic field. The mechanism of the scheme is as followed; first, the REB gets velocity modulated in the modulator region and then on travelling through the drift space, the velocity modulation is translated into the density modulation. The density modulated REB travels through the waveguide space in close proximity with the dielectric lining. The poynting flux is concentrated largely in the dielectric space and the velocity of the electromagnetic mode is reduced so that it becomes comparable with the beam velocity. At the expense of beam energy, the radiation wave grows. In Sec. 5.3 the dispersion characteristics of a TM mode in the waveguide is discussed. The premodulation of REB and its interaction with dielectric lined waveguide is shown in Sec. 5.4. The results are included in Sec. 5.5 and Sec. 5.6 concludes the investigations.

5.3 Physical Model

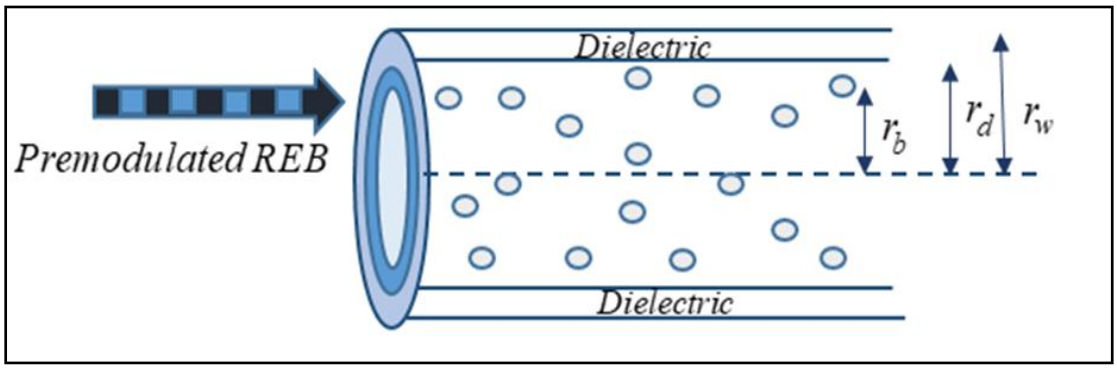

Fig 5.1. Schematic of interaction of density modulated REB with plasma filled dielectric lined waveguide.

In the present model, we examine the emission of THz radiation wave by taking into account the interaction of density modulated REB with a dielectric lined waveguide. First, for the premodulation of the REB, we consider two laser beams with frequencies ω_{l1} and ω_{l2}, respectively and with electric fields

$\overrightarrow{E_{l\eta}} = \overrightarrow{A_{l\eta}} e^{-i(\omega_{l\eta} t - k_{l\eta} z)}$, where $\eta = 1, 2$ for Laser 1 and 2, respectively.

A REB is propagating in z-direction with initial beam velocity v_{ib} and beam density n_{ib}.

The laser beams interact with the REB in the modulator region, where the beam acquires a transverse velocity component as $\overrightarrow{v_{l\eta}} = \dfrac{e\overrightarrow{E_{l\eta}}}{m_e \gamma_0 i\omega_{l\eta}}$, where $\gamma_0 = \left(1 - \dfrac{v_{ib}^2}{c^2}\right)^{-1/2}$ is the relativistic gamma factor, m_e is the electronic mass. The beam then gets velocity modulated at the frequency difference of two lasers (i.e.,

$\omega_{eb} = \omega_{l1} - \omega_{l2}$) due to the ponderomotive force $\overrightarrow{F_{bp}}$ exerted on the beam electrons due to the laser beams.

$$\overrightarrow{F_{bp}} = \frac{-e}{2c}\left[\overrightarrow{v_{l\eta}} \times \overrightarrow{B^*_{l\eta}} + \overrightarrow{v^*_{l\eta}} \times \overrightarrow{B_{l\eta}}\right] = F_{0b} e^{-i(\omega_{eb} t - k_{eb} z)}, \tag{5.1}$$

where $\overrightarrow{B_{l\eta}} = \frac{c(\overrightarrow{k_{l\eta}} \times \overrightarrow{E_{l\eta}})}{\omega_{l\eta}}$ is the magnetic field of laser beams, $F_{0b} = \frac{eA_{l1}A_{l2}k_{eb}}{2m_e\gamma_0\omega_{l1}\omega_{l2}}$, (ω_{eb}, k_{eb}) is frequency and wave number, respectively of the REB.

The beam electrons respond to ponderomotive force through relativistic equation of motion $\frac{d(\gamma\vec{v})}{dt} = \frac{\overrightarrow{F_b}}{m_e}$, which can be linearized to yield modulated beam velocity (v_b^m) using $\vec{v} = v_{ib}\hat{z} + v_b^m\hat{z}$ and $\gamma = \gamma_0 + \frac{v_{ib}\gamma_0^3 v_b^m}{c^2}$ as

$$v_b^m = -\xi_m v_{ib} \sin(\omega_{eb} t_M + \theta_m), \tag{5.2}$$

where $\xi_m = \frac{k_{eb} l_d}{2\gamma_0^4} \frac{c^2}{v_{ib}^2} \frac{e^2 A_{l1} A_{l2}^*}{m_e \omega_{l1} \omega_{l2} c^2} \frac{\sin\theta_m}{\theta_m}$, $\theta_m = \frac{(\omega_{em} - k_{em} v_{ib}) l_M}{2v_{ib}}$ is the phase angle of modulator, t_M is the time when beam enters the modulator region and l_M is the length of the modulator space.

The velocity modulated beam then travels through the drift space, where due to acceleration and deceleration, the velocity modulation translates into density modulation. Further following the analysis by Kumar and Tripathi [34], the expression of modulated beam density (n_b^m) can be given as

$$n_b^m = -2n_{ib}J_1\left(\frac{\omega_{eb}l_D\xi_m}{v_{ib}}\right)\cos(\omega_{eb}t_D - \phi_m), \tag{5.3}$$

where t_D is the time at which the beam leaves the drift space and enters the waveguide, $\phi_m = \frac{\omega_{eb}(l_M + l_D)}{v_{ib}} - \theta_m$, l_D is the length of the drift space and J_1 is the first order Bessel's function.

Next, we consider the interaction of density modulated REB with the TM mode. A cylindrical waveguide with dielectric lining is considered. The radius of the waveguide is r_w with plasma filled in the region I ($0 < r < r_d$) and the dielectric lining in the region II ($r_d < r < r_w$). Azimuthally symmetric TM mode is supported by the waveguide with $\overrightarrow{E_t^m} = \overrightarrow{A_t^m}e^{-i(\omega_t t - k_t z)}$, where (ω_t, k_t) is the frequency and wave number of the TM waveguide mode, respectively. The permittivity of the dielectric medium is ε_d and that of the plasma medium is $\varepsilon_p\left(=1-\frac{\omega_p^2}{\omega_t^2}\right)$, where $\omega_p\left(=\frac{4\pi n_{ep}e^2}{m_e}\right)^{1/2}$ is the electron plasma frequency, n_{ep} is the plasma electron density.

The current density of the premodulated electron beam leads to the excitation of TM mode in the plasma filled waveguide. The density profile of the electron beam is considered as $n_{ib} = N\delta(r - r_b)$, where $N = \frac{n_0}{2\pi r_b}$ and r_b is the radius of the electron beam. The premodulated beam travels in close proximity with the dielectric lining. A magnetostatic wiggler magnetic field, $\overrightarrow{B_h} = B_{0h}e^{-ik_h z}\hat{x}$ is introduced in the waveguide which acts as a pump field and a strong guide magnetic field B_s is externally applied such that it guides the beam in the axial direction in the waveguide.

The oscillatory velocity acquired by the beam electrons due to the pump wave in the frame of electron moving with velocity v_{ib} is obtained as $\overrightarrow{v'_{ob}} = \frac{e\overrightarrow{E'_h}}{im_e(\omega'_h - \omega'_{ce})}$, where ' denotes the quantities in the moving electron frame, $E'_h = \frac{\gamma_0}{c}\left(\overrightarrow{v_{ib}} \times \overrightarrow{B_h}\right)$, $\omega'_h = \gamma_0 k_h v_{ib}$ and $\omega'_{ce}\left(= \frac{eB'_s}{m_e c}\right)$ is the electron cyclotron frequency.

The equilibrium is perturbed by an electromagnetic perturbation due to the TM mode and the response of the mode to the electron beam in terms of perturbed beam velocity $\left(\overrightarrow{v'_{1b}}\right)$ is

$$\overrightarrow{v'_{1b}} = \frac{e\overrightarrow{E_t^{m'}}}{m_e i(\omega'_t - \omega'_{ce})}.$$

The pump wave and the electromagnetic perturbation exerts a pondermotive force ($\overrightarrow{F_{1p}}$) on the beam electrons, given as $F'_{1p} = eik'_{eb}\phi'_{1p}\hat{z}$, where

$$\phi'_{1p} = -\frac{m_e}{2e} v'^{*}_{ib} \cdot v'_{1b} = \frac{eE'^{*}_{hr} E^{m*}_{tr}}{2m_e(\omega'_h - \omega'_{ce})(\omega'_t - \omega'_{ce})}, \tag{5.4}$$

ϕ'_{1p} is the ponderomotive potential, phase matching condition demands $\omega'_t = \omega'_{eb} + \omega'_h$ and $k'_t = k'_{eb} + k'_h$.

The response of beam electrons to the ponderomotive potential in terms of perturbed beam velocity (v'_{bp}) and density (n'_{bp}) can be obtained as

$$v'_{bp} = -\frac{e\nabla'\phi'_{1p}}{m_e i\omega'_{eb}}$$

$$n_{bp}^{'}=\frac{\nabla^{'}\cdot\left(\left(n_{ib}^{'}+n_{b}^{m'}\right)v_{bp}^{'}\right)}{i\omega_{eb}^{'}}=\frac{en_{ib}^{'}\nabla^{'2}\phi_{1p}^{'}}{m_e\omega_{eb}^{'2}}, \tag{5.5}$$

where $n_{ib}^{'}=\frac{n_{ib}}{\gamma_0}$, $\phi_{1p}^{'}=\frac{\phi_{1p}k_{eb}}{k_{eb}^{'}}$, $k_{eb}^{'}=\gamma_0\left(k_{eb}-\frac{\omega_{eb}v_{ib}}{c^2}\right)$ and $\omega_{eb}^{'}=\gamma_0\left(\omega_{eb}-\kappa_{eb}v_{ib}\right)$ are the Lorentz transformed quantities from electron frame to the lab frame. The density of particles at $\left(\omega_t^{'},k_t^{'}\right)$ can be written as $n_{bp}^{1'}=\frac{\nabla'.\left(n_{bp}^{'}\overrightarrow{v_{ob}^{'}}\right)}{2i\left(\omega_t^{'}-\omega_{ce}^{'}\right)}$.

On using the Lorentz transformed quantities, the expression for nonlinear current density (J_{1b}) in the axial direction can be simplified to

$$J_{1bz}=-n_{bp}^{1}ev_{ib}=\frac{e^3\left(n_{ib}+n_b^m\right)v_{ib}^2B_h\nabla\cdot(\nabla^2\phi_{1p})}{2m_e^2\gamma_0^2\left(k_hv_{ib}-\omega_{ce}\right)(\omega_t-\omega_{ce})\left(\omega_{eb}-k_{eb}v_{ib}\right)^2}. \tag{5.6}$$

To analyse the TM mode, the wave equation is employed as

$$\frac{\partial^2\overrightarrow{E_{tz}}}{\partial r^2}+\frac{1}{r}\frac{\partial\overrightarrow{E_{tz}}}{\partial r}-\left(\frac{\omega_t^2}{c^2}\varepsilon-k_t^2\right)\overrightarrow{E_{tz}}=\frac{-4\pi i\omega_t}{c^2}\overrightarrow{J_{1bz}}. \tag{5.7}$$

The R.H.S of the above wave equation can be simplified to

$$\frac{e^4\pi\omega_t\left(n_{ib}+n_b^m\right)k_tv_{ib}^2B_h^2\left(1-\frac{v_{ib}}{\sqrt{\varepsilon}c}\right)\frac{\partial}{\partial r}\left(\frac{\partial^2E_{tr}}{\partial r^2}+\frac{1}{r}\frac{\partial E_{tr}}{\partial r}-k_t^2E_{tr}\right)}{m_e^3\gamma_0^3c\alpha^2\left(k_hv_{ib}-\omega_{ce}\right)^2\left(\omega_t-\omega_{ce}\right)^2\left(\omega_{eb}-k_{eb}v_{ib}\right)^2}. \tag{5.8}$$

where $E_{tr}=-i\left(\frac{k_t}{\alpha^2}\right)\frac{\partial E_{tz}}{\partial r}$.

The above expression drops to zero for region I and the solution is same as mentioned in Eq. (5.2) i.e., $E_{tz} = \varphi(r)$, where $\varphi(r) = A_{t1} I_0(\alpha r)$ for region I $\left(0 < r < r_d\right)$ and

$$\varphi(r) = A_{t2}\left[J_0(\beta r) - \frac{J_0(\beta r_w) Y_0(\beta r)}{Y_0(\beta r_w)} \right] \text{for region II } \left(r_d < r < r_w\right).$$

On considering the R.H.S expression (cf. Eq. 5.8), it is assumed that the eigenvalues are altered whereas the eigen function remains unchanged. For region II, the R.H.S. (cf. Eq. 5.8) tends to zero as there is no beam propagation. Eq. (5.7) is multiplied by $\varphi(r)\ r\ d\ r$ and on integrating it from $r = 0$ to r_w, we get

$$P \int_0^{r_d} I_0^2(\alpha r) r dr + Q \frac{A_{t2}^2}{A_{t1}^2} \int_{r_d}^{r_w} \left[J_0(\beta r) - \frac{J_0(\beta r_w) Y_0(\beta r)}{Y_0(\beta r_w)} \right]^2 r dr = \frac{R}{\left(\omega_{eb} - k_{eb} v_{ib}\right)^2}, \quad (5.9)$$

where $P = \left(\alpha^2 + \frac{\omega_t^2}{c^2} \varepsilon_p - k_t^2 \right)$, $Q = \left(\beta^2 - \frac{\omega_t^2}{c^2} \varepsilon_d + k_t^2 \right)$ and

$$R = \frac{e^4 \pi \omega_t \left(n_{ib} + n_b^m\right) v_{ib}^2 B_h^2 \left(1 - \frac{v_{ib}}{\sqrt{\varepsilon} c}\right) \int_0^{r_d} \frac{\partial}{\partial r} \left(\frac{\partial^3}{\partial r^3} + \frac{1}{r} \frac{\partial^2}{\partial r^2} - k_t^2 \frac{\partial}{\partial r} \right) I_0^2(\alpha r) r dr}{m_e^3 \gamma_0^3 c^3 \left(k_h v_{ib} - \omega_{ce}\right)^2 \left(\omega_t - \omega_{ce}\right)^2},$$

On taking k_t to be a constant value and varying the TM mode frequency around $\omega_t = \omega_{tm}$, we obtain

$$\left(\omega_t - \omega_{tm}\right) \left(\frac{\partial \alpha^2}{\partial \omega_t} + \frac{2\omega_t}{c^2} \varepsilon_p \right) \int_0^{r_d} I_0^2(\alpha r) r dr + \left(\frac{\partial \beta^2}{\partial \omega_t} - \frac{2\omega_t}{c^2} \varepsilon_d \right) \frac{A_{t2}^2}{A_{t1}^2} \times$$

$$\times \int_{r_d}^{r_w} \left[J_0(\beta r) - \frac{J_0(\beta r_w) Y_0(\beta r)}{Y_0(\beta r_w)} \right]^2 r dr = \frac{R}{\left(\omega_{eb} - k_{eb} v_{ib}\right)^2}. \quad (5.10)$$

The equation (5.10) is further simplified to

$$(\omega_t - \omega_{tm})\left(\omega_t - (k_t - k_h)v_{ib}\right)^2 = \frac{R}{\mathrm{T}\left(\frac{\partial\beta^2}{\partial\omega_t} - \frac{2\omega_t}{c^2}\varepsilon_d\right)}, \tag{5.11}$$

where

$$\mathrm{T} = \int_0^{r_d} I_0^2(\alpha r)\,r\,dr + \left[\frac{\frac{\varepsilon_d}{\varepsilon_p} I_0(\alpha r_d)Y_0(\beta r_w)}{J_0(\beta r_d)Y_0(\beta r_w) - J_0(\beta r_w)Y_0(\alpha r_d)}\right]^2 \times \int_{r_d}^{r_w}\left[J_0(\beta r) - \frac{J_0(\beta r_w)Y_0(\beta r)}{Y_0(\beta r_w)}\right]^2 r\,dr.$$

The growth rate Γ_{tm} of the radiation wave can be defined by using $\omega_t = \omega_{tm} + \delta_t = (k_t - k_h)v_{ib} + \delta_t$ and taking the imaginary part of δ_t,

$$\Gamma_{tm} = \frac{\sqrt{3}}{2}\left(\frac{Rc^2}{2\mathrm{T}\omega_t}\right)^{1/3}, \tag{5.12}$$

where δ_t is the small frequency mismatch.

For a completely plasma filled waveguide ($0 < r < r_d$), the dispersion relation for the TM mode is given as

$$\omega_t^2 = \omega_c^2 + \frac{k_t^2 c^2}{\varepsilon_p}, \tag{5.13}$$

where ω_c is the mode cut off frequency of the waveguide.

From the relation $\varepsilon_p = \left(1 - \frac{\omega_p^2}{\omega_t^2}\right)$, it can be inferred that the increase in plasma density leads to the decrease in plasma permittivity and from Eq. (5.13), it can be seen that this will lead to increase in radiation frequency. Thus, the growth rate of the radiation wave falls off with the increase of plasma density.

The efficiency (η_{tm}) of the radiation wave can be expressed as

$$\eta_{tm} = \frac{\Gamma_{tm}}{\omega_t} \frac{\gamma_0^3}{\sqrt{3}(\gamma_0 - 1)} = \frac{1}{2}\left(\frac{Rc^2\gamma_0^9}{T\omega_t^4(\gamma_0 - 1)^3}\right)^{1/3}. \quad (5.14)$$

5.4 Results and Discussion

The present study has been done to analyze the growth rate and efficiency of the radiation wave by considering an analytical model in which density modulated REB interacts with the slow wave structure. The effect of beam and dielectric medium has been realized on the output THz radiation for which the following typical parameters are considered, namely, REB velocity $v_{ib} = 0.94c$, relativistic gamma factor $\gamma_0 = 2.94$, density of beam $n_{ib} = 9 \times 10^{14} cm^{-3}$, length of the modulator space $l_M = 0.55cm$, drift space length $l_D = 1.2cm$, electron beam radius $r_b = 0.02cm$, radius of waveguide $r_w = 0.04cm$, width of dielectric lining $(r_w - r_d) = 0.01cm$.

The influence of different beam densities on the growth rate of the output radiation with radiation frequency has been depicted in Fig. 5.2. The figure shows that the growth rate of the wave rises with the increase in the density of the electron beam. This is because with the increase in the beam density, more number of electrons are

available to transfer their energy to the radiation wave, at the expense of which the wave grows. Further, the growth rate declines with the increase of the radiation frequency.

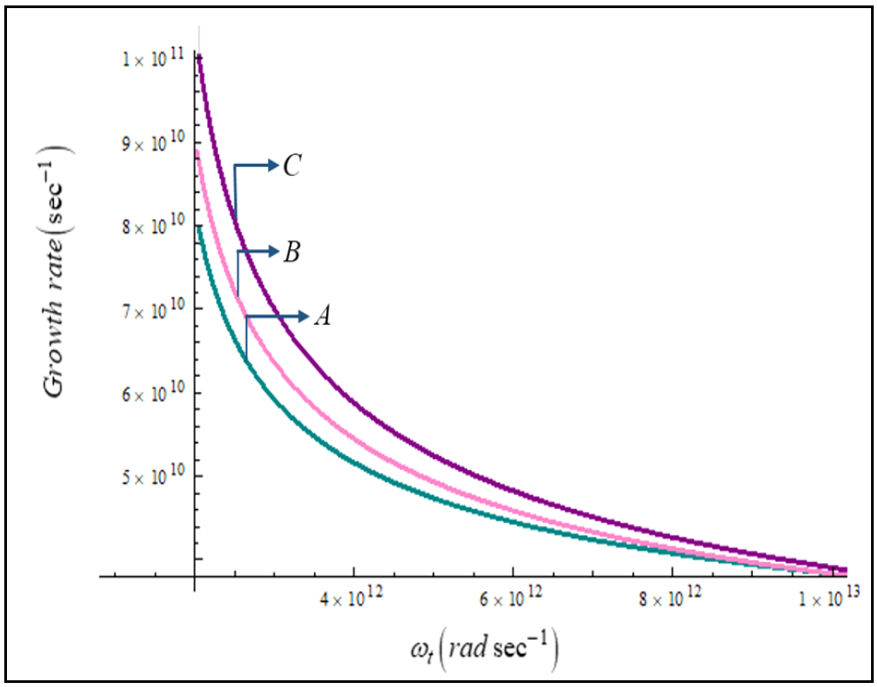

Fig 5.2. Growth rate variation with radiation frequency for different beam densities for (A) $n_{ib} = 8\times10^{14} cm^{-3}$, *(B)* $n_{ib} = 10\times10^{14} cm^{-3}$, *(C)* $n_{ib} = 12\times10^{14} cm^{-3}$.

Fig. 5.3 illustrates the effect of beam velocity on the growth rate of the radiation wave for different dielectric constant. As the dielectric constant increases, the phase velocity of the electromagnetic mode is reduced in order to have substantial interaction with the electron beam and hence the growth rate enhances. Further with the increase of beam energy the frequency of the wave increases and hence the growth rate declines with the beam velocity.

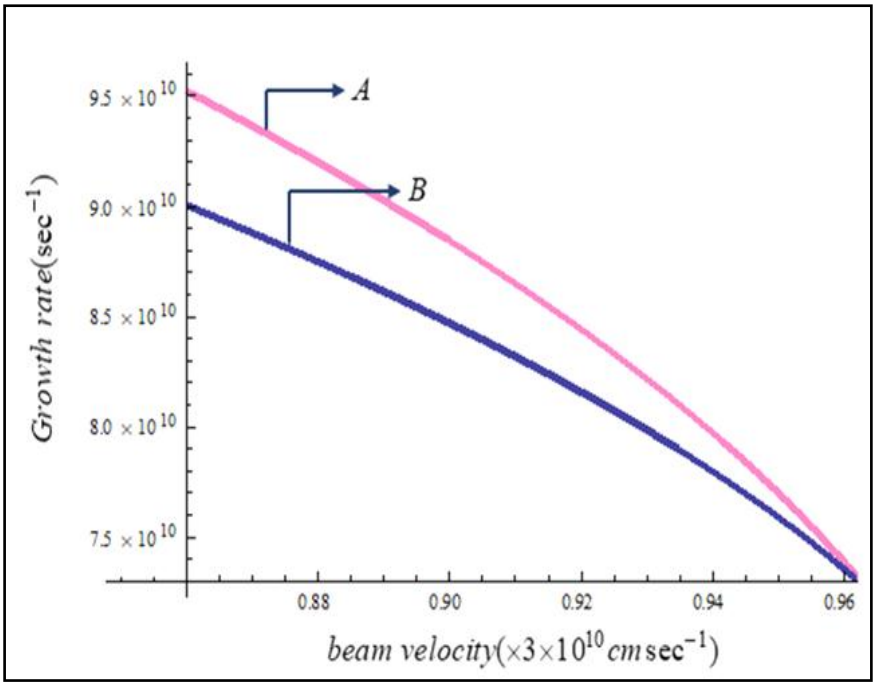

Fig 5.3. Variation of growth rate with beam velocities for different dielectric constant for (A) $\varepsilon_d = 2.1$, *(B)* $\varepsilon_d = 1.7$.

The influence of applied external magnetic field on the THz radiation has been shown in Fig. 5.4. The growth rate initially rises as the magnetic field is increased but at particular value of the magnetic field, the frequency of the pump field becomes comparable to the electron cyclotron frequency, where a peak with maximum growth rate is achieved.

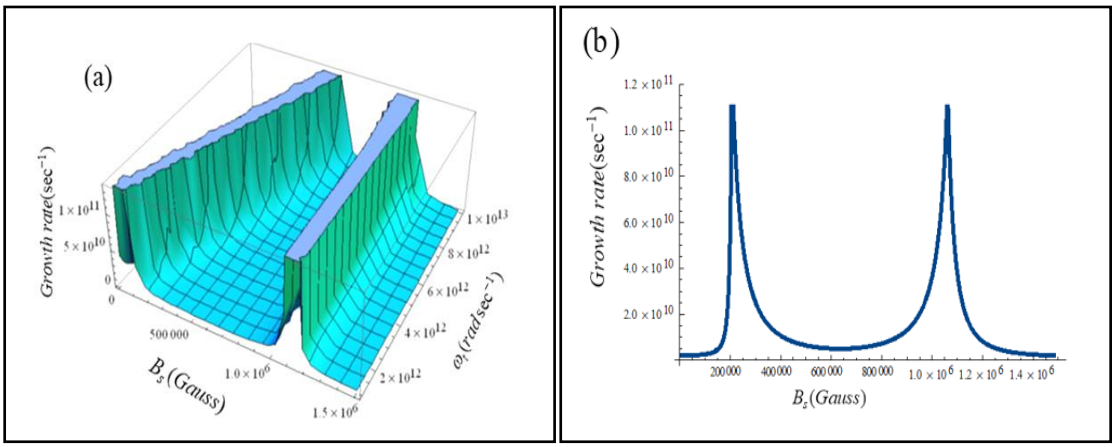

Fig 5.4. Influence of external magnetic field and radiation frequency on the growth rate of the output radiation. (b) Shows the 2-D profile of the plot.

The other peak corresponds to the resonance between the electron beam and the cyclotron frequency. The maximum emission of electromagnetic wave at the resonance has been observed by Krafft *et al*. [35]. With further increase of the field, the growth rate drops down. This behaviour complements with the theoretical observations of Bhasin and Sharma [36].

Fig. 5.5 investigates the variation of growth rate with the magnitude of the field of the pump wave and the radiation frequency. With the increase of the field of the pump wave, the pondermotive force is exerted more strongly on the beam electrons which leads to efficient interaction and hence the growth rate augments.

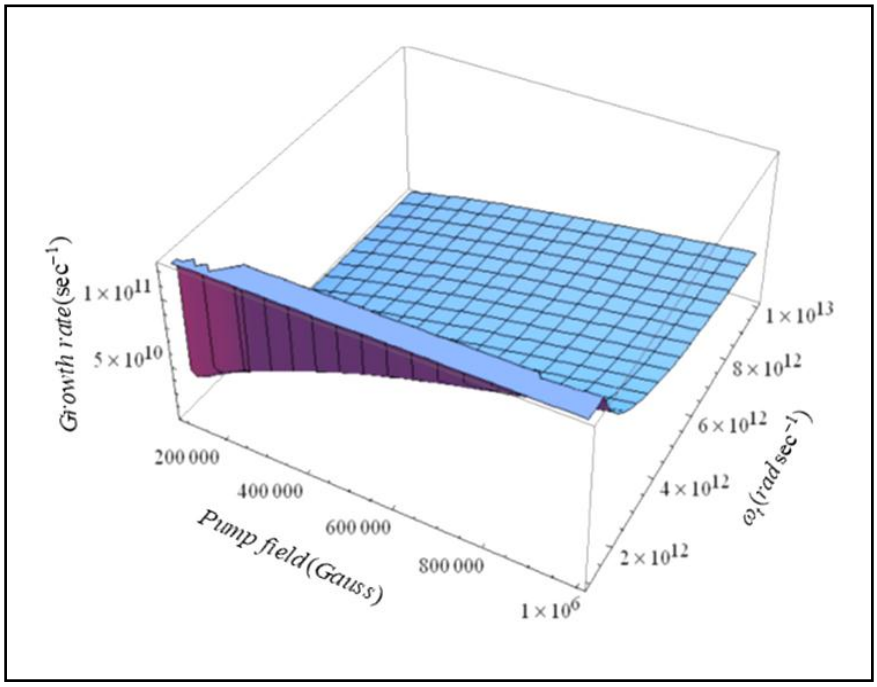

Fig 5.5. Variation of growth rate with the field of the pump wave and the radiation frequency.

Fig. 5.6 shows the variation of the efficiency of the system with the radiation frequency for modulated and unmodulated electron beam. The efficiency falls off with the frequency of the radiation wave and for the density modulated beam, nearly 21% higher efficiency is achieved.

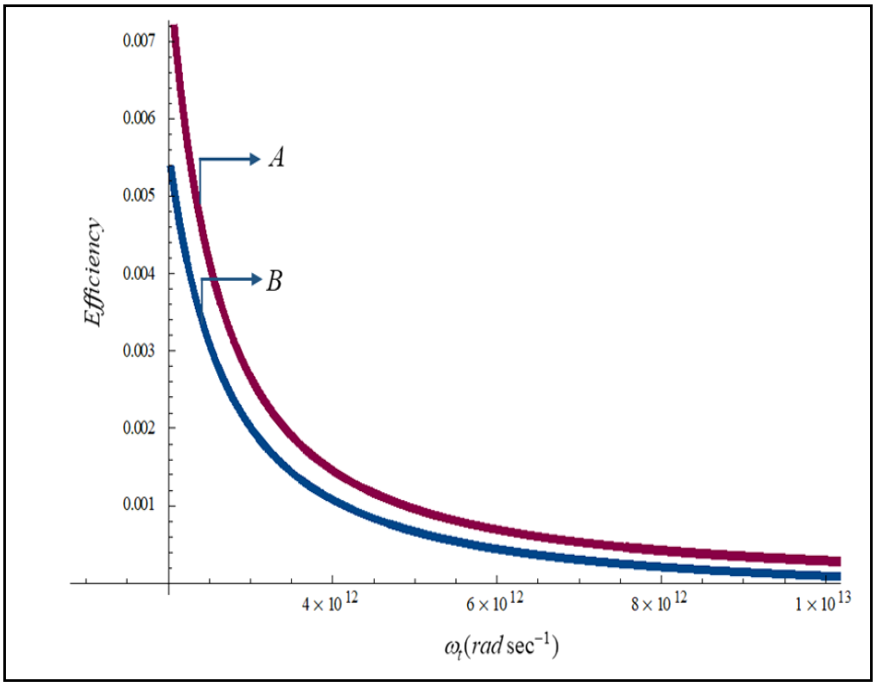

Fig 5.6. Variation of efficiency with radiation frequency for (A) Modulated beam and (B) Unmodulated beam.

5.5 Conclusion

For the efficient generation of the THz radiation wave, a premodulated REB is taken into consideration. A dielectric lined waveguide acts as a slow wave structure which slows down the phase velocity of the pondermotive wave and thus leads to the more effective interaction between the beam and the electromagnetic mode at lower beam energies. The growth rate and efficiency of the radiation wave falls off monotonically with the radiation frequency. The tunability of the radiation wave is determined by the beam parameters and the dielectric of the waveguide. The increase in beam density and the dielectric constant of the waveguide leads to the increment in the growth rate. For the applied magnetic field, the growth rate reaches a maximum value when the wiggler wave frequency is comparable to the electron cyclotron frequency. The model seems to be an effective way for the generation of tunable THz radiation which can be particularized for practical applications.

References

[1] M. Hangyo, T. Nagashima and S. Nashima, Meas. Sci. Technol. **13**,1727-1738 (2002).

[2] A. R. Orlando and G. P. Gallerano, J Infrared Milli Terahz Waves **30**, 1308-1318 (2009).

[3] J. F. Federici, B. Schulkin, F. Huang, D. Gary, R. Barat, F. Oliveira and D. Zimdars, Semicond. Sci. Technol. **20**, S266-S280 (2005).

[4] Zhu B, Chen Y, Deng K and Hu W, Yao Z S, PIERS Proceedings, 1166-1170 (2009).

[5] P. Malik, S. C. Sharma and R. Sharma, Phys. Plasmas **24**, 073101 (2017).

[6] A. Gover, Phys. Rev. Spec. Top.-Accel. Beams **8**, 030701 (2005).

[7] J. Panwar and S. C. Sharma, Phys. Plasmas **24**, 083101 (2017).

[8] A. K. Malik, H. K. Malik and S. Kawata, J. Appl. Phys. **107**, 113105 (2010).

[9] M. Singh, S. Kumar, R. P. Sharma, Phys. Plasmas **18**, 022304 (2011).

[10] F. Bakhtiari, S. Golmohammady, M. Yousefi and B. Ghafary, Phys. Plasmas **23**, 123105 (2016).

[11] V.A. Namiot and L.Yu. Shchurova, Physics Letters A **375**, 2759-2766 (2011).

[12] D.N. Gupta, V.V. Kulagin and H. Suk, Optics Communications **401**, 71-74 (2017).

[13] B. Schütte , S. Bauch, U. Frühling, M. Wieland, M. Gensch, E. Plönjes, T. Gaumnitz, A. Azima, M. Bonitz and M. Drescher, Phys. Rev. Lett. **108**, 253003 (2012).

[14] A. K. Malik, H. K. Malik and U. Stroth, Phys. Rev. E **85**, 016401 (2012).

[15] K.-Y. Kim, Phys. Plasmas **16**, 056706 (2009).

[16] S. Yang, Q. Zhou, C. Tang and S. Chen, Phys. Plasmas **24**, 123107 (2017).

[17] W.-M. Wang, Z.-M. Sheng, X.-G. Dong, H.-W. Du, Y.-T. Li and J. Zhang, J. Appl. Phys. **107**, 023113 (2010).

[18] A. M. Cook, R. Tikhoplav, S.Y. Tochitsky, G. Travish, O. B. Williams and J. B. Rosenzweig, Phys. Rev. Lett. **103**, 095003 (2009).

[19] G. Andonian, , O. Williams, X. Wei, P. Niknejadi, E. Hemsing, J. B. Rosenzweig, P. Muggli, M. Babzien, M. Fedurin, K. Kusche, R. Malone and V. Yakimenko, Appl. Phys. Lett. **98**, 202901 (2011).

[20] H.P. Freund and A.K. Ganguly, Nucl. Instrum. Methods Phys. Res. A **296**, 462-467 (1990).

[21] M. Cohen, A. Kugel, D. Chairman, M. Arbel, H. Kleinman, D. Ben-Haim, A. Eichenbaum, M. Draznin, Y. Pinhasi, I. Yakover, A. Gover, Nucl. Instrum. Methods Phys. Res. A **358**, 82-85 (1995) .

[22] M. Cohen, A. Eichenbaum, M. Arbel, D. Ben-Haim, H. Kleinman, M. Draznin, A. Kugel, I. M. Yacover, A. Gover, Phys. Rev. Lett., **74**, 3812-3815 (1995).

[23] S. C. Sharma and A. Bhasin, Phys. Plasmas **14**, 053101(2007).

[24] V. K. Tripathi and C. S. Liu, IEEE Trans. Plasma Sci. **17**, 583-587 (1989).

[25] O. V. Kibis, M. R. da Costa and M. E. Portnoi, Nano Lett. **7**, 3414-3417 (2007).

[26] R. Hedayati, S. Jafari and S. Batebi, Plasma Phys. Control. Fusion **57**, 085007 (2015).

[27] V. K. Tripathi and C. S. Liu, IEEE Trans. Plasma Sci. **18**, 466-471 (1990).

[28] T. M. Antonsen, J. Palastro and H. M. Milchberg, Phys. Plasmas **14**, 033107 (2007).

[29] S. Chauhan and J. Parashar, Phys. Plasmas **21**, 103113 (2014).

[30] V. B. Gildenburg and N.V. Vvedenskii, Phys. Rev. Lett. **98**, 245002 (2007).

[31] H. K. Malik, Phys. Lett. A **379**, 2826-2829 **(**2015).

[32] M.-Ku Chen, J. H. Kim, C.-E. Yang, S. S. Yin, R. Hui and P. Ruffin, Appl. Phys. Lett. **93**, 231102 (2008**)**.

[33] D. Singh and H. K. Malik, Phys. Plasmas **21**, 083105 (2014).

[34] M. Kumar and V. K. Tripathi, Phys. Plasmas **19**, 073109 **(**2012).

[35] C. Krafft, G. Matthieussent, P. Thevenet and S. Bresson, Phys. Plasmas **1**, 2163-2171 (1994).

[36] A. Bhasin and S. C. Sharma, IEEE J. Quantum Electron. **45**, 1129-1132 (2009).

Chapter 6

RELATIVISTIC ELECTRON BEAM DRIVEN TERAHERTZ RADIATION USING PLASMA SLAB

6.1 Brief Outline of the Chapter

An analytical model for the emission of terahertz radiation using interaction of premodulated relativistic electron beam (REB) with electromagnetic wave in the plasma slab that acts as a pump wave has been developed. The two laser beams interact obliquely with the REB which leads to the energy modulation of the beam due to the nonlinear ponderomotive force. The energy modulated beam translates into a density modulation when travels through the drift space. In the plasma slab, the transverse velocity acquired by the beam electrons couples with the modulated density that give rise to nonlinear current density which leads to the emission of terahertz radiation. The radiation can be tuned by varying the beam and plasma parameters which can be particularised for practical applications.

6.2 Introduction

The field of terahertz radiation which lies in the frequency range of 0.1 to 10 THz has contributed to the research area due to potentiality of its various applications [1-5]. The various sources which are employed for the generation of terahertz radiation involves the optical methods, quantum cascade lasers, free electron lasers [6-11].

The emission of THz radiation via a short pulse Bessel beam by using optical rectification has been studied by Xu *et al.* [12]. They observed that the power of the THz radiation has been enhanced to considerable amount due to the non-diffracting property of the Bessel beam in comparison to the Gaussian beam. Yardimci *et al.* [13] have employed the photoconductive antennas via electrodes with plasmonic contact for the generation of THz radiation which improves the conversion efficiency from optical to terahertz. Vidal *et al*. [14] have observed that the energy of the THz radiation can be optimized by optical rectification in ZnTe crystal using a chirped pulse. Maier *et al*. [15] have suggested the confinement of the radiation at millimeter and sub millimeter wavelength range by using grooves for corrugating the surface of the metal wires which alters the surface plasmons dispersion characteristics which propagates along the surface. The generation of narrow band, tunable THz radiation by the propagation of femtosecond laser pulses in LiNbO3 through optical rectification has been experimentally demonstrated by Stepanov *et al.* [16].

The free electron lasers which involves the interaction of relativistic electron beams with the wiggler have proved to be the potent source for the generation of terahertz radiation due to its tunability, high power and efficiency. Sharma and Bhasin [17] have investigated the terahertz radiation using a dielectric loaded Cerenkov free electron laser with the density modulated electron beam and concluded that the gain and efficiency of the system improves with the modulation index and prebunching of the beam. Hasanbeigi et al [18] have studied the effect of ion channel guiding on

the emission of THz radiation by using prebunched electron beam. They found that the power of the radiation can be enhanced by incorporating the ion channel and it becomes tunable with the density of the ion channel.

The use of plasma medium leads to the increase in field strength as it can sustain large beam currents which are required during the radiation process. The emission of terahertz radiation has been studied by Kumar et al [19] by the nonlinear interaction of laser pulses with the density gradient plasma with the consideration of thermal velocity and observed that the growth rate of the THz radiation increases with the electron temperature and also with the distance to the peak of the plasma density. Dorannian et al [20] have examined the emission of short pulse coherent radiation by the interaction of high intense laser with the magnetized plasma. They studied the role of plasma density and the sharp plasma boundary on the intensity of the radiation.

The emission of THz radiation by the interaction of a density modulated electron beam with the rippled density plasma has been investigated by Malik *et al.* [21]. They observed that the growth rate of the output radiation is improved by the densities of the plasma and electron beam, and also concluded that the mechanism optimizes for mild relativistic electron beams as at higher beam energies, the wave gets attenuated. Tripathi et al [22] have observed the resonant excitation of the terahertz radiation when the amplitude modulated 2-D laser pulse interacts non linearly with the rippled density plasma. They found that the amplitude of the THz radiation augments with the THz frequency and therefore with the plasma density.

In this chapter, the interaction of a density modulated REB with the electromagnetic plasma wave which is used as a wiggler in the presence of an externally applied static magnetic field has been considered by using an analytical formalism. The following mechanism for the above scheme is tracked as; primarily, the velocity modulation of the REB takes place on interaction with the two laser beams in the modulator space, which then translates to the density modulation on passing through

the drift space. The beam on leaving the drift space enters the plasma slab where it interacts with the electromagnetic pump plasma wave and acquires a transverse component of velocity that couples with the modulated beam density to give nonlinear current density, which provides a path for the emission of frequency in the terahertz range. Sec 6.3 involves the physical model for the excitation of THz radiation by the prebunched REB. The results are conferred in Sec 6.4 and the Sec 6.5 concludes the observations.

6.3 Physical Model

In the present work, the emission of terahertz radiation by considering the interaction of premodulated REB with the electromagnetic pump wave wiggler has been studied.

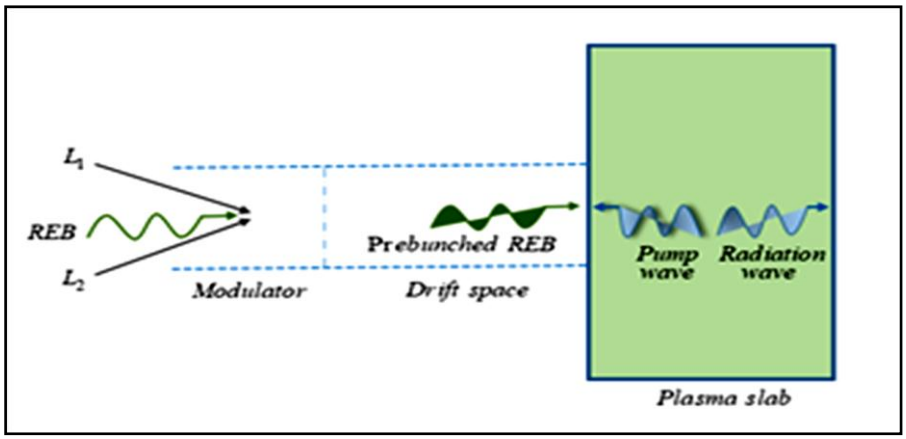

Fig 6.1. Schematic of interaction of prebunched REB with the pump wave.

The modulation of the REB is accounted by the interaction of two laser beams with the electron beam. A REB propagates in z-direction with initial velocity $v_{be}\hat{z}$ and beam density n_{be}. The electric and magnetic fields of the laser beams, L_1 and L_2 are taken as $\vec{E_l^j} = \vec{A_l^j}\exp\left[-i\left(\omega_{bj}t - k_{bj}z\right)\right]$ and $\vec{B_l^j} = \frac{c\left(\vec{k_l^j}\times\vec{E_l^j}\right)}{\omega_{bj}}\hat{y}$, where j = 1, 2 for lasers L_1 and L_2, respectively.

The beam electrons acquires an oscillatory velocity $\overrightarrow{v_0^j} = \frac{e\overrightarrow{E_l^j}}{im_e\omega_{bj}\gamma_0}$ due to the interaction of laser beams with the REB in the modulator space, where m_e is the electronic mass, $\gamma_0 = \left(1 - \frac{v_{be}^2}{c^2}\right)^{-1/2}$ is the relativistic gamma factor.

The nonlinear THz ponderomotive force $\overrightarrow{F_{el}}$ exerted on the beam electrons due to the laser beams leads to the velocity modulation of the REB.

$$\overrightarrow{F_{el}} = -\frac{e^2 k_b^e A_l^1 A_l^{2*}}{2im_e\omega_l^1\omega_l^2\gamma_0}\cos(\theta_i)e^{-i\left(\omega_b^e t - k_b^e z\right)}\hat{z},$$

where $\omega_b^e\left(=\omega_{b1}-\omega_{b2}\right)$ and $k_b^e\left(=k_{b1}-k_{b2}\right)$ are the frequency and wave number of the REB, respectively and θ_i is the angle at which the laser beams interact with each other.

The time at which the electrons enter the modulator is taken to be t_{im} and at $t = t_{id}$, the beam enters the drift space.

The modulated velocity of the REB $\overrightarrow{v_{lm}}$ due to the ponderomotive force is obtained by using relativistic equation of motion as

$$\overrightarrow{v_{lm}} = \frac{k_b^e l_1 e^2 A_l^1 A_l^{2*}}{2\gamma_0^4 m_e^2 c^2 v_{be}\omega_l^1\omega_l^2}\frac{\sin(\theta_v)}{\theta_v}\sin\left(\omega_b^e t_{im} + \theta_v\right), \tag{6.1}$$

where $\theta_v\left(=\frac{\omega_b^e - k_b^e v_{be}}{2v_{be}}\right)l_1$ is the phase angle of the modulator and l_1 is the modulator region length.

Now, the velocity modulated REB will travel through the drift space where the fast and slow moving electrons catch each other leading to the formation of bunches and this leads to the translation into a density modulated REB. The modulated density of the beam[11] n_{lm} can be expressed as.

$$n_{lm} = -2n_{be}J_1\left(\frac{\omega_b^e l_2 \lambda}{v_{be}}\right)\cos\left(\omega_b^e t_{id} - \phi\right), \tag{6.2}$$

where $\lambda = \frac{k_b^e l_1 e^2 A_l^1 A_l^{2*}}{2\gamma_0^4 m_e^2 c^2 v_{be} \omega_l^1 \omega_l^2}\frac{\sin(\theta_v)}{\theta_v}$, l_2 is the drift space length, $\phi = \frac{\omega_b^e(l_1+l_2)}{v_{be}} - \theta_v$ and $t_{id}\left(= t_{im} + \frac{l_1}{v_{be}} + \frac{\left(l_2\left(1+\lambda\sin\left(\omega_b^e t_{im} + \theta_v\right)\right)\right)}{v_{be}}\right)$ is the time at which the beam enters the plasma slab.

Next, a slab filled with plasma of uniform density n_p^i is considered. The electromagnetic plasma wave acts as a pump wave in the present case. An external magnetic field $B_0\hat{y}$ is applied in the medium. The transverse velocity component $\overrightarrow{v_{e0}}$ attained by the beam electrons on interaction of the density modulated REB with the pump wave can be obtained using relativistic equation of motion

$$\frac{\partial(\gamma\vec{v})}{\partial t} + \vec{v}.\nabla(\gamma\vec{v}) = -\frac{e}{m_e}\left(\overrightarrow{E_{em}} + \frac{1}{c}\left(\vec{v}\times\overrightarrow{B_{em}}\right) + \frac{1}{c}\left(\vec{v}\times\overrightarrow{B_0}\right)\right) \text{ as}$$

$$\overrightarrow{v_{e0}} = \frac{\frac{e}{m_e}\left(\overrightarrow{E_{em}} - \frac{v_{be}}{c}\overrightarrow{B_{em}}\right)}{i\gamma_0^3\left(\omega_m - \frac{\omega_{ce}}{\gamma_0^3}\right)}, \tag{6.3}$$

where $\vec{v} = \overrightarrow{v_{be}} + \overrightarrow{v_{e0}}$, $\overrightarrow{E_{em}}\left(= A_{em}\hat{x}\exp -i\left(\omega_m t - k_m z\right)\right)$

and $\overrightarrow{B_{em}} = \frac{c}{\omega_m}\left(\overrightarrow{k_m} \times \overrightarrow{E_{em}}\right) = A_{bm} \exp\left[-i\left(\omega_m t - k_m z\right)\right]\hat{y}$ are the electric and magnetic fields, respectively of the electromagnetic pump wave, ω_m and k_m are the electromagnetic pump wave frequency and wave number, respectively and $\omega_{ce}\left(=\frac{eB_0}{m_e c}\right)$ is the electron cyclotron frequency.

The modulated beam density now couples with the oscillatory velocity acquired by the beam to give rise to nonlinear current density $\overrightarrow{J_{nl}}$ that drives the radiation wave.

$$\begin{aligned}\overrightarrow{J_{nl}} &= -n_{lm} e \overrightarrow{v_{e0}} \\ &= \frac{2n_{be} J_1\left(\frac{\omega_b^e l_2 \lambda}{v_{be}}\right) e^{-i\phi} e^2 \left(\overrightarrow{E_{em}} - \frac{v_{be}}{c}\overrightarrow{B_{em}}\right)}{i m_e \gamma_0^3 \left(\omega_m - \frac{\omega_{ce}}{\gamma_0^3}\right)} e^{-i\left(\omega_t t - k_t z\right)},\end{aligned} \tag{6.4}$$

where t_{ip} is taken as $t_{ip} = t - \frac{z}{v_{be}}$, $\omega_t\left(=\omega_b^e + \omega_m\right)$ and $k_t\left(=k_b^e + k_m\right)$ are the frequency and wave number, respectively of the THz radiation.

The retarded vector potential is evaluated for obtaining the magnetic field

$$\begin{aligned}\overrightarrow{A} = \frac{\mu}{4\pi}\frac{\int \overrightarrow{J_{nl}}\left(\vec{r}', t_r\right)}{R} d^3 r' = \\ -\frac{\mu n_{be} r_{be}^2 J_1\left(\frac{\omega_b^e l_2 \lambda}{v_{be}}\right) e^{-i\phi} e^2 \left(\overrightarrow{E_{em}} - \frac{v_{be}}{c}\overrightarrow{B_{em}}\right)}{2i m_e \gamma_0^3 r \left(\omega_m - \frac{\omega_{ce}}{\gamma_0^3}\right)} \hat{z} \times \\ \int_0^{l_e} \exp\left[-i\left(\frac{\omega_t}{c}\left(\frac{c}{v_{be}} - \cos\varphi\right) - k_t\right) z'\right] dz',\end{aligned} \tag{6.5}$$

where $t_r\left(=t-\frac{R}{c}\right)$ is the retarded time, $R=\left|r-r'\right|\simeq r-z'\cos\varphi$, l_e is the length of the electron bunch, μ_0 is the permeability of the medium.

For the oscillating field of the wave, consider the real part of the poynting vector as

$$\overline{S_r}=\frac{1}{2}\frac{c}{\mu}|B|^2=\frac{1}{2}\frac{c}{\mu}\left[\frac{\mu n_{be}r_{be}^2J_1\left(\frac{\omega_b^e l_2\lambda}{v_{be}}\right)e^{-i\phi}e^2\left(A_{em}-\frac{v_{be}}{c}A_{bm}\right)}{2icm_e\gamma_0^3 r\left(\omega_m-\frac{\omega_{ce}}{\gamma_0^3}\right)}\right.$$
$$\left.\frac{\exp\left(i\left(\frac{\omega_t l_e}{c}\left(\frac{c}{v_{be}}-\cos\varphi+\frac{ck_t}{\omega_t}\right)\right)\right)-1}{\left(\frac{c}{v_{be}}-\cos\varphi+\frac{ck_t}{\omega_t}\right)}\right]^2,$$

where $\vec{B}$ is obtained using $\vec{B}=\nabla\times\vec{A}$.

On taking $\frac{\omega_t l_e}{c}\left(\frac{c}{v_{be}}-\cos\varphi+\frac{ck_t}{\omega_t}\right)=\beta$, the above expression can be simplified to

$$\overline{S_r}=\frac{1}{2}\frac{c}{\mu}\left[\frac{\mu_0 n_{be}r_{be}^2J_1\left(\frac{\omega_b^e l_2\lambda}{v_{be}}\right)e^{-i\phi}e^2\left(\overrightarrow{E_{em}}-\frac{v_{be}}{c}\overrightarrow{B_{em}}\right)}{icm_e\gamma_0^3 r\left(\omega_m-\frac{\omega_{ce}}{\gamma_0^3}\right)}\frac{\sin^2(\beta)}{\beta^2}\right]. \qquad (6.6)$$

Normalized terahertz power P_{THz} can be evaluated using

$$P_{THz} = \frac{4\pi r^2 \overrightarrow{S_r}}{4\pi l_p^2 c B_{em}^2 / 2\mu}$$

$$= \left[\frac{\omega_{be}^2 r_{be}^2 \omega_t l_e J_1\left(\frac{\omega_b^e l_2 \lambda}{v_{be}}\right) e^{-i\phi}\left(A_{em} - \frac{v_{be}}{c} A_{bm}\right)}{i2\eta c^3 \gamma_0^3 l_p B_{em}\left(\omega_m - \frac{\omega_{ce}}{\gamma_0^3}\right)} \frac{\sin^2(\beta)^2}{\beta^2} \right]^2, \tag{6.7}$$

where $\omega_{be} = \left(\frac{n_{be} e^2}{m_e \varepsilon_0}\right)^{1/2}$ is the electron beam plasma frequency, $\eta\left(=\sqrt{\varepsilon_{p0}}\right)$ is the refractive index of the medium, $\varepsilon_{p0}\left(=1-\frac{\omega_{pe}^2}{\omega_m^2}\right)$ is the dielectric constant of plasma medium, $\omega_{pe}\left(=\frac{n_{pe} e^2}{m_e \varepsilon_0}\right)^{1/2}$ is the electron plasma frequency, n_{pe} is the electron plasma density.

To evaluate the amplitude of the THz radiation, the wave equation is employed as

$$\nabla^2 \overrightarrow{E_{1t}} + \frac{\partial^2}{\partial t^2} \overrightarrow{E_{1t}} = -4\pi i \frac{\omega_t}{c^2} \overrightarrow{J_{nl}}, \tag{6.8}$$

where $\overrightarrow{E_{1t}}\left(= A_{1t} e^{-i\left(\omega_t - k_t z\right)} \hat{x}\right)$ is the electric field of the radiation wave.

Using, $k_t = \frac{\omega_b^e}{v_{be}} + k_{em}$, Eq. (6.8) can be re-written as

$$k_t \frac{\partial A_{1t}}{\partial z} + \frac{k_t}{v_g^t} \frac{\partial A_{1t}}{\partial t} + \left(\frac{\omega_t^2}{c^2} \varepsilon_{p0} - k_t^2\right) A_{1t}$$

$$= \frac{-4\pi n_{be} \omega_t J_1\left(\frac{\omega_b^e l_2 \lambda}{v_{be}}\right) e^{-i\phi} e^2 \left(A_{em} - \frac{v_{be}}{c} A_{bm}\right)}{i m_e c^2 \gamma_0^3 \left(\omega_m - \frac{\omega_{ce}}{\gamma_0^3}\right)}, \tag{6.9}$$

where $v_g^t \left(= \frac{c^2 k_t}{\omega_t} \right)$ is the radiation group velocity and at $\frac{\omega_t^2}{c^2} \varepsilon_{p0} = k_t^2$, exact phase matching condition is satisfied. Eq. (6.9) can be simplified to

$$\frac{\partial A_{1t}}{\partial \rho} = -\frac{\omega_b^{e2} \omega_t J_1 \left(\frac{\omega_b^e l_2 \lambda}{v_{be}} \right) e^{-i\phi} \left(A_{em} - \frac{v_{be}}{c} A_{bm} \right)}{i k_t c^2 \gamma_0^3 \left(\omega_m - \frac{\omega_{ce}}{\gamma_0^3} \right)}, \tag{6.10}$$

where $\rho = v_g^t \left(t - \frac{z}{v_g^t} \right)$.

The amplitude of the radiation wave can be obtained by integrating Eq. (6.10) and considering the real part as

$$A_{1t} = -\frac{\omega_b^{e2} \omega_t l_p J_1 \left(\frac{\omega_b^e l_2 \lambda}{v_{be}} \right) \sin(-\phi) \left(A_{em} - \frac{v_{be}}{c} A_{bm} \right)}{\left(k_m + \frac{\omega_b^e}{v_{be}} \right) c^2 \gamma_0^3 \left(\omega_m - \frac{\omega_{ce}}{\gamma_0^3} \right)}, \tag{6.11}$$

6.4 Results and Discussion

The present model has been studied analytically to evaluate the power and amplitude of the output THz radiation. The outcome of beam and wiggler parameters on the radiation wave is analyzed by considering the following typical parameters, i.e., beam velocity $v_{be} = 0.92c$, beam density $n_{be} = 1.5 \times 10^{15} cm^{-3}$, relativistic gamma factor $\gamma_0 = 2.56$, electron bunch length $l_e = 0.3cm$, beam radius $r_{be} = 2 \times 10^{-3} cm$, modulator region length $l_1 = 0.45cm$, length of the drift space $l_2 = 0.8cm$, length of the wiggler space $l_p = 0.5cm$.

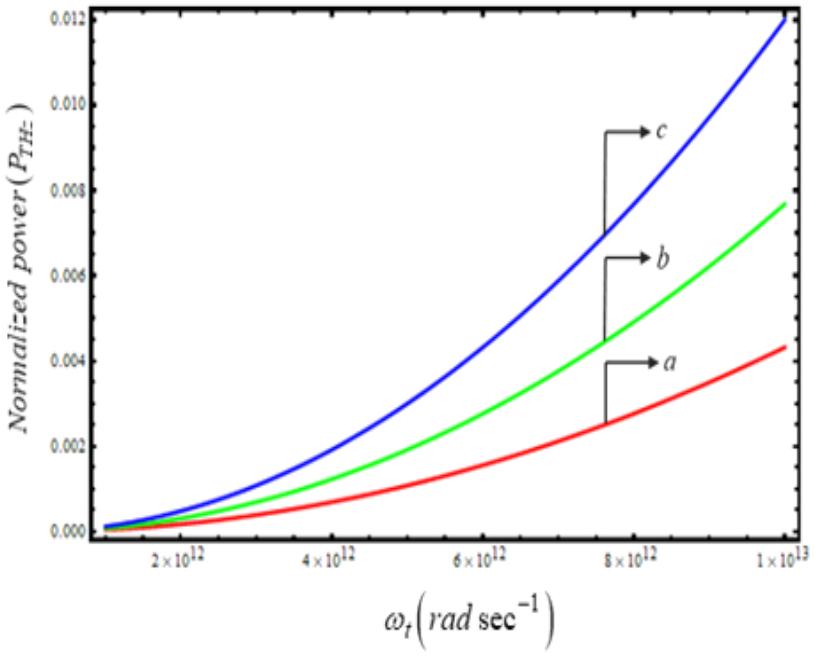

Fig 6.2. Variation of normalized output power with the radiation frequency for different beam densities (a) $n_{be}=1.5\times10^{15}cm^{-3}$, *(b)* $n_{be}=2\times10^{15}cm^{-3}$, *(c)* $n_{be}=2.5\times10^{15}cm^{-3}$.

Figure 6.2 indicates the variation of the power of the output radiation with the radiation wave frequency for different beam densities. As the beam density augments, more the number of energy carrying electrons become available to transfer the energy to the radiation wave. Thus the power increases with the beam density. Further, the power enhances with the radiation frequency also.

The effect of externally applied static magnetic field on the variation of the THz power is illustrated in Figure 6.3. The figure shows the increase in power with the magnetic field upto a point where the frequency of the pump wave matches the electron cyclotron frequency and maximum value of normalized power is achieved when the pump wave frequency is comparable to the electron cyclotron frequency. With the further increases of the magnetic field, the power declines.

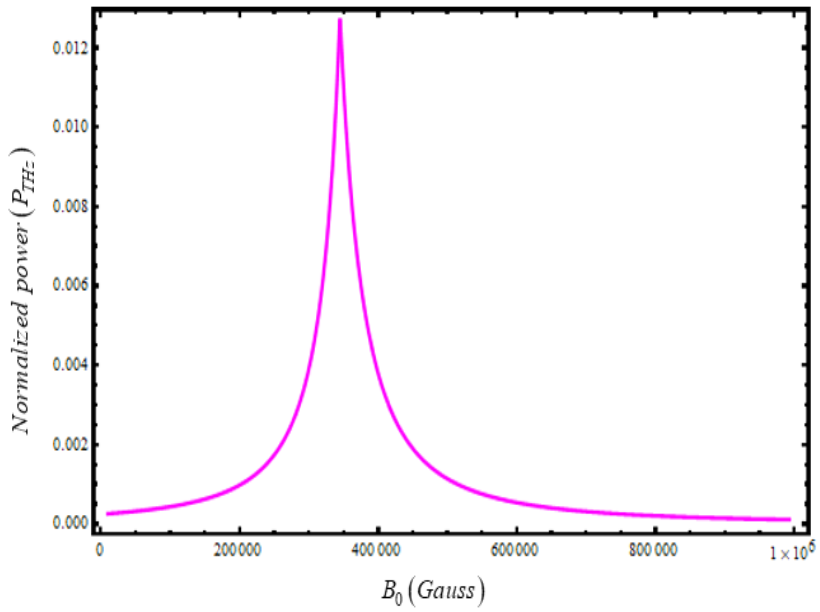

Fig 6.3. Effect of externally applied magnetic field on the power of the output radiation.

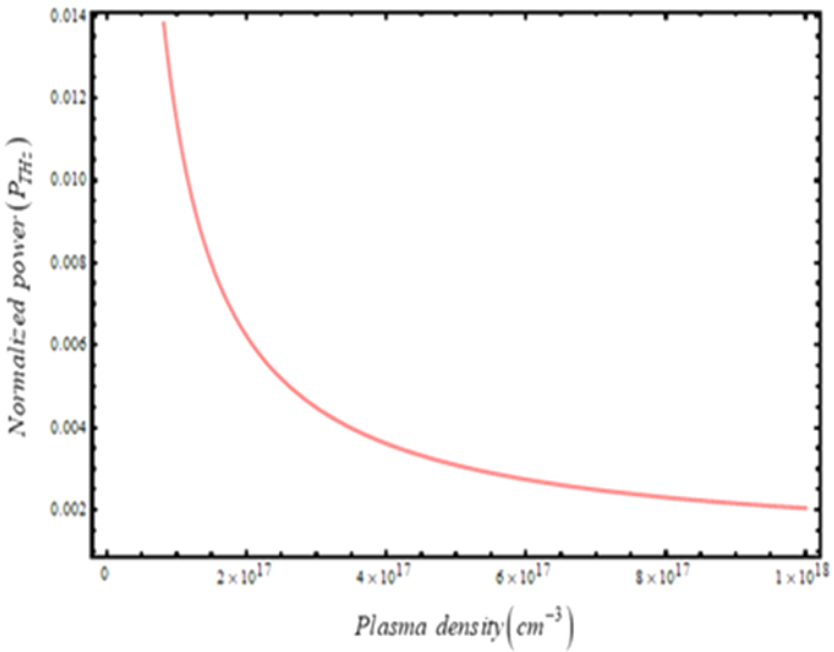

Fig 6.4. Normalized power as function of plasma density.

The influence of plasma density on the power of the radiation wave is shown in Figure 6.4. The figure shows that the increase in density of the plasma electrons, leads to the decrease in power of the radiation wave upto a certain level and then it saturates.

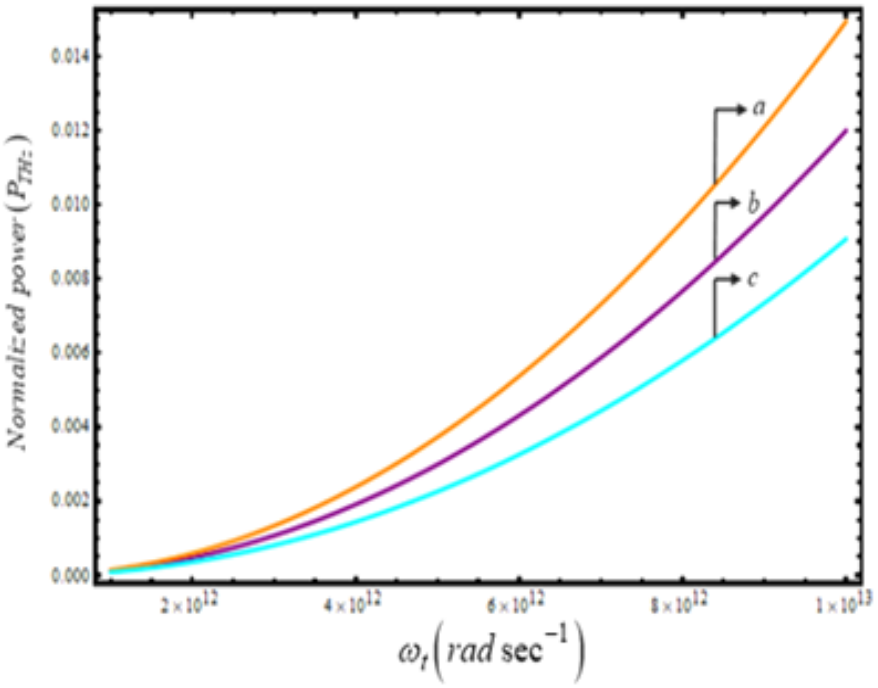

Fig 6.5. Variation of normalized output power with the radiation frequency for different beam velocities (a) $v_{be}=0.88c$, *(b)* $v_{be}=0.91c$, *(c)* $v_{be}=0.94c$.

Figure 6.6 depicts the variation of amplitude of the THz radiation wave with the amplitude of the field of the pump wave. With the increase in strength of the field of the pump wave, the ponderomotive force is exerted more strongly on the beam electrons which leads to the efficient interaction with the electromagnetic wave and therefore, the amplitude of the radiation wave increases linearly with the strength of the electric field of the pump wave.

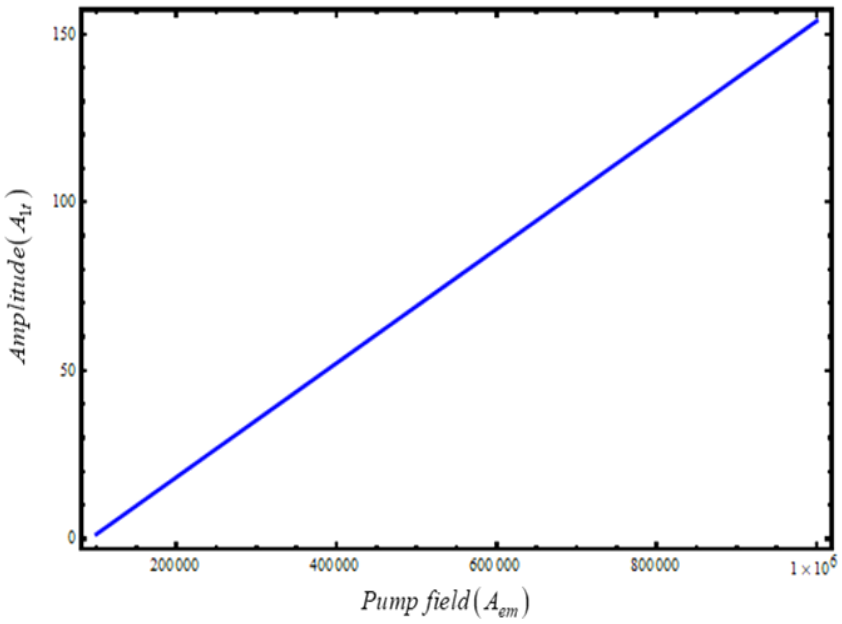

Fig 6.6. Variation of THz amplitude with the field of the pump wave.

6.5 Conclusion

In this scheme, the emission of terahertz radiation by using premodulated REB interaction with the electromagnetic plasma pump wave has been deliberated analytically. The effect of beam and plasma parameters on the power and amplitude of the radiation wave has been analyzed. The normalized power of the wave varies as square of the beam density and the field of the pump wave. The amplitude varies linearly with the beam density and amplitude of the pump field. The power and amplitude of the wave is improved by the beam energy and the density of the beam electrons. It is inferred that at the condition of resonance, the frequency of the pump wave becomes comparable to the electron cyclotron frequency which leads to the maximum emission of power. The THz power enhances with the plasma density upto a saturation point. The scheme thus holds importance in obtaining tunable radiation in the frequency range of terahertz which can be particularised for various applications such as spectroscopy, imaging, security analysis etc.

References

[1] H. A. Hafez, X. Chai, A. Ibrahim, S. Mondal, D. Férachou, X. Ropagnol and T. Ozaki, J. Opt. **18**, 093004 (2016).

[2] E. Pickwell and V. P. Wallace, J. Phys. D. Appl. Phys. **39**, R301–R310 (2006).

[3] W. L. Chan, J. Deibel, and D. M. Mittleman, Reports Prog. Phys. **70**, 1325–1379 (2007).

[4] J. F. Federici, B. Schulkin, F. Huang, D. Gary, R. Barat, F. Oliveira and D. Zimdars, Semicond. Sci. Technol. **20**, S266–S280 (2005).

[5] G. K. Kitaeva, Laser Phys. Lett. **5**, 559–576 (2008).

[6] S. V Sazonov, JETP Lett. **96**, 263–274 (2012).

[7] P. Dean, A. Valavanis, J. Keeley, K. Bertling, Y. L. Lim, and R. Alhathlool, *J. Phys. D: Appl. Phys.* ***47*** , 374008 (2017).

[8] S. C. Sharma, J. Panwar, and R. Sharma, Contrib. to Plasma Phys. **57**, 167–175 (2017).

[9] S. C. Sharma and P. Malik, Phys. Plasmas **22** 043301 (2015).

[10] J. Panwar and S. C. Sharma, Phys. Plasmas **24**, 083101 (2017).

[11] M. Kumar and V. K. Tripathi, Phys. Plasmas **19**, 073109 (2012).

[12] S. Xu, Y. Li, X. Liang, H. Cao, M. Hu, L. Chai, and C. Wang, "Generation of Terahertz Radiation by Optical Rectification Using Femtosecond Bessel Beam," vol. 23, no. 4, 2017.

[13] N. T. Yardimci, S. H. Yang, C. W. Berry, and M. Jarrahi, IEEE Trans. Terahertz Sci. Technol. **5**, 223–229, 5100406 2015.

[14] S. Vidal, J. Degert, M. Tondusson, E. Freysz, and J. Oberlé, J. Opt. Soc. Am. B **31**, 149 (2014).

[15] S. A. Maier, S. R. Andrews, L. Martín-Moreno, and F. J. García-Vidal, Phys. Rev. Lett. **97**, 1–4 (2006).

[16] A. Stepanov, J. Hebling, and J. Kuhl, Opt. Express **12**, 4650 (2004).

[17] S. C. Sharma and A. Bhasin, Phys. Plasmas **14**, 10 (2007).

[18] A. Hasanbeigi, H. Mehdian, and P. Gomar, Phys. Plasmas **22**, 123116 (2015).

[19] M. Kumar, K. Lee, S. H. Park, Y. U. Jeong, and N. Vinokurov, Phys. Plasmas **24**, 033104 (2017).

[20] D. Dorranian, M. Starodubtsev, H. Kawakami, H. Ito, N. Yugami, and Y. Nishida, Phys. Rev. E - Stat. Nonlinear, Soft Matter Phys. **68**, 026409 (2003).

[21] P. Malik, S. C. Sharma, and R. Sharma, Phys. Plasmas **24**, 073101 (2017).

[22] D. Tripathi, L. Bhasin, R. Uma, and V. K. Tripathi, Phys. Scr. **82**, 035504 (2010).

Chapter 7

SUMMARY AND FUTURE ASPECTS

The present work emphases on the emission of high power THz radiation using free electron laser (FEL). FEL is a classical device opted for the generation of the radiation with the widest frequency range tuned as per the requirement with wavelength lying in the spectrum range from microwaves to X- rays. The frequency of the output radiation is determined mainly by the energy of the electron beam, strength of the field of the wiggler wave and density of the plasma electrons. We have incorporated the effect of premodulated REB for enhancing the beam efficiency. The premodulation of the beam is accounted by two laser beams which is similar to klystron based principle. The ponderomotive force exerted on the beam electrons results prebunching of the electron beam.

The strength and size of the wiggler plays a significant role in determining the wavelength of the output radiation. Some of the plasma based wigglers such as Langmuir wave, surface plasma wave are used as a pump wave in the interaction process which helps in achieving high peak powers due to the plasma characteristics. We have also used a dielectric lined plasma filled waveguide as a slow wave structure that offers low beam energy requirement. The plasma wiggler provides shorter wavelengths leading to reduction in wiggler period. Other plasma based sources which have not been used can be taken into consideration with different plasma conditions and density profiles to have more effective route for the emission.

FEL requires relativistic electron beams which are obtained by accelerating the beam electrons through large size accelerators. The demand for high frequency requires increase of beam energy which results in high cost and maintenance of the device. The setup for FEL cannot be established in a laboratory for performing the experiments and thus the implementation of the outcomes is little restricted. The work can therefore be extended to reduce the size and consequently cost of the device so as to make it accessible on a larger scale.

Further, THz radiation has tremendous properties and applications but the use of the radiation is still restricted to some areas. Therefore, there exists a great scope to extend the present work done to have a better knowledge of generating the THz radiation on a common scale such that the use of the THz radiation mentioned in various fields can be extended to a large scale.

The work has been carried out analytically by following fluid theory approach. The same can be improved by employing kinetic theory such that effect of collisions and microscopic processes that leads to pressure and temperature variation can also be incorporated.

Further, the numerical simulation can also be carried out for the work done in the thesis and verified with the current analytical outcomes for more accuracy and optimization of the parameters.